

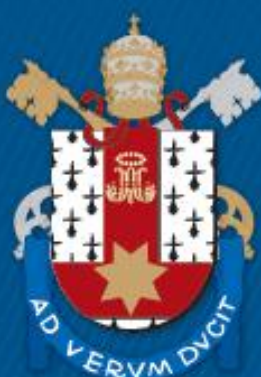
FACULDADE DE BIOCIÊNCIAS
PROGRAMA DE PÓS-GRADUAÇÃO EM BIOLOGIA CELULAR E MOLECULAR
MESTRADO EM BIOLOGIA CELULAR E MOLECULAR

FERNANDA SOUZA MACCHI

**3,4-DIIDROQUINAZOLIN-4-ONAS E 1H-BENZO[*d*]IMIDAZÓIS: PLANEJAMENTO
UTILIZANDO HIBRIDAÇÃO MOLECULAR, SÍNTESE E ATIVIDADE INIBITÓRIA
SOBRE O CRESCIMENTO DE *Mycobacterium tuberculosis***

Porto Alegre
2017

PÓS-GRADUAÇÃO - STRICTO SENSU



Pontifícia Universidade Católica
do Rio Grande do Sul

FERNANDA SOUZA MACCHI

**3,4-DIIDROQUINAZOLIN-4-ONAS E 1*H*-BENZO[*d*]IMIDAZÓIS:
PLANEJAMENTO UTILIZANDO HIBRIDAÇÃO MOLECULAR, SÍNTESE E
ATIVIDADE INIBITÓRIA SOBRE O CRESCIMENTO DE *MYCOBACTERIUM
TUBERCULOSIS***

Dissertação apresentada ao Programa
de Pós-Graduação em Biologia Celular
e Molecular da Faculdade de
Biociências como requisito para
obtenção do título de mestre em
Biologia Celular e Molecular.

Orientador: Prof. Dr. Pablo Machado

Coorientadora: Dra. Kenia Pissinate

Porto Alegre

2017

Ficha Catalográfica

M124 Macchi, Fernanda Souza

3,4-Diidroquinazolin-4-onas e 1H-benzo[d]imidazóis planejamento utilizando
hibridação molecular, síntese e atividade inibitória sobre o crescimento
de *Mycobacterium tuberculosis* / Fernanda Souza Macchi . – 2017.

115 f.

Dissertação (Mestrado) – Programa de Pós-Graduação em Biologia Celular
e Molecular, PUCRS.

Orientador: Prof. Dr. Pablo Machado.

Co-orientadora: Profa. Dra. Kenia Pissinate.

1. *Mycobacterium tuberculosis*. 2. tuberculose. 3. hibridação molecular. 4. cepas
resistentes à fármacos. 5. cardiotoxicidade. I. Machado, Pablo. II. Pissinate,
Kenia. III. Título.

Elaborada pelo Sistema de Geração Automática de Ficha Catalográfica da PUCRS
com os dados fornecidos pelo(a) autor(a).

FERNANDA SOUZA MACCHI

**3,4-DIIDROQUINAZOLIN-4-ONAS E 1*H*-BENZO[*d*]IMIDAZÓIS:
PLANEJAMENTO UTILIZANDO HIBRIDAÇÃO MOLECULAR, SÍNTESE E
ATIVIDADE INIBITÓRIA SOBRE O CRESCIMENTO DE *MYCOBACTERIUM
TUBERCULOSIS***

Dissertação apresentada ao Programa
de Pós-Graduação em Biologia Celular
e Molecular da Faculdade de
Biociências como requisito para
obtenção do título de mestre em
Biologia Celular e Molecular.

Aprovada em: ____ de ____ de ____.

BANCA EXAMINADORA:

Prof. Dr. Wilson João Cunico Filho – UFPel

Prof. Dr. Lucas Pizzuti – UFGD

Prof. Dr. Jarbas Rodrigues de Oliveira - PUCRS

Porto Alegre

2017

Dedico este trabalho aos meus
pais, amigos e ao Lucas.

AGRADECIMENTOS

Aos meus orientadores Professor Pablo Machado e Dra. Kenia Pissinate, pela ajuda, conhecimento compartilhado e confiança durante estes dois anos. Obrigada pelos momentos divididos.

Ao Professor Diógenes Santiago Santos (*in memoriam*) por ter aberto as portas do seu laboratório, ter me recebido e contribuído com meu crescimento pessoal e profissional.

Aos colegas do Centro de Pesquisas em Biologia Celular e Molecular, pela colaboração para desenvolver e concluir este trabalho, pelos momentos de descontração e pelas palavras de apoio.

À Ana Paula e à Talita, que sempre se mostraram interessadas, por toda ajuda, pelo companheirismo, dedicação e disponibilidade.

À Renata e ao Bruno, pelo afeto, risadas, auxílio, compartilhamento de experiências e pela amizade construída. Esses dois anos não teriam sido tudo o que foram sem a presença de vocês.

Aos meus pais, que sempre acreditaram em mim e estiveram presentes em toda minha caminhada até aqui. Obrigada pelo apoio, amor, suporte e carinho. Amo vocês e tudo é por/para vocês.

Ao Lucas, companheiro incansável, compreensivo e presente em todos os momentos. Obrigada pelo carinho, pelo suporte, pelo ouvinte atento e ótimo conselheiro, por me fazer bem, pelo amor.

Aos meus amigos, por escutarem minhas angústias e felicidades, por entenderem a ausência e estimularem meu crescimento, pelos momentos divididos e por tantos anos de amizade.

À PUCRS, pelas oportunidades e também à CAPES e BNDES pelo suporte financeiro.

“Happiness can be found, even in the darkest of times, if one only remembers to turn on the light.”

Albus Dumbledore (J.K. Rowling)

RESUMO

Usando a abordagem clássica de hibridação molecular, séries de *1H*-benzo[*d*]imidazóis e 3,4-diidroquinazolin-4-onas foram sintetizadas e ensaiadas como inibidores de crescimento de *Mycobacterium tuberculosis*. Modificações químicas e estudos de relação estrutura-atividade nos conduziram a potentes agentes antituberculose com valores submicromolares de concentração inibitória mínima. Os compostos sintetizados também foram ativos contra cepas resistentes à fármacos e demonstraram desprovida citotoxicidade aparente em células HepG2, HaCat e Vero. Além disso, algumas 3,4-diidroquinazolin-4-onas apresentaram baixo risco de toxicidade cardíaca, e nenhum sinal de neurotoxicidade ou alteração morfológica em modelo de peixe-zebra (*Danio rerio*). Sendo assim, os resultados indicam que essa classe de molécular pode fornecer condidatos para o desenvolvimento futuro de novos fármacos contra a tuberculose.

Palavras-chave: *Mycobacterium tuberculosis*, tuberculose, hibridação molecular, cepas resistentes a fármacos, carditoxicidade.

ABSTRACT

Using the classical hybridization approach series of $1H$ -benzo[d]imidazoles and 3,4-dihydroquinazolin-4-ones were synthesized and evaluated as inhibitors of *Mycobacterium tuberculosis* growth. Chemical modifications and structure-activity relationship studies yielding potent antitubercular agents with minimum inhibitory concentration values in submicromolar range. Further, the synthesized compounds were active against drug-resistant strains and were devoid of apparent toxicity to HepG2, HaCat, and Vero cells. In addition, some 3,4-dihydroquinazolin-4-ones showed low risk of cardiac toxicity, no signals of neurotoxicity or morphological alteration in zebrafish (*Danio rerio*) models. Therefore, these data denote that this class of molecules may furnish candidates for future development of novel anti-TB drug alternatives.

Keywords: *Mycobacterium tuberculosis*, tuberculosis, molecular hybridization, drug-resistant strains, cardiotoxicity.

LISTA DE FIGURAS

Figura 1. Tendências globais no número estimado de casos de TB incidente e o número de casos de mortes por TB entre os anos de 2000 - 2015. Adaptado de WHO, 2016.....	12
Figura 2. Estimativa de novos casos de TB (todas as formas) a cada 100.000 habitantes no ano de 2015. Adaptado de WHO, 2016	13
Figura 3. Composição do granuloma maduro. Adaptado de ZAHRT, 2003.	14
Figura 4. Estrutura química da bedaquilina (a) da delamanida (b).....	18
Figura 5. Tipos de hibridação molecular. Adaptado de NEPALI et al., 2014....	22
Figura 6. Estrutura química do lansoprazol (LPZ) (a) e do sulfeto de lansoprazol (LPZS) (b).....	23
Figura 7. Estruturas químicas dos principais isômeros quinazolinônicos e sua numeração.	24
Figura 8. Estrutura química das moléculas sintetizadas por Pedgaonkar et al., 2014.	25
Figura 9. Hibridação molecular utilizando substituintes N-substituídas- α -bromoacetamidas provenientes dos compostos 2-(quinolin-4-iloxi)acetamidas com núcleos 1H-benzo[d]imidazóis e 3,4-diidroquinazolin-4-onas.....	26

SUMÁRIO

CAPÍTULO 1 – INTRODUÇÃO E OBJETIVOS	11
1.INTRODUÇÃO	12
1.1 Tuberculose	12
1.2 Patogenia e Diagnóstico	14
1.3 Tratamento e Resistência aos fármacos	15
1.4 Fármacos em desenvolvimento contra a tuberculose.....	18
1.5 Hibridação Molecular	21
1.6 1 <i>H</i> -Benzo[<i>d</i>]imidazóis, 3,4-diidroquinazolin-4-onas e 2-(quinolin-4-iloxo)acetamidas	22
2.JUSTIFICATIVA	27
3.OBJETIVOS	28
3.1 Objetivo Geral.....	28
3.2 Objetivos Específicos	28
CAPÍTULO 2 – ARTIGO CIENTÍFICO	30
CAPÍTULO 3 – CONSIDERAÇÕES FINAIS	106
REFERÊNCIAS	109
ANEXOS	114

CAPÍTULO 1

INTRODUÇÃO E OBJETIVOS

1. INTRODUÇÃO

1.1 Tuberculose

A tuberculose (TB) é uma doença infectocontagiosa, causada predominantemente pelo *Mycobacterium tuberculosis* (Mtb), que afeta principalmente os pulmões, mas pode causar doença em outros órgãos do paciente (PAI et al., 2016). A sua transmissão se dá pela difusão de aerossóis que contenham o bacilo, que quando inalados são fagocitados pelos macrófagos ou pelas células dendríticas (WORLD HEALTH ORGANIZATION, 2015).

Atualmente a Organização Mundial da Saúde (OMS) considera a TB a principal doença infectocontagiosa causada por um único agente infeccioso, estando a frente do Vírus da Imunodeficiência Humana (HIV). No ano de 2015 foram estimados pela OMS 10,4 milhões de novos casos de TB no mundo, dos quais 56% foram em homens, 34% em mulheres e 10% em crianças. Em relação à mortalidade foram estimados 1,4 milhão de mortes no ano de 2015 com um adicional de 0,4 milhão de mortes resultantes da coinfecção HIV-TB (Figura 1) (WORLD HEALTH ORGANIZATION, 2016). Apesar dos números de mortes por TB terem diminuído 22% entre os anos 2000 e 2015, a doença continua sendo uma das 10 principais causas de mortes do mundo em 2015, com a persistência de lacunas entre diagnóstico e tratamento (WORLD HEALTH ORGANIZATION, 2016).

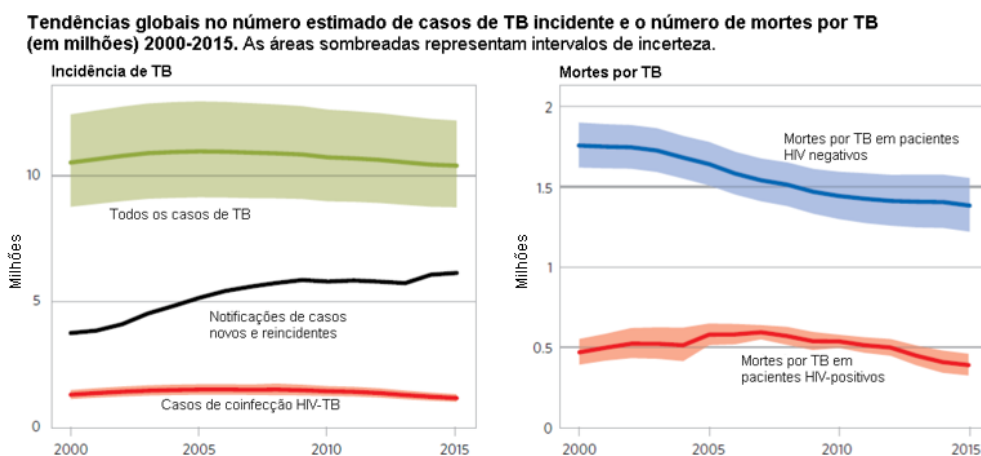


Figura 1. Tendências globais no número estimado de casos de TB incidente e o número de casos de mortes por TB entre os anos de 2000 - 2015. Adaptado de WHO, 2016

O número de casos de TB continua aumentando e todos os países ao redor do mundo registram casos da doença, sendo a África a região com maior registro de casos e óbitos (Figura 2) (WORLD HEALTH ORGANIZATION, 2016). O perfil de ampla distribuição da doença e o sucessivo aumento no número de casos é atribuído às estratégias de tratamento atuais, as quais são recomendadas pela OMS, e ao precário sistema de saúde, principalmente dos países menos favorecidos (KOUL et al., 2011).

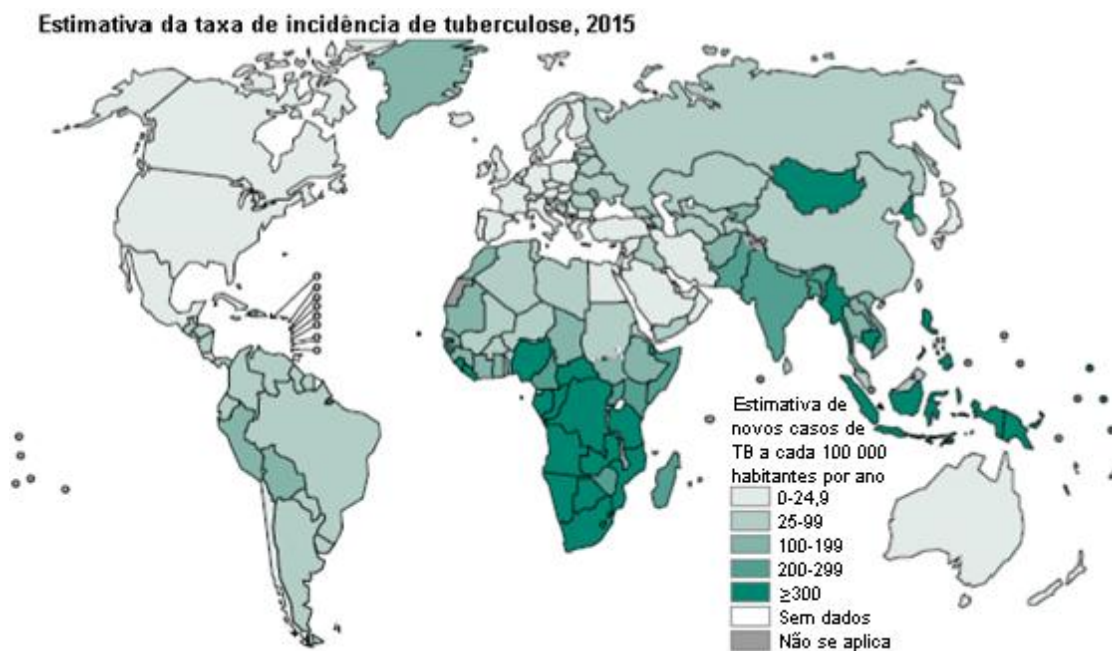


Figura 2. Estimativa de novos casos de TB (todas as formas) a cada 100.000 habitantes no ano de 2015. Adaptado de WHO, 2016

Em relação ao Brasil, a OMS estimou no ano de 2015, 84 mil casos e 5,5 mil mortes por TB. Em relação a indivíduos que convivem com a coinfecção HIV-TB foram estimados 13 mil casos e 2,2 mil mortes no mesmo ano (WORLD HEALTH ORGANIZATION, 2016). Se tratando do estado do Rio Grande do Sul (RS), a incidência de casos notificados de TB no ano de 2016 foi de 1.422 casos, sendo 330 destes casos notificados como pacientes HIV positivos (BRASIL, 2017).

1.2 Patogenia e diagnóstico

A tuberculose pulmonar é a forma mais comum da doença, ainda que o Mtb consiga infectar outros órgãos (FLYNN; CHAN, 2001; KAUFMANN, 2001).

Normalmente o sistema imune do paciente é capaz de conter, mas não de erradicar o patógeno. Dessa maneira, a TB ativa é encontrada em uma pequena porcentagem de pacientes que possuem sistema imune debilitado e, nos outros muitos casos, esses pacientes são assintomáticos e portadores da doença na forma não infecciosa. A TB no estado de latência oferece uma maior sobrevida ao paciente, contudo a reativação da infecção pode ocorrer em resposta a perturbações do sistema imune do paciente, como ocorre na infecção por HIV, tratamento com corticosteroides, idade avançada, abuso de drogas ou álcool (FLYNN; CHAN, 2001). Dessa forma a preocupação em relação à TB é aumentada em pacientes portadores do vírus HIV, uma vez que esses têm diminuição da atividade do sistema imune, levando então a uma maior manifestação da doença (KOUL et al., 2011; WORLD HEALTH ORGANIZATION, 2015).

Após o Mtb ser internalizado pelo sistema respiratório do paciente, ele é fagocitado pelos macrófagos, mas não é combatido, células T específicas são estimuladas para induzir a formação de granulomas (Figura 3), os quais são definidos como agregados de células do sistema imune juntamente com o Mtb, que não são eficientes em erradicar a infecção. Quando a doença está na fase ativa, o bacilo se replica, causando danos, necrose e a formação de cavitações no tecido pulmonar. Por outro lado, em pacientes que se encontram na fase latente da doença não há a replicação do bacilo e dessa forma, não há sintomas clínicos (FLYNN; CHAN, 2001; KAUFMANN, 2001).

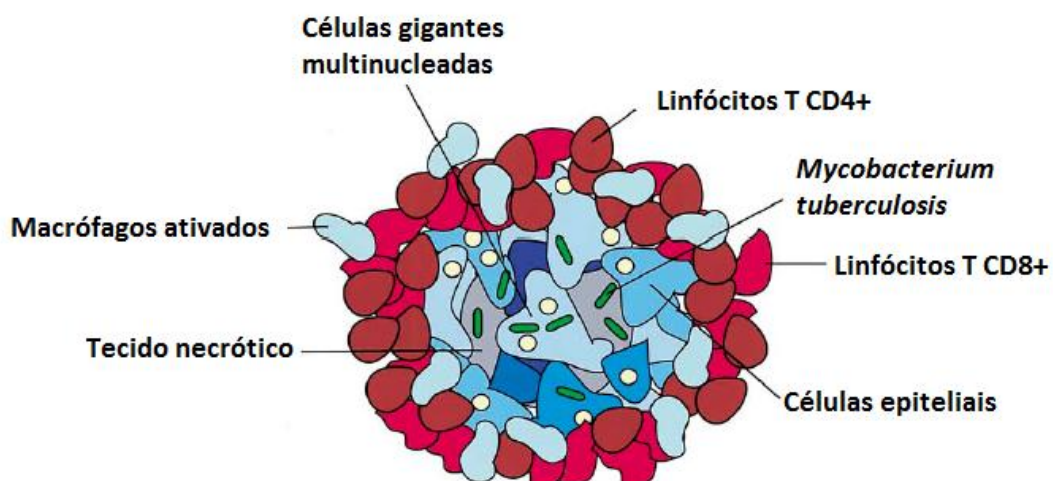


Figura 3. Composição do granuloma maduro. Adaptado de ZAHRT, 2003.

O diagnóstico do paciente com suspeita de TB é considerado positivo quando o mesmo possui o exame bacteriológico confirmado, cultura ou bacilosscopia positivos. Além disso, o diagnóstico deve ser baseado em dados clínico-epidemiológicos e em resultados de exames complementares (BRASIL, 2012). Os pacientes diagnosticados que estão infectados com a TB na forma latente, também denominada dormente, não manifestam sintomas, já que o Mtb se encontra em estado metabólico não ativo devido a diversos fatores de estresse das células hospedeiras, como a hipoxia. Em contraponto, se o paciente apresentar a forma ativa da doença, sintomas clínicos como tosse, febre, cansaço e emagrecimento serão manifestados em até um ano, caracterizando a forma primária da doença (YOUNG; STARK; KIRSCHNER, 2008; KOUL et al., 2011).

1.3 Tratamento e resistência aos fármacos

Atualmente, o tratamento da tuberculose é realizado de acordo com as recomendações da OMS, conhecido como DOTS (do inglês, *Directly Observed Treatment Short Course*), que consiste em uma fase inicial de 2 meses com a administração de isoniazida (INH), rifampicina (RIF), pirazinamida (PZA) e etambutol (ETB), seguida por uma fase de 4 meses com a continuação dos fármacos INH e RIF (RAMASWAMY; MUSSER, 1998; WORLD HEALTH ORGANIZATION, 2003; KOUL et al., 2011). É descrito que esse tratamento pode curar até 95% dos casos de tuberculose (KOUL et al., 2011), além de ser efetivo contra subpopulações da bactéria, sendo elas: 1) as bactérias ativas, as quais são suscetíveis à INH; 2) bactérias de crescimento acelerado, que são atacadas pela RIF e; 3) os bacilos de baixo estado metabólico, suscetíveis à PZA. No entanto, não há nenhum fármaco entre os preconizados para o tratamento que seja ativo contra os bacilos em estado dormente (CHAN; ISEMAN, 2002; DOVER; COXON, 2011; RAWAL; BUTANI, 2016). Muito além do tratamento, o DOTS prevê também outras estratégias de saúde contra a TB, sendo elas: o estabelecimento de indivíduos treinados para administração e supervisão do DOTS, laboratórios e indivíduos treinados para o diagnóstico, implementação de um sistema confiável e efetivo de distribuição dos medicamentos, compromisso

governamental e acompanhamento dos resultados (WORLD HEALTH ORGANIZATION, 2003; YEW; LEUNG, 2008).

Embora as estratégias propostas pela OMS tenham apresentado resultados significativos, o número de casos de cepas resistentes aos fármacos de primeira escolha continua crescendo, podendo estar relacionado à falha no tratamento e/ou à falta de adesão dos pacientes (RAMASWAMY; MUSSER, 1998; ELSTON; THAKER, 2008; MA et al., 2010; WORLD HEALTH ORGANIZATION, 2015; RAWAL; BUTANI, 2016).

A resistência aos fármacos é caracterizada por uma mutação genética que altera a suscetibilidade dos microrganismos, e no caso do Mtb, a resistência surge com a seleção de cepas que possuem resistência inata a agentes individuais seguida da exposição aos fármacos que o Mtb não apresenta suscetibilidade (DORMAN; CHAISSON, 2007). Alguns mecanismos de resistência aos antimicobacterianos já são conhecidos e as rotas metabólicas que o bacilo utiliza para impedir a ação dos fármacos utilizados na clínica têm sido elucidadas (Tabela 1).

Tabela 1. Mecanismo de resistência aos principais fármacos de escolha (adaptado de HOAGLAND et al., 2016).

Fármaco	Mecanismo de ação	Mecanismo comum de resistência
Rifampicina	Inibição da síntese de DNA.	Mutação no gene <i>rpoB</i> induz uma mudança conformacional da RNA polimerase, diminuindo a afinidade de ligação do fármaco.
Isoniazida	Inibição da síntese dos ácidos micólicos	Supressão de KatG diminui a ativação do fármaco (pró-droga) e a mutação no promotor da <i>InhA</i> causa uma superexpressão da enzima.

Pirazinamida	Não é totalmente resolvido, mas inclui reduz a conversão à ruptura de membrana	Mutações no gene <i>pncA</i> reduz a conversão à forma ativa.
Etambutol	Inibição da biossíntese de aracnogalactano.	Mutações no gene <i>embB</i> no códon <i>embB306</i> .
Fluoroquinolonas	Inibidores da DNA girase e topoisomerase IV.	Mutações no gene <i>rpsL</i> conferem modulação do sítio de ligação. Mutações no gene <i>gyrA</i> e <i>gyrB</i> conferem mutações nos sítios de ligação das DNA girase A e B.

As cepas resistentes são definidas como: (a) resistente aos múltiplos fármacos (MDR-TB), onde o bacilo se torna resistente à, pelo menos, INH e RIF, principais fármacos de primeira linha; (b) extensivamente resistente aos fármacos (XDR-TB), quando é observada uma resistência à INH e RIF juntamente com alguma fluoroquinolona e algum dos fármacos anti-TB injetáveis de segunda linha (KOUL et al., 2011; PALOMINO; MARTIN, 2013; RAWAL; BUTANI, 2016) e; (c) resistentes a todos os fármacos (TDR-TB), onde a cepa de Mtb é resistente a todos os fármacos utilizados para o tratamento (VELAYATI et al., 2009).

Considerando as circunstâncias atuais, onde os casos de resistências têm aumentado a cada ano, torna-se necessário o desenvolvimento de novos fármacos para o tratamento da TB. Dessa forma, busca-se novos tratamentos de custos reduzidos, desprovido ou com menores efeitos adversos e com maior efetividade contra às cepas MDR-TB, XDR-TB e TDR-TB (ZAHRT, 2003; JASSAL; BISHAI, 2009).

1.4 Fármacos em desenvolvimento contra a tuberculose

Após mais de 50 anos sem descobertas de fármacos novos contra a tuberculose, o que demonstra o quanto defasado vem sendo o desenvolvimento de alternativas terapêuticas contra a doença, o cenário começou a mudar (HOAGLAND et al., 2016). Os novos candidatos ao tratamento da doença têm sido planejados visando um mecanismo de ação capaz de atuar sobre cepas resistentes, apresentando uma rápida ação bactericida para diminuir o tempo de tratamento, farmacocinética e farmacodinâmica otimizadas para obtenção de menor número de administrações diárias, um baixo potencial para interações medicamentosas e um bom perfil de segurança para que possa ser administrado em gestantes e crianças (HOAGLAND et al., 2016; WALLIS et al., 2016).

Recentemente, alguns fármacos estão sendo testados em fases clínicas, dentre eles os principais são a bedaquilina e a delamanida, compostos que se encontram em ensaios clínicos de fase 3. Ambos os fármacos receberam aprovação acelerada baseada em ensaios clínicos de fase 2 e têm sido utilizados para o tratamento de infecções causadas por cepas de *Mtb* resistentes aos fármacos disponibilizados na clínica (WALLIS et al., 2016).

A bedaquilina foi desenvolvida pela Janssen Pharmaceuticals da Bélgica (Figura 4a). Originalmente chamada de TMC207, é uma diarilquinolina de peso molecular 555,51 Da que teve sua estrutura completamente elucidada em uma combinação de estudos de ressonância magnética nuclear (RMN), modelagem molecular e difração de raios-X (ANDRIES et al., 2005; GAURRAND et al., 2006; PETIT et al., 2007; PALOMINO; MARTIN, 2013).

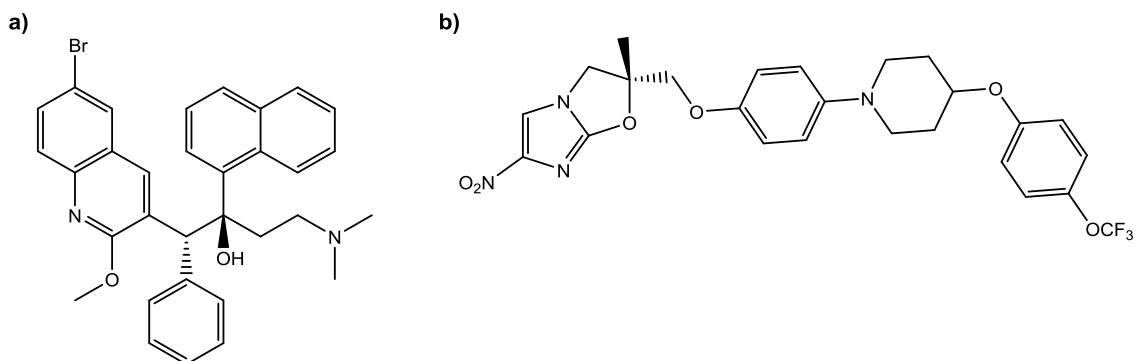


Figura 4. Estrutura química da bedaquilina (a) da delamanida (b).

O modo de ação da bedaquilina é a inibição de maneira específica e seletiva da atividade da enzima ATP sintase, tanto no *Mtb* ativo quanto em cepas

com fenótipo dormente. Além disso, o fármaco exerce efeito inibitório contra cepas MDR-TB (ANDRIES et al., 2005; PALOMINO; MARTIN, 2013; HOAGLAND et al., 2016). O fármaco é ativo principalmente contra espécies de *Mycobacterium*, com uma concentração inibitória mínima (CIM) de 0,03-0,12 µg/mL em relação à cepa laboratorial H37Rv de *Mtb* e outras seis cepas suscetíveis. Valores semelhantes foram encontrados quando foi realizada a CIM contra cepas resistentes à RIF, INH, ETB, PZA, estreptomicina ou moxifloxacino (ANDRIES et al., 2005; HUITRIC et al., 2010; PALOMINO; MARTIN, 2013).

Em relação ao perfil de segurança, pacientes tratados com bedaquilina nos ensaios clínicos apresentaram alguns efeitos adversos tais como: náusea, artralgia, dores de cabeça, hiperuricemia, vômito, mialgia, aumento das transaminases e aumento do intervalo QT no Eco cardiograma (CENTERS FOR DISEASE CONTROL AND PREVENTION, 2013).

A bedaquilina foi aprovada como fármaco que pode ser adicionado ao regime de tratamento para MDR-TB, desde que alguns critérios e recomendações sejam seguidos: (a) o regime de tratamento que contém quatro fármacos de segunda linha e PZA não pode ser seguido; (b) A cepa MDR-TB apresenta resistência a alguma fluoroquinolona adicional; (c) o paciente deve ser informado do processo de decisão; (d) deve-se manter o uso cauteloso em pacientes com HIV, com alguma comorbidade ou abuso de álcool; (e) utilizar por no máximo 6 meses, em uma dose recomendada de 400 mg por dia nas primeiras duas semanas e, posteriormente, 200 mg três vezes ao dia; (f) não adicionar a bedaquilina sozinha ao tratamento; (g) testes e monitoramento do intervalo QT e arritmias devem ser realizados; (h) deve ser realizado o monitoramento e manejo das comorbidades; (i) deve-se manter uma farmacovigilância ativa; (j) a suscetibilidade à bedaquilina deve ser monitorada por CIM, assim como a suscetibilidade a outros fármacos (CENTERS FOR DISEASE CONTROL AND PREVENTION, 2013).

Outro antimicobacteriano promissor é a delamanida, um nitroimidazol de nome químico (2*R*)-2-metil-6-nitro-2-[4-{4-[4-(trifluorometoxi)fenoxy]-1-piperidinil}fenoxy]metil]-2,3-diidroimidazol[2,1-*b*][1,3]oxazol (Figura 4b), primeiramente conhecido como OPC-67683 e fabricado pelo nome de Deltyba™ pela indústria Otsuka Pharmaceutical Co., Ltd (Tóquio, Japão) (SZUMOWSK; LYNCH, 2015).

O mecanismo de ação deste fármaco ainda não é bem descrito, mas acredita-se que envolva a inibição da síntese de ácidos micólicos, essenciais para a formação da parede celular do Mtb (MATSUMOTO et al., 2006; PALOMINO; MARTIN, 2013; SZUMOWSK; LYNCH, 2015). Alguns parâmetros relacionados com a farmacocinética do composto têm sido descritos, como: (a) baixa solubilidade aquosa; (b) absorção aumentada quando administrado com alimentos; (c) biodisponibilidade desconhecida, mas estimada entre 25% e 47%; (d) mais do que 99% de ligação às proteínas plasmáticas, principalmente albumina; (e) alto volume de distribuição; (f) meia vida de 30-38 horas (EUROPEAN MEDICINES AGENCY, 2013; SZUMOWSK; LYNCH, 2015).

Ensaios *in vitro* realizados não demonstraram possíveis interações com os fármacos de primeira linha contra a TB (INH, RIF, etambutol ou estreptomicina) e poucos dados são encontrados em relação às possíveis interações com antirretrovirais, contudo é reportada a não significância de efeitos com tenofovir, lopinavir-ritonavir ou efavirenz (EUROPEAN MEDICINES AGENCY, 2013; SZUMOWSK; LYNCH, 2015).

Em relação à toxicidade, os ensaios clínicos realizados relataram náusea, vômito e tontura como sendo os efeitos adversos mais comuns. A análise do risco de aumento do prolongamento QT nos pacientes tratados com delamanida parece estar relacionado com hipoalbuminemia (EUROPEAN MEDICINES AGENCY, 2013).

As recomendações de uso da delamanida para tratar infecções causadas por MDR-TB, segundo a OMS, são: (a) dose de 100 mg por seis meses; (b) pacientes que possuem intolerância ou resistência às fluoroquinolonas ou fármacos injetáveis de segunda linha, bem como paciente com XDR-TB; (c) exclusão dos pacientes com prolongamento QT; (d) a delamanida nunca deve ser administrada sozinha; (e) as recomendações descritas incluem HIV positivos; (f) cuidado extremos em pacientes grávidas, amamentando, crianças ou com MDR-TB extrapulmonar, visto que há poucos ou nenhum estudo sobre o efeito do fármaco nessas populações; (g) o uso para pacientes com MDR-TB extrapulmonar deve ser realizado considerando os estudos para MDR-TB pulmonar. Além disso, para que o paciente seja incluído nas recomendações, ele deve ter mais do que 18 anos e cuidados especiais são exigidos para pacientes com mais de 65 anos (WORLD HEALTH ORGANIZATION, 2014).

Já foi relatado o primeiro caso de infecção por cepa MDR-TB tratada com a combinação de bedaquilina e delamanida. O caso foi documentado no hospital Delek, em Dharamshala, Índia. A paciente (mulher, 39 anos, 4 casos prévios de TB) apresentou aumento no intervalo QT e a administração de bedaquilina teve de ser interrompida. Entretanto, foi observada a conversão do escarro da paciente com resultado negativo para o Mtb na bacilosscopia (TADOLINI et al., 2016).

Assim, considerando o surgimento de cepas de Mtb resistentes aos fármacos disponíveis, o tratamento longo com os fármacos disponibilizados na clínica que ocasiona baixa adesão, a incapacidade dos tratamentos existentes de combater as cepas em estado latente e as interações medicamentosas entre os fármacos de primeira escolha com o tratamento antirretroviral, há uma proeminente necessidade de desenvolvimento de fármacos novos, idealmente, com mecanismos de ação inovadores.

1.5 Hibridação molecular

Hibridação molecular (HM) é uma estratégia clássica em química medicinal para o desenvolvimento de compostos ativos novos. A premissa é que a reunião de partes estruturais com função farmacofórica provenientes de estruturas distintas podem produzir estruturas químicas novas com atividade otimizada (VIEGAS-JUNIOR et al., 2007). A junção dessas estruturas pode se basear na junção de dois fármacos distintos (HM do tipo fármaco-fármaco) ou dos grupos farmacofóricos de fármacos distintos (HM do tipo farmacofórica), como é exemplificado na Figura 5. Em ambos os casos, o composto novo obtido é chamado de híbrido e se espera que apresente atividade farmacológica similar ou melhorada quando comparado às estruturas que lhe deram origem (NEPALI et al., 2014).

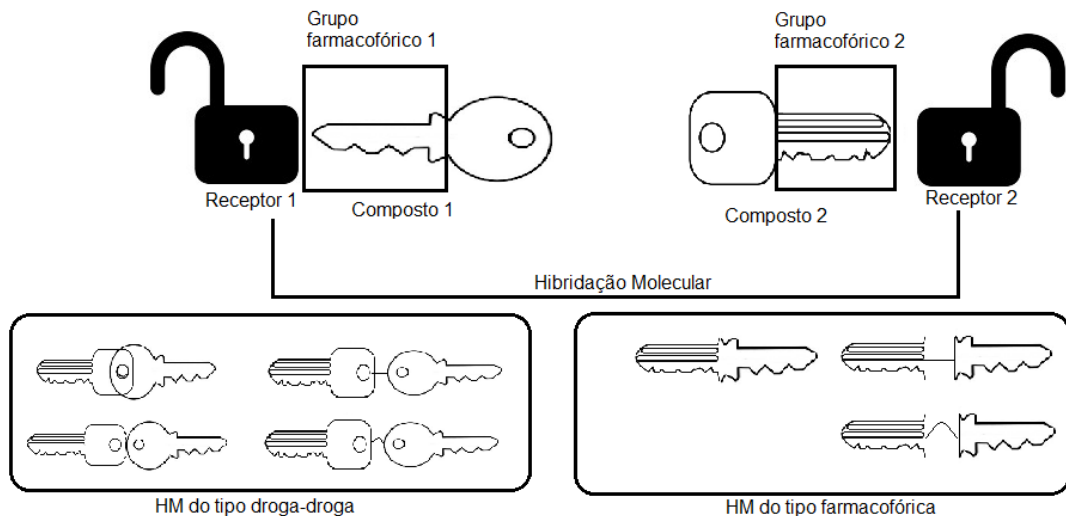


Figura 5. Tipos de hibridação molecular. Adaptado de NEPALI et al., 2014.

A realização de hibridação molecular visa alcançar alguns dos seguintes objetivos: (a) sinergismo de ação farmacológica; (b) terapia de dupla ação farmacológica ou (c) modulação de efeitos indesejáveis.

Por meio desse processo, pode-se obter uma grande biblioteca de compostos químicos obtidos por diferentes combinações de fármacos ou de grupamentos farmacofóricos e, dessa forma, pode-se criar estruturas químicas otimizadas com efeitos farmacológicos pronunciados em menor tempo (VIEGAS-JUNIOR et al., 2007).

1.6 1*H*-Benzo[*d*]imidazóis, 3,4-diidroquinazolin-4-onas, e 2-(quinolin-4-iloxi)acetamidas

O sulfeto de lansoprazol (LPZS), metabólito do fármaco lansoprazol (LPZ) é apontado como uma estrutura promissora para inibição de cepas de Mtb. As estruturas químicas do lansoprazol e de seu metabólito reduzido contém o anel heterocíclico 1*H*-benzo[*d*]imidazol em sua constituição (Figura 6). O LPZ é um fármaco já aprovado pelo FDA para o tratamento de úlceras gastrointestinais e suas complicações, que age como inibidor da bomba de prótons reduzindo a secreção do ácido gástrico da membrana celular das células parietais do estômago. Recentemente, tem sido descrito que o LPZ atua como um pró-fármaco ativo contra cepas Mtb em modelos *in vitro* e *in vivo* (RYBNIKER et al., 2015).

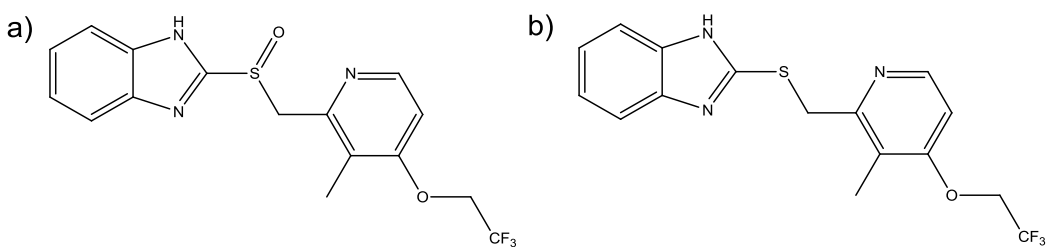


Figura 6. Estrutura química do lansoprazol (LPZ) (a) e do sulfeto de lansoprazol (LPZS) (b).

Rybniker e colaboradores testaram um painel de fármacos, já aprovados pelo FDA, contra o Mtb em um modelo de infecção intracelular. Nestes ensaios o LPZ foi o fármaco que mais se destacou. Após os resultados promissores a atividade foi verificada em meio líquido, contudo o fármaco não demonstrou atividade, indicando que ele possivelmente agiria como um pró-fármaco ativado intracelularmente. Posteriormente, analisando os metabólitos intracelulares utilizando espectrometria de massas foi verificado quantidades elevadas do metabólito LPZS (Figura 6). Em ensaios contra a micobactéria intracelular e em meio líquido o LPZS se mostrou altamente efetivo com IC₅₀ de 0,59 μM e IC₅₀ de 0,46 μM, respectivamente. A seletividade contra o bacilo foi determinada utilizando cepas bacterianas Gram positivas e Gram negativas e não foram constatadas quaisquer atividades nas maiores concentrações testadas. Em estudos utilizando o sequenciamento completo do genoma de cepas resistentes ao LPZS foi encontrada uma mutação em um único nucleotídeo (leucina – 176 para prolina) na subunidade *b* do complexo do citocromo *bc*₁. Dessa maneira, nas cepas tratadas com LPZS se observa uma rápida e massiva depleção de ATP e uma razão ADP/ATP elevada, indicando que este seria realmente o alvo do composto (RYBNIKER et al., 2015). Observando os resultados descritos no estudo de Rybniker e seus colaboradores, o composto LPZS pode ser uma estrutura promissora para estudos de hibridação molecular.

Outro composto identificado como promissor contém o núcleo quinazolinônico. Esses compostos são heterocíclicos com dois anéis geminados, ou seja, contendo dois átomos de carbono compartilhados por ambos os anéis, um anel é o benzeno e o outro ciclo contém dois átomos de nitrogênio e um carbono oxidado na forma de grupamento cetona (Figura 7). Essa classe é

amplamente encontrada em alcaloides naturais (KSHIRSAGAR, 2015), além de representar muitas moléculas sintéticas reportadas com propriedades anticâncer, diuréticas, anti-inflamatórias, anticonvulsivantes, anti-hipertensivas e antimicrobianas (ASIF, 2014; JAFARI et al., 2016).

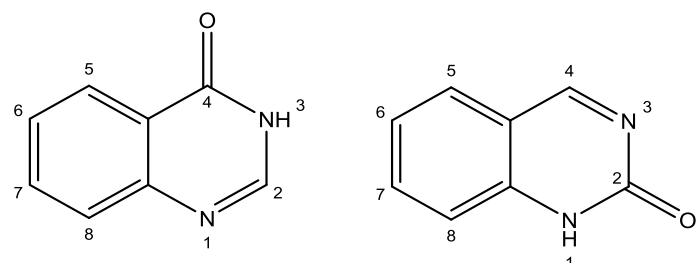


Figura 7. Estruturas químicas dos principais isômeros quinazolinônicos e sua numeração.

O efeito antimicrobiano desses heterocíclicos tem sido estudado e a relação da estrutura química com atividade biológica delineada (JAFARI et al., 2016). Jafari e colaboradores realizaram a determinação da relação estrutura atividade (REA) para esta classe de antimicrobianos e apresentaram que substituições na posição 2 e 3, um átomo de halogênio nas posições 6 ou 8 e um grupamento amínico na posição 4 aumentam a atividade antimicrobiana da molécula. Por outro lado, substituições na posição 3 do anel aromático e um grupamento metil, aminínico ou tiol na posição 2 são essenciais para a atividade antimicrobiana (DEVI; SARANGAPANI; SRIRAM, 2012; DAVE et al., 2012; EL-BADRY; ANTER; EL-SHESHTAWY, 2012; ZAYED; GHORAB et al., 2013; HASSAN, 2014; JAFARI et al., 2016).

As quinazolinonas também vêm sendo estudadas como inibidores do crescimento do Mtb *in vitro* e da enzima 2-*trans*-enoil-ACP redutase (InhA) de Mtb (PEDGAONKAR et al., 2014). Pedgaonkar e colaboradores sintetizaram 28 compostos (Figura 8) e os testaram frente a cepas sensíveis e resistentes de Mtb. Também foram realizados testes de citotoxicidade, bem como inibição e docagem molecular da enzima InhA.

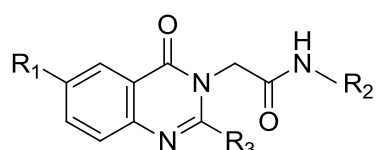


Figura 8. Estrutura química das moléculas sintetizadas por PEDGAONKAR et al., 2014.

Dentre a biblioteca química sintetizada, o composto 21 (onde R₁ = cloro; R₂ = fenila e; R₃ = metil) foi identificado como o mais promissor da série com valores de CIM de 4,76 µM e 19,06 µM frente a cepa sensível de Mtb e XDR-TB, respectivamente. Este derivado inibiu a atividade enzimática da InhA em 88% na concentração de 10 µM com valor de IC₅₀ = 3,12 µM. Favoravelmente, a análise *in silico* do perfil de interação molecular no sítio ativo mostrou que essa molécula estabelece duas ligações de hidrogênio, sendo uma com a cadeia lateral do resíduo tirosina 158 e a outra com o grupamento hidroxila da ribose do substrato NAD⁺. Além disso, frente à linhagem celular RAW 264,7 o composto não apresentou citotoxicidade na concentração de 100 µM (PEDGAONKAR et al., 2014). Dessa forma, os compostos contendo o núcleo 3,4-diidroquinazolin-4-ona se mostram como uma alternativa na investigação de novas moléculas ativas contra o Mtb.

O nosso grupo de pesquisa tem se dedicado ao desenvolvimento de novos compostos anti-TB utilizando estratégias baseadas em alvos moleculares e a partir da otimização estrutural de compostos químicos obtidos em triagens fenotípicas. Recentemente, utilizando a estrutura GSK358607A (BALLELL et al., 2013) como ponto de partida para subsequentes derivatizações químicas, foi obtida uma série de 2-(quinolin-4-iloxi)acetamidas (Figura 9) que, apesar da baixa solubilidade aquosa, apresentaram CIM na faixa submicromolar (0,8-0,05 µM). O composto mais promissor obtido foi o composto 5s, com CIM de 0,05 µM. Nesta estrutura, os grupos 2-metil, 6-metóxi e arilacetamida foram descritos como grupos farmacofóricos da molécula. Importante destacar que nas mesmas condições experimentais a isoniazida apresentou resultados de CIM de 1,46 µM. Além disso, o composto foi capaz de inibir cepas resistentes provenientes de isolados clínicos resistentes à isoniazida e, quando testada em células Vero e HaCat (20 µM), não apresentou citotoxicidade aparente (PISSINATE et al., 2016). Recentemente, utilizando cepas de Mtb contendo modificações no gene *qcrB*, tem sido sugerido que alvo molecular das 2-(quinolin-4-iloxi)acetamidas é o complexo menaquinol citocromo c oxidoreductase (*bc₁*) o qual tem sido descrito como um componente essencial da cadeia respiratória bacteriana. Além disso,

a atividade dos compostos desta classe contra cepa *knock-out* para o citocromo *bd* oxidase tem corroborado com esta possibilidade (PHUMMARIN et al., 2016).

Considerando os dados apresentados, a proposta para o desenvolvimento de novos compostos nesse trabalho foi a realização da hibridação molecular utilizando substituintes conhecidos provenientes dos compostos 2-(quinolin-4-iloxi)acetamidas (1) juntamente com os núcleos 1*H*-benzo[*d*]imidazol (2) ou 3,4-diidroquinazolin-4-onas (3) (Figura 9). Foram realizadas modificações estruturais trazendo a função acetamida presente no composto 5s (PISSINATE et al., 2016). A utilização dessa estratégia de desenvolvimento de moléculas novas visava obter compostos menos lipossolúveis, uma vez que os núcleos 3,4-diidroquinazolin-4-onas e 2-tio-1*H*-benzo[*d*]imidazol apresentam menor lipossolubilidade do que o núcleo quinolínico.

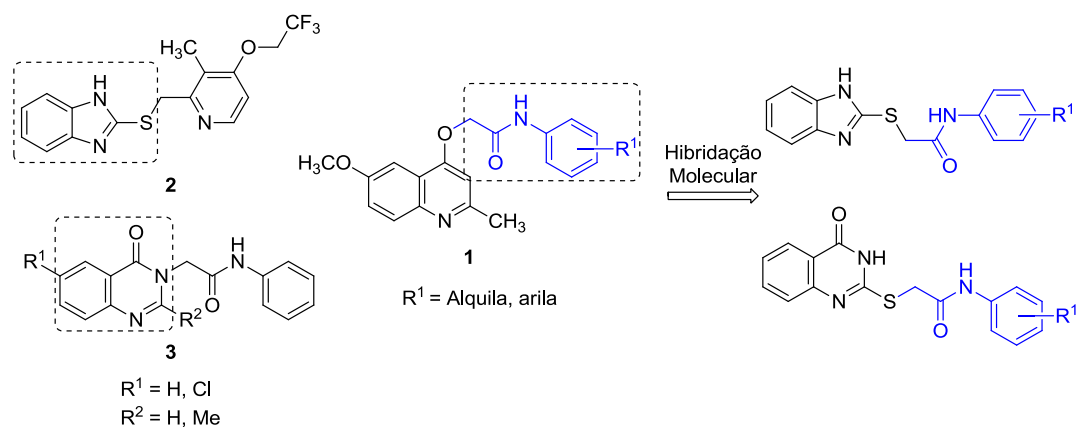


Figura 9. Hibridação molecular utilizando substituintes *N*-substituídas- α -bromoacetamidas provenientes dos compostos 2-(quinolin-4-iloxi)acetamidas com núcleos 1*H*-benzo[*d*]imidazóis e 3,4-diidroquinazolin-4-onas.

2. JUSTIFICATIVA

É notável a necessidade de desenvolvimento de novas moléculas para o tratamento da tuberculose, tendo em vista a alta taxa de incidência, mortalidade e a resistência aos fármacos de primeira escolha (WORLD HEALTH ORGANIZATION, 2016). Contudo as indústrias farmacêuticas acabam se afastando desse campo de estudo devido às condições geográficas e econômicas dos acometidos pela doença. Além disso, existe um alto custo ligado ao desenvolvimento de fármacos novos, o que acaba por influenciar que grupos de pesquisa presentes em instituições de ensino desenvolvam pesquisas nessa área.

Nosso grupo de pesquisa já vem trabalhando com o desenvolvimento de fármacos novos contra a tuberculose, obtendo alguns resultados promissores com a classe das 2-(quinolin-4-iloxi)acetamidas (PISSINATE et al., 2016; GIACOBBO et al., 2017). Assim, incorporar o conhecimento já obtido com pesquisas anteriores a novos estudos parece ser uma estratégia interessante para incrementar a procura por moléculas novas candidatas a fármacos contra a TB. Nesse contexto, aliar os núcleos heterocíclicos 3,4-diidroquinazolin-4-ona e $1H$ -benzo[*d*]imidazol a dois grupos farmacofóricos das 2-(quinolin-4-iloxi)acetamidas poderá gerar novos compostos com ação antimicobacteriana mais pronunciada e propriedades físico-químicas otimizadas.

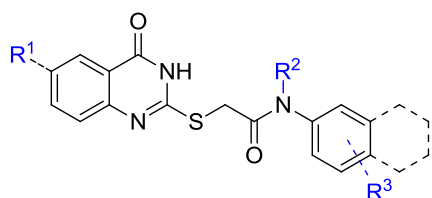
3. OBJETIVOS

3.1 Objetivo Geral

Desenvolver uma nova série de compostos químicos híbridos contendo os núcleos 3,4-diidroquinazolin-4-ona e 1*H*-benzo[*d*]imidazol, caracterizar estruturalmente essas novas moléculas e determinar sua capacidade de inibir o crescimento do *Mycobacterium tuberculosis* *in vitro*.

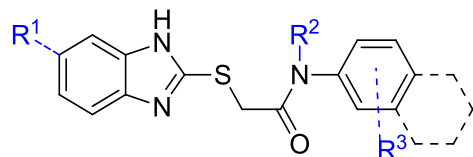
3.2 Objetivos Específicos

- a) Sintetizar uma série de moléculas híbridas contendo o núcleo 3,4-diidroquinazolin-4-ona.



Onde $R^1 = H$, $R^2 = \text{arilas ou alquilas substituídas}$ e $R^3 = \text{arilas, alquilas, halogênios ou naftilas}$.

- b) Sintetizar uma série de moléculas híbridas contendo o núcleo 1*H*-benzo[*d*]imidazol.



Onde $R^1 = H$, $R^2 = \text{arilas ou alquilas substituídas}$ e $R^3 = \text{arilas, alquilas, halogênios ou naftilas}$.

- c) Caracterizar estruturalmente os compostos sintetizados utilizando técnicas de ressonância magnética nuclear (RMN) de ^1H e ^{13}C , espectrometria de massas de alta resolução (HRMS) e infravermelho (FTIR), ponto de fusão (PF) e pureza, sendo a última realizada por cromatografia líquida de alta eficiência (CLAE).
- d) Determinar a concentração inibitória mínima (CIM) em relação à cepa laboratorial H37Rv de *Mycobacterium tuberculosis*.
- e) Determinar a concentração inibitória mínima em relação a cepas de *Mycobacterium tuberculosis* resistente aos fármacos de primeira linha e/ou segunda linha.

- f) Avaliar o efeito citotóxico dos compostos sintetizados em diferentes linhagens celulares (Vero, HaCat, RAW 293).
- g) Realizar estudos de relação estrutura-atividade (REA) dos compostos sintetizados.
- h) Realizar estudos de citotoxicidade *in vivo* utilizando modelo animal de *Zebrafish* (*Danio rerio*).
- i) Avaliar a estabilidade dos compostos sintetizados a 25 °C e 37 °C.

CAPÍTULO 2

ARTIGO CIENTÍFICO

Manuscrito submetido para publicação no periódico internacional *European Journal of Medicinal Chemistry.* (F.I. 4,519)

1*H*-Benzo[*d*]imidazoles and 3,4-dihydroquinazolin-4-ones: design, synthesis and antitubercular activity

Fernanda Souza Macchi^{a,b}, Kenia Pissinate^a, Anne Drumond Villela^a, Bruno Lopes Abbadi^{a,b}, Valnês Rodrigues-Junior^a, Débora Dreher Nabinger^{b,d}, Stefani Altenhofen^{b,d}, Nathalia Sperotto^{a,c}, Adílio da Silva Dadda^{a,b}, Fernanda Teixeira Subtil^{a,b}, Talita Freitas de Freitas^a, Ana Paula Erhart Rauber^a, Ana Flávia Borsoi^a, Carla Denise Bonan^{b,c,d}, Cristiano Valim Bizarro^{a,b}, Luiz Augusto Basso^{a,b,c}, Diógenes Santiago Santos^{a,b}, Pablo Machado^{a,b,*}

^aInstituto Nacional de Ciência e Tecnologia em Tuberculose, Centro de Pesquisas em Biologia Molecular e Funcional, Pontifícia Universidade Católica do Rio Grande do Sul, 90616-900, Porto Alegre, Rio Grande do Sul, Brazil

^bPrograma de Pós-Graduação em Biologia Celular e Molecular, Pontifícia Universidade Católica do Rio Grande do Sul, 90616-900, Porto Alegre, Rio Grande do Sul, Brazil

^cPrograma de Pós-Graduação em Medicina e Ciências da Saúde, Pontifícia Universidade Católica do Rio Grande do Sul, 90616-900, Porto Alegre, Rio Grande do Sul, Brazil

^dLaboratório de Neuroquímica e Psicofarmacologia, Pontifícia Universidade Católica do Rio Grande do Sul, 90616-900, Porto Alegre, Rio Grande do Sul, Brazil

*Corresponding author.

E-mail address: pablo.machado@pucrs.br (Pablo Machado)

Abstract

Using a classical hybridization approach, a series of 1*H*-benzo[*d*]imidazoles and 3,4-dihydroquinazolin-4-ones were synthesized and evaluated as inhibitors of *Mycobacterium tuberculosis* growth. Chemical modification studies yielded potent antitubercular agents with minimum inhibitory concentration (MIC) values in the submicromolar range. Further, the synthesized compounds were active against drug-resistant strains and were devoid of apparent toxicity to HepG2, HaCat, and Vero cells. Viability in mammalian cell cultures was evaluated using MTT and neutral red assays. In addition, some 3,4-dihydroquinazolin-4-ones showed low risk of cardiac toxicity, no signals of neurotoxicity or morphological alteration in zebrafish (*Danio rerio*) toxicity models. Taken together, these data indicate that this class of molecules may furnish candidates for future development of novel anti-TB drugs.

Keywords: *Mycobacterium tuberculosis*, tuberculosis, molecular hybridization, drug-resistant strains, SAR, cardiotoxicity.

1. Introduction

Human tuberculosis (TB) is an infectious disease caused mainly by *Mycobacterium tuberculosis* (Mtb), and has been responsible for the deaths of thousands of people annually [1]. Only in 2015, 9.6 million new cases of the disease and 1.8 million deaths were reported by the World Health Organization (WHO) worldwide [2]. The emergence of multidrug-resistant TB (MDR-TB) and extensively drug-resistant TB (XDR-TB), HIV coinfection, and the elevated number of individuals infected with latent or dormant bacilli have contributed to complicate this scenario [1, 2]. The recommended treatment includes two months of isoniazid (INH), rifampicin (RIF), ethambutol (ETH) and pyrazinamide (PZA), followed by four more months of INH and RIF [3, 4]. Although it has a cure rate of up to 95%, the regime suffers with increasing number of cases of individuals infected with drug-resistant strains [3]. In these cases, the treatment can be extended and requires the use of second-line drugs that are, in general, more expensive and toxic [5]. Furthermore, the low levels of compliance with treatment, adverse effects, toxicity and impossibility of co-administration with some antiretroviral drugs have limited the use of this therapeutic strategy [6].

Within this context, there is an urgent need to obtain new therapeutic alternatives for tuberculosis treatment; if possible, with innovative mechanisms of action capable of overcoming the drug resistance concern. Although the approval of new drugs such as bedaquiline and delamanid [7] for treatment of drug-resistant TB has brought some hope, the adaptive capacity of Mtb has already led to the emergence of resistant strains for these drugs, evidencing the continued need for new options [8].

As part of our ongoing research we have studied the antimycobacterial activity of 2-quinolin-4-yloxy)acetamides **1** (**Figure 1**) and their derivatives, with some encouraging

in vitro results [9, 10]. The compounds have been active against resistant and non-resistant Mtb strains and have exhibited selective inhibition of bacillus growth. Recently, the menaquinol cytochrome c oxidoreductase (bc₁ complex) was proposed as a molecular target of this chemical class by using whole-genome sequencing [11], corroborating other findings already described in the literature [12]. In addition, SAR studies have shown that acetamide moiety is part of the molecules' pharmacophore, which is prone to be used in molecular hybridization-based approaches (**Figure 1**). In line with this purpose, 1*H*-benzo[*d*]imidazole and 3,4-dihydroquinazolin-4-one were used as molecular scaffolds to evaluate the possibility of obtaining new anti-TB drug candidates by hybridization between the titled heterocycles and acetamide group (**Figure 1**). Indeed, these scaffolds have been obtained as part of the structure of compounds endowed with selective antimycobacterial activity. Lansoprazole sulfate (**2**) (**Figure 1**), the active metabolite from the drug lanzoprazole, have presented significant activity against intracellular and in-broth cultures of Mtb with IC₅₀ of 0.59 μM and 0.46 μM, respectively [13]. Interestingly, whole-genome sequencing of resistant strains to LPZS revealed a unique nucleotide mutation in the b subunit of bc₁ cytochrome [13]. 3,4-Dihydroquinazolin-4-ones **3** have also been described as *in vitro* inhibitors of Mtb growth with Minimal Inhibitory Concentration (MIC) as low as 4.76 μM (**Figure 1**). These compounds were described to inhibit the *Mycobacterium tuberculosis* enoyl acyl carrier protein reductase, a validated molecular target for TB drug development [14].

Therefore, in an attempt to obtain new compounds with activity against drug-resistant Mtb strains, new series of hybridized 1*H*-benzo[*d*]imidazoles and 3,4-dihydroquinazolin-4-ones were synthesized and assayed against *M. tuberculosis* H37Rv. First, the basic structural requirements for potency of compounds (SAR) were evaluated. Thereafter, the most active structures against *M. tuberculosis* H37Rv were tested against a panel of

clinically isolated drug-resistant strains, and the viability of HepG2, HaCat and Vero cells after exposure to the compounds was determined. Finally, cardiotoxicity, neurotoxicity and possible morphological alterations by exposure to the compounds using zebrafish (*Danio rerio*) models were also evaluated.

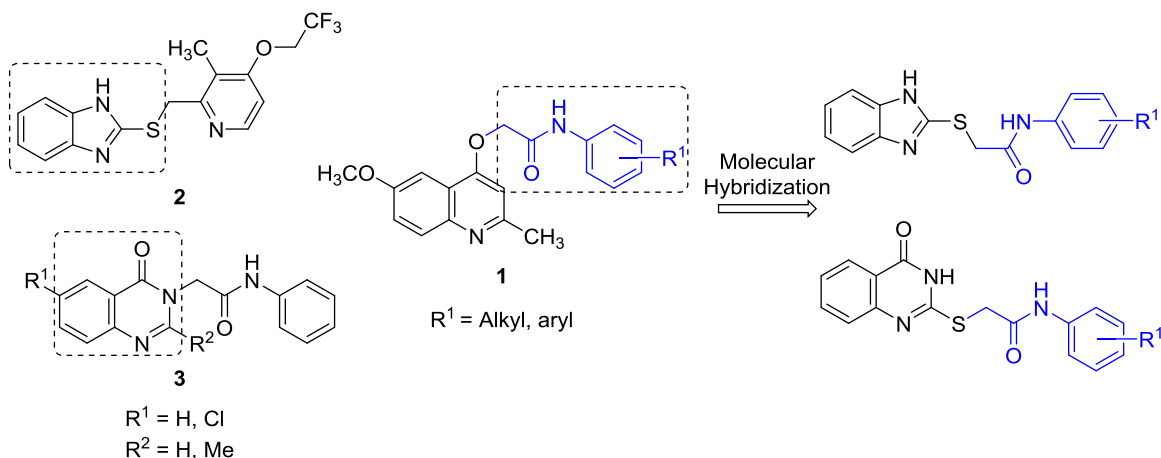
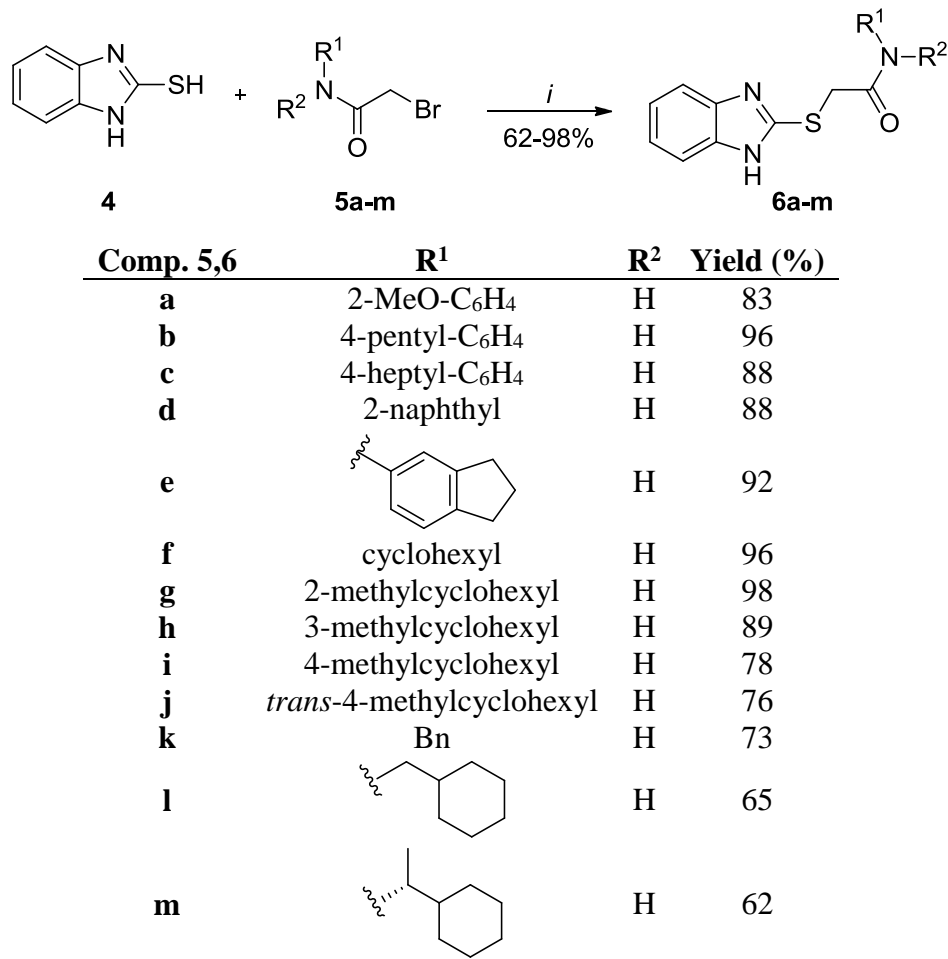


Figure 1. Molecular hybridization using acetamide moieties from 2-(quinolin-4-yloxy)acetamides with 1*H*-benzo[d]imidazole and 3,4-dihydroquinazolin-4-one scaffolds.

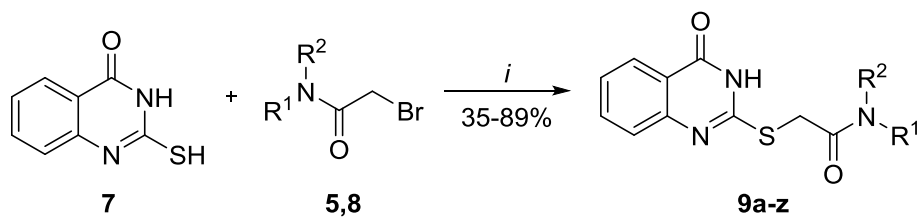
2. Results and Discussion

The synthesis of the designed compounds was performed in two synthetic steps. First, bromoacetamides **5** and **8** were obtained in an acylation reaction between primary or secondary amines and bromoacetyl chloride according to already-reported protocols [9, 10]. It is important to mention that the substituents were chosen based on the best antimycobacterial results presented by the 2-(quinolin-4-yloxy)acetamides, including published [9, 10] and unpublished data. The second step was accomplished through a second-order nucleophilic substitution reaction (S_N2). The 1*H*-benzo[d]imidazoles **6a–m**

were obtained from reaction of 2-mercaptopbenzoimidazole (**4**) and bromoacetamides **5a–m** using potassium carbonate (K_2CO_3) as base, according to a previously described method [15]. The reactants were stirred for 4 h at 40 °C leading to products with 62–98% yields (**Scheme 1**). On the other hand, the synthesis of 3,4-dihydroquinazolin-4-ones **9a–z** was accomplished by reaction of 2-mercaptopquinazolin-4(3H)-one (**7**) and bromoacetamides **5** and **8** in the presence of diisopropylethylamine (DIPEA) using dimethylformamide (DMF) as solvent. The reaction mixtures were stirred for 16 h at 0–25 °C to afford the desired products **9a–z** with 35–89% yields (**Scheme 2**). Spectroscopic and spectrometric data were obtained in agreement with the proposed structures.



Scheme 1. Reagents and conditions: *i* = K_2CO_3 , CH_3CN , 40 °C, 4 h.



Comp. 5,8,9	R¹	R²	Yield (%)
a	Ph	H	86
b	4-MeO-C ₆ H ₄	H	81
c	4-Me-C ₆ H ₄	H	69
d	4-F-C ₆ H ₄	H	68
e	4-Cl-C ₆ H ₄	H	81
f	4-Br-C ₆ H ₄	H	89
g	4-I-C ₆ H ₄	H	86
h	4-O ₂ N-C ₆ H ₄	H	50
i	4-propyl-C ₆ H ₄	H	75
j	4-pentyl-C ₆ H ₄	H	88
k	2-naphthyl	H	81
l		H	37
m		H	80
n	cyclohexyl	H	65
o	cyclohexyl	Me	52
p	2-methylcyclohexyl	H	55
q	3-methylcyclohexyl	H	35
r	4-methylcyclohexyl	H	45
s	<i>trans</i> -4-methylcyclohexyl	H	59
t	cyclopentyl	H	60
u	cycloheptyl	H	76
v	Bn	H	41
w		H	46
x		H	59
y		H	82
z	CH ₂ -(CH ₂) ₃ -CH ₂		72

Scheme 2. Reagents and conditions: *i* = DIPEA, DMF, 0–25 °C, 16 h.

The synthesized compounds **6a–m** and **9a–z** were tested in whole-cell assay against *M. tuberculosis* H37Rv, using the first-line drug isoniazid as reference [16, 17]. The 1*H*-

benzo[*d*]imidazoles **6a–m** presented only moderate activity against the bacillus under the tested conditions (**Table 1**). Considering the data shown, one can conclude that cycloalkyl substituents exhibited better activity than did aromatic groups. In addition, the extent of the chain using a carbon with cycloalkyl or aromatic substituents did not lead to higher activity. The most active compound **6j** inhibited the Mtb growth with an MIC of 16.5 μM . This compound shows the 4-methyl group in a *trans* position relative to the amidic nitrogen attached to the cyclohexane ring. Interestingly, when a mixture of *cis* and *trans* isomers was used the activity of the compound **6i** was nearly 2.5-fold less than 1*H*-benzo[*d*]imidazole **6j**. This finding demonstrates a possible stereochemical preference for increasing antimycobacterial activity of this class of compounds. Changing the methyl group to the 2- or 3-position of the cyclohexane ring in the compounds **6g** and **6h** did not maintain the activity, with MIC values $>33 \mu\text{M}$. It is noteworthy that the lipophilicities of 1*H*-benzo[*d*]imidazoles **6g–j** are the same, with CLogP of 3.81, denoting that structural factors, rather than the physicochemical properties, appear to be linked to the activity of the molecules. The importance of the 4-methyl group attached to the cyclohexane ring can be inferred by the result obtained for compounds **6f–h**, which were ineffective at the highest tested concentration (MIC $>31.3 \mu\text{M}$). Finally, chain extension using a methylene group in the compounds **6k–m** and the presence of aromatic substituents on the molecules **6a–e** did not result in better activities when compared to cyclohexyl derivatives (**Table 1**).

Table 1. ClogP values and *in vitro* activities of the 1*H*-benzo[*d*]imidazoles **6a–m** against *M. tuberculosis* H37Rv.

Entry	ClogP ^a	MIC H37Rv (μM)
6a	2.73	>31.9
6b	5.86	70.7
6c	3.85	>65.5
6d	4.42	>75.0

6e	4.81	>29.63
6f	3.29	>31.3
6g	3.81	>33.0
6h	3.81	>33.0
6i	3.81	41.2
6j	3.81	16.5
6k	3.14	>33.6
6l	3.91	82.4
6m	4.22	>31.5
INH	-	2.9

^aClogP calculated by ChemBioDraw Ultra, version 13.0.0.3015. INH, isoniazid.

In the second round of obtaining new drug candidates to treat tuberculosis, the antimycobacterial activity of 3,4-dihydroquinazolin-4-ones **9a–z** against *M. tuberculosis* H37Rv strain was determined (**Table 2**). Once more, the cycloalkyl substituents presented the best inhibition activities on bacillus growth, with MICs in the submicromolar range. Substituents containing aromatic groups, which had produced highly potent compounds when present in the 2-(quinolin-4-yloxy)acetamides, led to products with moderate or no activity at the highest concentrations assayed. As expected, ClogP values of the 3,4-dihydroquinazolin-4-ones **9** were reduced when compared to the analogs containing the quinoline scaffold. ClogP values were obtained ranging from 1.38 to 4.63 for the synthesized compounds (**Table 2**). Variation using electron-donating, electron-withdrawing or alkyl groups attached at the 4-position of the phenyl group in molecules **9a–j** yielded structures with moderate or no activity against Mtb. Increasing the molecular volume by using a 2-naphthyl group in the 3,4-dihydroquinazolin-4-one **9k** also failed to produce satisfactory results (MIC >27.7 μM). Afterwards, the importance of the planarity of the naphthyl group was evaluated by the insertion of the tetrahydronaphthyl groups in the **9l** and **9m** structures. Whereas the stereoisomer of S configuration (**9l**) exhibited an MIC >27.4 μM, the R isomer (**9m**) was able to inhibit the bacillus growth with an MIC of 17.1 μM. The apparent stereospecificity of the molecules

will be rationalized when subsequent studies reveal the molecular target responsible for the antimycobacterial activity. This moderate MIC value with tetrahydronaphthyl group in **9m** prompted us to investigate its molecular simplification by the removal of the phenyl group and evaluation of the cyclohexyl group. Indeed, 3,4-dihydroquinazolin-4-one **9n** exhibited an MIC of 0.97 μM , which was approximately 18-fold more potent than tetrahydronaphthyl-containing compound **9m**. Moreover, this compound was almost 3-fold more potent than isoniazid drug (MIC = 2.9 μM). These findings corroborated data already described in the literature [18]. Interestingly, the secondary amide seems to be crucial for the activity of the 3,4-dihydroquinazolin-4-ones, as substitution of hydrogen for a methyl abolished completely the antimycobacterial activity of compound **9o** (MIC >75.4 μM). Amidic hydrogen may be involved in hydrogen bond(s) with a putative molecular target, stabilizing the protein-ligand complex, or may be responsible for the correct conformation of the structure through intramolecular stabilization. Following SAR evaluation, the presence of methyl at the 2-position of the cyclohexyl ring did not significantly alter the activity of compounds, as 3,4-dihydroquinazolin-4-one **9p** showed an MIC of 0.94 μM . By contrast, 3-methyl-, 4-methyl-, and *trans*-4-methylcyclohexyl substituents yielded molecules with an MIC of 0.24 μM , a potency increase of more than 4-fold compared to the non-substituted **9n**. Reduction in molecular volume by using a cyclopentyl group (**9t**) reduced the antitubercular potency. Cyclopentyl-substituted **9t** exhibited an MIC of 2.07 μM , which was 2.1-fold less active than cyclohexyl-based compound **9n**. The use of a cycloheptyl substituent again yielded a structure with an MIC in the submicromolar range. 3,4-Dihydroquinazolin-4-one **9u** presented an MIC of 0.48 μM . In the same manner as for the *1H*-benzo[*d*]imidazoles series, the 3,4-dihydroquinazolin-4-one side chain was extended with an additional methylene. First, using a benzyl group (**9v**) the MIC obtained was 4.8 μM , which was more promising than

phenyl-substituted **9a**. By contrast, the presence of methylene separating the amidic nitrogen from the cyclohexyl ring did not alter the potency of compound **9w** (MIC = 0.94 μ M) compared to **9n** (MIC = 0.97 μ M). Another interesting observation was that the presence of an additional methyl group creating stereogenic centers abolished the activity of the 3,4-dihydroquinazolin-4-ones **9x** and **9y** (MICs >28.9 μ M). Finally, piperidinyl-containing compound **9z** was devoid of activity at the evaluated concentration (MIC >33.0 μ M), evidencing, once more, the necessity of the secondary amide for the potent activity of the 3,4-dihydroquinazolin-4-ones.

Table 2. ClogP values and *in vitro* activities of the 3,4-dihydroquinazolin-4-ones **9a-z** against *M. tuberculosis* H37Rv and clinical resistant isolates.

Entry	ClogP ^a	MIC H37Rv (μ M)	MIC CDCT10 (μ M)	MIC CDCT16 (μ M)	MIC CDCT27 (μ M)	MIC CDCT28 (μ M)
9a	2.02	>32.1	-	-	-	-
9b	2.09	>29.3	-	-	-	-
9c	2.52	>30.7	-	-	-	-
9d	2.42	>30.4	-	-	-	-
9e	2.99	28.9	-	-	-	-
9f	3.14	>25.6	-	-	-	-
9g	3.40	>22.9	-	-	-	-
9h	2.31	>28.1	-	-	-	-
9i	3.57	>28.3	-	-	-	-
9j	4.63	26.2	-	-	-	-
9k	3.19	>27.7	-	-	-	-
9l	2.58	>27.4	-	-	-	-
9m	2.58	17.1	-	-	-	-
9n	2.07	0.97	0.50	0.97	0.25	0.5
9o	2.27	>75.4	-	-	-	-

9p	2.58	0.94	0.95	3.9	0.96	1.9
9q	2.58	0.24	0.94	0.9	0.24	0.93
9r	2.58	0.24	0.24	0.48	0.12	0.24
9s	2.58	0.24	0.12	0.24	0.04	0.12
9t	1.51	2.07	-	-	-	-
9u	2.62	0.48	0.48	0.93	0.24	0.48
9v	1.92	4.8	-	-	-	-
9w	2.68	0.94	0.93	0.93	0.48	0.93
9x	2.99	>28.9	-	-	-	-
9y	2.99	>28.9	-	-	-	-
9z	1.38	>33.0	-	-	-	-
INH	-	2.9	45.6	729.2	182.3	2.84

^aClogP calculated by ChemBioDraw Ultra, version 13.0.0.3015. INH, isoniazid.

3,4-Dihydroquinazolin-4-ones with MIC values lower than 1 µM (**9n**, **9p-s**, **9u** and **9w**) were selected for further evaluation of their inhibitory activity against a panel of clinical isolate strains (**Table 2**). The CDCT10 and CDCT16 strains are described as multidrug-resistant clinical isolates. CDCT10 presents resistance to drugs such as isoniazid, rifampin and ethambutol, whereas CDCT16 strain exhibits resistance to isoniazid, rifampin, ethambutol and streptomycin. Targeted sequencing from CDCT10 strain has revealed mutations in the rpoB and katG genes. Also using targeted sequencing, mutations in the rpo, katG and inhA regulatory region C(-15)T were observed for CDCT16 strain. Additionally, CDCT27 was also evaluated; this drug-resistant strain shows resistance to drugs such as isoniazid and ethambutol. CDCT27 has displayed mutations in the katG gene. Finally, clinical isolate CDCT28 does not present resistance to the first-line drugs, and targeted sequencing has also presented mutation in the rpoB gene. Notably, the selected compounds exhibited identical activity or were even more

potent against CDCT10, CDCT27, and CDCT28 strains than against *M. tuberculosis* H37Rv strain (**Table 2**). By contrast, 3,4-dihydroquinazolin-4-ones **9p–r** and **9u** increased MIC values when assayed against CDCT16 strain. Only compounds **9n** and **9w** did not alter MIC values against this strain compared to those presented for *M. tuberculosis* H37Rv. Although these results may suggest the participation of the inhA gene product in the activity elicited by the compounds, the mutations in the clinical isolate strains were obtained by target sequencing, and alterations elsewhere in the genome cannot be excluded. Thus, inferences about the mechanism of action of the compounds based on modifications in MIC values for these strains should be made with caution, and further studies are needed to clarify this point.

Cellular viability was carried out after incubation with the test compounds using the neutral red uptake assay [19] and MTT method [10] (**Table 3**). Exposing the HepG2, HaCat, and Vero cell lineages to 3,4-dihydroquinazolin-4-ones **9n**, **9p–s**, **9u** and **9w** for 72 h did not significantly affect the cell viability [20]. The assayed concentration was at least 32 times higher than the MICs of the synthesized compounds against *M. tuberculosis* H37Rv. These results suggest a possible low toxicity of the compounds to mammalian cells and a likely high degree of selectivity for Mtb.

Table 3. Percentage of cell viability of HepG2, HaCat, and Vero cell lineages after exposition to 3,4-dihydroquinazolin-4-ones **9n**, **9p–s**, **9u** and **9w**.

Entry	% of cell viability ± SEM ^a					
	HepG2		HaCat		Vero	
	MTT	Neutral red	MTT	Neutral red	MTT	Neutral red
9n	86 ± 6	95 ± 4	100 ± 8	97 ± 3	90 ± 12	92 ± 4
9p	94 ± 5	101 ± 3	100 ± 8	99 ± 12	102 ± 7	95 ± 12

9q	89 ± 6	95 ± 3	94 ± 9	88 ± 7	89 ± 7	95 ± 5
9r	89 ± 3	96 ± 3	95 ± 8	94 ± 3	84 ± 4	95 ± 2
9s	83 ± 7	97 ± 2	97 ± 2	97 ± 4	88 ± 12	93 ± 6
9u	99 ± 3	105 ± 5	100 ± 10	88 ± 6	91 ± 4	94 ± 5
9w	79 ± 3	97 ± 3	98 ± 8	88 ± 3	89 ± 5	97 ± 3

^aData are expressed as the mean cell viability ± SEM for each compound, tested at 10 µg/mL. Results were obtained in triplicate from three independent experiments.

The promising and selective activity showed by the compounds prompted us to investigate other *in vivo* toxicological parameters such as cardiotoxicity, neurotoxicity and morphological alterations, using zebrafish (*Danio rerio*) models [21–23]. In particular, there are possible cardiac side effects under study attributed to the new antitubercular drug bedaquiline [24]. Therefore, cardiac risk assessment for novel compounds should ideally be evaluated in the early drug discovery stages. The 3,4-dihydroquinazolin-4-ones **9n**, **9p–s**, **9u** and **9w** were evaluated for the heartbeat rate in viable embryos at 2 and 5 dpf (days post-fertilization) using concentrations of 3, 15 and 20 µM (**Table 4**). Except for compounds **9p** and **9r**, the molecules did not change the heartbeat rates in tested animals at 2 dpf at 3 µM concentration. By contrast, at the highest dose assayed (20 µM) six of the seven structures tested induced changes in the heartbeat rate of animals at 2 dpf. Notably, 3,4-dihydroquinazolin-4-one **9q** did not alter heartbeat rates in any of the concentrations tested. Considering animals at 5 dpf, only compound **9u** was able significantly to alter the rate of heartbeats. This finding indicates an apparent cardiac safety of compounds **9n**, **9p–s**, and **9w** in animals at 5 dpf.

Table 4. Cardiac evaluation of 3,4-dihydroquinazolin-4-ones **9n**, **9p–s**, **9u** and **9w** in viable embryos at 2 and 5 dpf (days post-fertilization).

Zebra fish heart rate (Mean ± SD/min) – Embryos 2 dpf					
Entry	Control	1% DMSO	3 µM	15 µM	20 µM
9n	141.6 ± 15.8	147.3 ± 16.1	149.5 ± 16.3	155.0 ± 14.8 **	155.7 ± 14.1 **
9p	141.6 ± 15.8	147.3 ± 16.1	156.3 ± 14.8 **	151.7 ± 14.2	153.9 ± 16.1 *
9q	146.3 ± 9.3	148.8 ± 9.6	151.2 ± 7.1	151.7 ± 9.4	152.2 ± 8.5
9r	128.7 ± 21.7	134.4 ± 11.7	122.3 ± 9.6 ##	127.2 ± 6.6	146.4 ± 10.9 **** / ##
9s	128.7 ± 21.7	134.4 ± 11.7	135.5 ± 7.3	134.0 ± 6.1	150.2 ± 8.2 **** / ###
9u	138.3 ± 10.7	139.9 ± 12.4	139.6 ± 15.0	136.5 ± 16.4	148.4 ± 10.8 *
9w	138.3 ± 10.7	139.9 ± 12.4	140.7 ± 12.2	143.2 ± 14.1	152.6 ± 8.8 **** / ###

Zebra fish heart rate (Mean ± SD/min) – Embryos 5 dpf					
Entry	Control	1% DMSO	3 µM	15 µM	20 µM
9n	158.2 ± 12.7	157.4 ± 9.7	162.8 ± 10.5	163.0 ± 8.4	158.4 ± 9.9
9p	156.7 ± 16.3	157.4 ± 9.7	162.6 ± 8.0	163.4 ± 7.2	160.6 ± 12.3
9q	155.9 ± 12.5	159.1 ± 9.7	157.2 ± 15.3	157.4 ± 9.3	160.9 ± 11.4
9r	148.1 ± 7.4	148.1 ± 11.3	147.7 ± 14.1	150.3 ± 13.5	152.2 ± 10.6
9s	148.1 ± 7.4	148.1 ± 11.3	149.2 ± 13.5	157.4 ± 18.6	153.8 ± 13.2
9u	153.2 ± 8.2	154.5 ± 6.8	160.1 ± 8.4 *	160.4 ± 7.7 *	153.8 ± 11.1
9w	153.2 ± 8.2	154.5 ± 6.8	157.8 ± 9.0	158.9 ± 11.9	152.5 ± 11.0

* $P < 0.5$ compared with control group (Tukey post-test). ** $P < 0.01$ compared with control group (Tukey post-test). *** $P < 0.0001$ compared with control group (Tukey post-test). ## $P < 0.01$ compared with the 1% DMSO group (Tukey post-test). ### $P < 0.001$ compared with the 1% DMSO group.

Furthermore, the distance traveled by the animals was used as a parameter to evaluate neurological impairment after exposure to the compounds. None of the evaluated compounds **9n**, **9p–s**, **9u**, and **9w** altered the locomotor activity of the animals (data not

shown). Morphological evaluation considered parameters such as body length, ocular distance, and surface area of the eyes. Except for compound **9s** which altered the body length of the larvae at 20 µM concentration, none of the compounds in any of the tested concentrations (3, 15 and 20 µM) shown modifications on the morphological parameters (data not shown). Finally, the larvae survival rate was not altered by exposure to 3,4-dihydroquinazolin-4-ones **9n**, **9p–s**, **9u**, and **9w** in the experimental conditions used (data not shown).

Aiming at further *in vivo* effectiveness trials in rodents and pharmaceutical formulation studies for oral administration, the stability of 3,4-dihydroquinazolin-4-ones **9n**, **9p–s**, **9u**, and **9w** in aqueous medium was determined (Supporting information). The experiments were carried out using 10% DMSO as co-solvent in PBS at 25 °C and 37 °C for up to 48 h. At room temperature (25 °C), only compound **9s** showed chemical instability. After 24 h, only 26% of the 3,4-dihydroquinazolin-4-one **9s** could be recovered. The other products remained stable over 48 h. Elevation of temperature to 37 °C appeared to be crucial for chemical instability of compound **9r**. After 6 h of incubation less than 70% of **9r** was recovered. Once more, the 3,4-dihydroquinazolin-4-one **9s** presented instability under the experimental conditions tested. In contrast, 3,4-dihydroquinazolin-4-ones **9n**, **9p–q**, **9u**, and **9w** were stable in aqueous medium for 48 h at 37 °C in the evaluated conditions.

3. Conclusion

In summary, herein was shown the synthesis of new series of hybridized 1*H*-benzo[*d*]imidazoles and 3,4-dihydroquinazolin-4-ones and their *in vitro* antitubercular activity. The simplicity of the route, easily accessible reactants and reagents, reasonable yields and high purity make the synthetic protocols attractive. In addition, the synthesized

compounds showed potent and selective activity against drug-sensitive and drug-resistant Mtb strains, with no apparent cytotoxicity to mammalian cells. The submicromolar antitubercular activity elicited by 3,4-dihydroquinazolin-4-ones, coupled with low risk of cardiotoxicity and neurotoxicity, suggests that this *class of compounds* may furnish candidates for future development of novel anti-TB drugs. Considering the data described so far, 3,4-dihydroquinazolin-4-ones **9q** and **9w** are considered the lead compounds of this series of synthesized molecules. Studies to identify the target(s) of the antimycobacterial action of the 3,4-dihydroquinazolin-4-ones, new structural modifications, and pharmaceutical formulation studies are in progress and these data will be reported to the scientific community soon.

4. Experimental Section

4.1 Synthesis and structure: apparatus and analysis

The commercially available reactants and solvents were obtained from commercial suppliers and were used without additional purification. The reactions were monitored by thin-layer chromatography (TLC) with Merck TLC Silica gel 60 F₂₅₄. The melting points were measured using a Microquímica MQAPF-302 apparatus. ¹H and ¹³C NMR spectra were acquired on a Avance III HD Bruker spectrometer (Pontifical Catholic University of Rio Grande do Sul). Chemical shifts (δ) were expressed in parts per million (ppm) relative to DMSO-*d*₆, which was used as the solvent, and to TMS, which was used as internal standard. High-resolution mass spectra (HRMS) were obtained for all the compounds on an LTQ Orbitrap Discovery mass spectrometer (Thermo Fisher Scientific, Bremer, Germany). This system combines an LTQ XL linear ion-trap mass spectrometer and an Orbitrap mass analyzer. The analyses were performed through the direct infusion

of the sample in MeOH/H₂O (1:1) with 0.1% formic acid (flow rate 10 µL/min) in a positive-ion mode using electrospray ionization (ESI). For elemental composition, calculations used the specific tool included in the Qual Browser module of Xcalibur (Thermo Fisher Scientific, release 2.0.7) software. Compound purity was determined using an Äkta HPLC system (GE Healthcare® Life Sciences) equipped with a binary pump, manual injector and UV detector. Unicorn 5.31 software (Build 743) was used for data acquisition and processing. The HPLC conditions were as follows: RP column 5 µm Nucleodur C-18 (250 × 4.6 mm); flow rate 1.5 mL/min; UV detection 254 nm; 100% water (0.1% acetic acid) was maintained from 0 to 7 min and was followed by a linear gradient from 100% water (0.1% acetic acid) to 90% acetonitrile/methanol (1:1, v/v) from 7 to 15 min (15–30 min) and subsequently returned to 100% water (0.1% acetic acid) in 5 min (30–35 min) and maintained for an additional 10 min (35–45 min). All the evaluated compounds were ≥ 90% pure.

4.2 General procedure for the synthesis of 1*H*-benzo-[*d*]-imidazoles **6a-m**

The synthesis of these compounds was adapted from previously described methodology [15]. The appropriately substituted bromoacetamide (1 mmol) was added to a mixture of 1*H*-benzimidazole-2-thiol (1 mmol), potassium carbonate (K₂CO₃, 2 mmol) in acetonitrile (10 mL). The reaction mixture was stirred at 40 °C (oil bath) for 4 h. The precipitated solid was filtered off, washed with chloroform (3 × 20 mL) and dried under reduced pressure to afford the products in good purity.

4.2.1. 2-((1*H*-Benzo[*d*]imidazol-2-yl)thio)-*N*-(2-methoxyphenyl)acetamide (6a**):** Yield 83%; m.p.: 127.5 – 129.3 °C; HPLC 93% (*t*_R = 15.90); ¹H NMR (400 MHz, DMSO-*d*₆) δ ppm 3.67 (s, 3 H), 4.22 (s, 2 H), 6.88 (td, *J* = 8.2, 1.3 Hz, 1 H), 6.97 (td, *J*=8.2, 1.3 Hz, 1 H), 7.02 (dd, *J* = 8.2, 1.3 Hz), 7.13-7.17 (m, 2 H), 7.48-7.50 (m, 2 H), 8.10 (d, *J* = 8.1, 1 H), 9.94 (s, 1 H). ¹³C NMR (101 MHz, DMSO-*d*₆) δ ppm 35.4, 55.6, 111.0, 120.3,

121.5, 124.1, 127.3, 148.7, 150.0, 166.8; FTMS (ESI) m/z 314.0954 [M+H]⁺; calcd for C₁₆H₁₅N₃O₂S: 314.0958.

4.2.2. 2-((1*H*-Benzo[*d*]imidazol-2-yl)thio)-*N*-(4-pentylphenyl)acetamide (6b**):** Yield 96%; m.p.: 103.5 – 104.7 °C; HPLC 94% (*t_R* = 19.10); ¹H NMR (400 MHz, DMSO-*d*₆) δ ppm 0.83 (t, *J* = 7.0 Hz, 3 H), 1.25 (m, 4 H), 1.51 (m, 2 H), 2.49 (m, 2 H), 4.21 (s, 2 H), 7.09-7.11 (m, 4 H), 7.43-7.48 (m, 4 H), 10.58 (s, 1H). ¹³C NMR (101 MHz, DMSO-*d*₆) δ ppm 13.8, 21.9, 30.6, 30.7, 34.4, 36.1, 109.4, 113.8, 118.9, 121.0, 128.4, 136.6, 137.3, 140.0, 150.5, 166.1; FTMS (ESI) m/z 354.1630 [M+H]⁺; calcd for C₂₀H₂₃N₃OS: 354.1635.

4.2.3. 2-((1*H*-Benzo[*d*]imidazol-2-yl)thio)-*N*-(4-heptylphenyl)acetamide (6c**):** Yield 88%; m.p.: 142.6 – 143.7 °C; HPLC 93% (*t_R* = 19.68); ¹H NMR (400 MHz, DMSO-*d*₆) δ ppm 0.84 (t, *J* = 6.8 Hz, 4 H), 1.23 (d, *J* = 6.1 Hz, 8 H), 1.51 (m, 2 H), 2.50 (m, 2 H), 4.13 (s, 2 H), 7.03-7.06 (m, 2 H), 7.10 (d, *J* = 8.6 Hz, 2 H), 7.42-7.44 (m, 2 H), 7.48 (d, *J* = 8.6 Hz, 2 H). ¹³C NMR (101 MHz, DMSO-*d*₆) δ ppm 13.8, 22.0, 28.4, 30.9, 31.2, 34.5, 36.1, 109.4, 113.8, 118.8, 120.2, 122.0, 128.4, 132.6, 136.8, 137.2, 141.3, 151.9, 166.7; FTMS (ESI) m/z 382.1977 [M+H]⁺; calcd for C₂₂H₂₇N₃OS: 382.1948.

4.2.4. 2-((1*H*-Benzo[*d*]imidazol-2-yl)thio)-*N*-(naphthalen-2-yl)acetamide (6d**):** Yield 88%; m.p.: 101.7 – 102.2 °C; HPLC 92% (*t_R* = 16.61); ¹H NMR (400 MHz, DMSO-*d*₆) δ ppm 4.33 (s, 2 H), 7.10-7.14 (m, 2 H), 7.37-7.43 (td, *J* = 7.5, 1.5 Hz, 1 H), 7.44-7.47 (m, 3 H), 7.56-7.59 (dd, *J* = 8.8, 2.2 Hz, 1 H), 7.81 (t, *J* = 8.8, 2 H), 7.86 (d, *J* = 9.0 Hz, 1 H), 8.29 (d, *J* = 1.7 Hz, 1 H), 10.73 (s, 1 H). ¹³C NMR (101 MHz, DMSO-*d*₆) δ ppm 36.2, 115.1, 119.6, 121.4, 124.6, 126.4, 127.2, 127.4, 128.4, 129.7, 133.3, 136.4, 149.8, 166.4; FTMS (ESI) m/z 334.1005 [M+H]⁺; calcd for C₁₉H₁₅N₃OS: 334.1009.

4.2.5. 2-((1*H*-Benzo[*d*]imidazol-2-yl)thio)-*N*-(2,3-dihydro-1*H*-inden-5-yl)acetamide (6e**):** Yield 92%; m.p.: 89.7 – 90.6 °C; HPLC 90% (*t_R* = 16.71); ¹H NMR (400 MHz, DMSO-*d*₆) δ ppm 1.97 (q, *J* = 7.4, Hz, 2 H), 2.79 (dt, *J* = 10.7, 7.4 Hz, 4 H), 4.23 (s, 2 H), 7.09-7.13 (m, 3 H), 7.26 (dd, *J* = 8.1, 1.5 Hz, 1 H), 7.42-7.46 (m, 2 H), 7.49 (s, 1 H) 10.40 (s, 1 H). ¹³C NMR (101 MHz, DMSO-*d*₆) δ ppm 25.0, 31.7, 32.4, 36.1, 115.2, 117.1, 121.3, 124.1, 137.0, 138.6, 144.1, 149.9, 165.8; FTMS (ESI) m/z 324.1161 [M+H]⁺; calcd for C₁₉H₁₉N₃OS: 324.1165.

4.2.6. 2-((1*H*-Benzo[*d*]imidazol-2-yl)thio)-*N*-cyclohexylacetamide (6f**):** Yield 96%; m.p.: 132.9 – 134.0 °C; HPLC 90% (*t_R* = 16.59); ¹H NMR (400 MHz, DMSO-*d*₆) δ ppm 1.08-1.25 (m, 5 H, 3'-H, 4'-H and 5'H), 1.45-1.48 (m, 1 H, 5'-H), 1.59-1.69 (m, 4 H, 2'-H and 6'-H), 3.54 (m, 1 H, 1'-H), 3.87 (s, 2 H, 8-H), 6.98-7.02 (m, 2 H, 5-H and 6-H), 7.35-7.39 (m, 2 H, 4-H and 7-H), 8.87 (s, 1 H, H-N). ¹³C NMR (101 MHz, DMSO-*d*₆) δ ppm 23.9, 25.2, 31.9, 35.1 (9-C), 47.5 (1'-C), 113.8 (4-C and 7-C), 120.1 (5-C and 6-C), 141.5 (3a-C and 7a-C), 152.1 (2-C), 167.3 (10-C); FTMS (ESI) m/z 290.1314 [M+H]⁺; calcd for C₁₅H₁₉N₃OS: 290.1322.

4.2.7. 2-((1*H*-Benzo[*d*]imidazol-2-yl)thio)-*N*-(2-methylcyclohexyl)acetamide (6g**):** Yield 98%; m.p.: 114.8 – 115.5 °C; HPLC 91% (*t_R* = 16.97 and 17.44); ¹H NMR (400 MHz, DMSO-*d*₆) δ ppm 0.74-0.75 (d, *J* = 6.8 Hz, 3 H), 0.79-0.80 (d, *J* = 6.6 Hz, 3 H), 0.84-0.86 (m, 1H), 0.96-1.02 (m, 1 H), 1.12-1.40 (m, 7 H), 1.58 (d, *J* = 11.7 Hz, 2 H), 1.64-1.75 (m, 4 H), 3.18-3.26 (m, 2 H), 3.88-4.03 (m, 4 H), 7.03-7.05 (m, 2 H), 7.06-7.09

(m, 2 H), 7.38-7.42 (m, 4 H), 8.41 (d, $J = 4.4$ Hz, 1 H), 8.88 (d, $J = 4.4$ Hz, 1 H). ^{13}C NMR (101 MHz, DMSO- d_6) δ ppm 18.8, 24.9, 25.2, 28.9, 29.7, 32.6, 33.7, 33.7, 34.9, 35.1, 37.1, 48.8, 53.7, 113.7, 120.3, 120.8, 140.2, 150.7, 166.8, 168.1; FTMS (ESI) m/z 304.1467 [M+H] $^+$; calcd for C₁₆H₂₁N₃OS: 304.1478.

4.2.8. 2-((1*H*-Benzo[*d*]imidazol-2-yl)thio)-*N*-(3-methylcyclohexyl)acetamide (**6h**): Yield 89%; m.p.: 128.7 – 129.4 °C; HPLC 90% ($t_R = 17.16$ and 17.48); ^1H NMR (400 MHz, DMSO- d_6) δ ppm 0.70-0.98 (m, 5 H), 1.01-1.27 (m, 3 H), 1.37-1.58 (m, 4 H), 1.65 (d, $J = 9.5$ Hz, 2 H), 1.68-1.77 (m, 2 H), 3.47-3.57 (m, 1 H), 3.98 (s, 2 H), 7.09-7.13 (m, 2 H) 7.41-7.46 (m, 2 H), 8.24 (d, $J = 4.4$ Hz, 1 H), 8.44 (d, $J = 4.4$ Hz, 1 H). ^{13}C NMR (101 MHz, DMSO- d_6) δ ppm 20.0, 21.6, 22.2, 24.3, 26.4, 29.8, 31.2, 31.8, 33.4, 33.8, 35.0, 35.3, 38.1, 41.0, 44.5, 48.2, 113.7, 121.2, 150.0, 166.3, 166.9; FTMS (ESI) m/z 304.1467 [M+H] $^+$; calcd for C₁₆H₂₁N₃OS: 304.1478.

4.2.9. 2-((1*H*-Benzo[*d*]imidazol-2-yl)thio)-*N*-(4-methylcyclohexyl)acetamide (**6i**): Yield 78%; m.p.: 98.2 – 99.0 °C; HPLC 96% ($t_R = 17.12$ and 17.41); ^1H NMR (400 MHz, DMSO- d_6) δ ppm 0.66 (d, $J = 6.1$ Hz, 3 H_{cis}), 0.84 (d, $J = 6.4$ Hz, 3 H_{trans}), 0.88-0.97 (m, 2 H_{trans}), 1.08-1.17 (m, 4 H_{cis/trans}), 1.26-1.44 (m, 7 H_{cis/trans}), 1.53-1.58 (m, 2 H_{cis}), 1.63 (dd, $J = 12.5, 2.7$ Hz, 2 H_{trans}), 1.77 (dd, $J = 12.5, 2.7$ Hz, 2 H_{trans}), 3.3-3.4 (m, 2 H_{cis/trans}), 3.8 (s, 2 H_{cis}), 3.9 (s, 2 H_{trans}), 6.96-7.05 (m, 2 H_{cis}), 7.02-7.05 (m, 2 H_{trans}), 7.35-7.41 (m, 4 H_{cis/trans}), 8.68 (s, 1 H_{trans}), 9.13 (d, $J = 4.4$ Hz, 1 H_{cis}). ^{13}C NMR (101 MHz, DMSO- d_6) δ ppm 21.4_{cis}, 22.0_{trans}, 29.0_{cis}, 29.1_{cis}, 30.8_{cis}, 31.3_{trans}, 32.0_{trans}, 33.3_{trans}, 34.7_{cis}, 35.1_{trans}, 44.2_{cis}, 48.1_{trans}, 113.7_{trans}, 113.9_{cis}, 119.6_{cis}, 120.3_{trans}, 141.0_{trans}, 142.2_{cis}, 151.6_{trans}, 153.1_{cis}, 167.0_{trans}, 168.0_{cis}; FTMS (ESI) m/z 304.1467 [M+H] $^+$; calcd for C₁₆H₂₁N₃OS: 304.1478.

4.2.10. 2-((1*H*-Benzo[*d*]imidazol-2-yl)thio)-*N*-(*trans*-4-methylcyclohexyl)acetamide (**6j**): Yield 76%; m.p.: 144.5 – 145.2 °C; HPLC 91% ($t_R = 17.17$); ^1H NMR (400 MHz, DMSO- d_6) δ ppm 0.84 (d, $J = 6.4$ Hz, 3 H), 0.88-0.98 (m, 2 H), 1.10-1.18 (m, 2 H), 1.22-1.39 (m, 1 H), 1.63 (d, $J = 12.7$ Hz, 2 H), 1.76 (d, $J = 9.5$ Hz, 2 H), 3.43 (m, 1 H), 3.92 (s, 2 H), 7.05-7.07 (m, 2 H), 7.40-7.41 (m, 2 H), 8.55 (s, 1 H). ^{13}C NMR (101 MHz, DMSO- d_6) δ ppm 22.0, 31.3, 32.0, 33.3, 35.2, 48.1, 113.8, 120.5, 120.6, 140.7, 151.2, 166.9; FTMS (ESI) m/z 304.1496 [M+H] $^+$; calcd for C₁₆H₂₁N₃OS: 304.1478.

4.2.11. 2-((1*H*-Benzo[*d*]imidazol-2-yl)thio)-*N*-benzylacetamide (**6k**): Yield 73%; m.p.: 175.5 – 177.0 °C; HPLC 91% ($t_R = 15.98$); ^1H NMR (400 MHz, DMSO- d_6) δ ppm 4.10 (s, 2 H), 4.32 (d, $J = 6.1$ Hz, 2 H), 7.12-7.19 (m, 2 H), 7.21-7.25 (m, 5 H), 7.44-7.46 (m, 2 H), 8.82 (t, $J = 5.4$ Hz, 1 H). ^{13}C NMR (101 MHz, DMSO- d_6) δ ppm 34.9, 42.4, 121.3, 126.6, 127.0, 128.1, 138.9, 149.7, 167.3; FTMS (ESI) m/z 298.1029 [M+H] $^+$; calcd for C₁₆H₁₅N₃OS: 298.1009.

4.2.12. 2-((1*H*-Benzo[*d*]imidazol-2-yl)thio)-*N*-(cyclohexylmethyl)acetamide (**6l**): Yield 65%; m.p.: 166.7 – 167.1 °C; HPLC 90% ($t_R = 17.21$); ^1H NMR (400 MHz, DMSO- d_6) δ ppm 0.77-0.88 (m, 2 H), 1.10-1.14 (m, 4 H), 1.34-1.35 (m, 1 H), 1.55-1.69 (m, 6 H), 2.94 (ddd, $J = 17.1, 10.8, 6.6$ Hz, 2 H), 4.00 (s, 2 H), 7.09-7.14 (m, 2 H), 7.41-7.45 (m, 2 H), 8.32 (s, 1 H). ^{13}C NMR (101 MHz, DMSO- d_6) δ ppm 25.3, 25.9, 30.1, 34.9, 37.3, 45.1, 113.7, 121.2, 139.6, 149.9, 167.3; FTMS (ESI) m/z 304.1474 [M+H] $^+$; calcd for C₁₆H₂₁N₃OS: 304.1478.

4.2.13. (*S*)-2-((1*H*-Benzo[*d*]imidazol-2-yl)thio)-*N*-(1-cyclohexylethyl)acetamide (**6m**): Yield 62%; m.p.: 139.7 – 140.2 °C; HPLC 92% (t_R = 17.59); ^1H NMR (400 MHz, DMSO-*d*₆) δ ppm 0.81-1.10 (m, 7 H), 1.22-1.26 (m, 1 H), 1.52-1.60 (m, 5 H), 3.55-3.60 (m, 1 H), 3.82-3.99 (m, 2 H), 7.02 (dd, J = 5.9, 3.2 Hz, 2 H), 7.37 (dd, J = 6.1, 3.2 Hz, 2 H), 8.56 (s, 1 H). ^{13}C NMR (101 MHz, DMSO-*d*₆) δ ppm 17.4, 25.7, 25.8, 28.2, 28.6, 35.0, 42.3, 48.9, 113.7, 120.3, 141.0, 151.5, 167.3; FTMS (ESI) m/z 318.1621 [M+H]⁺; calcd for C₁₇H₂₃N₃OS: 318.1635.

4.3 General procedure for the synthesis of 3,4-dihydroquinazolin-4-ones **9a-z**

2-Mercaptoquinazolin-4(3*H*)-one (1 mmol) was diluted in *N,N*-dimethylformamide (5 mL) with the addition of diisopropylethylamine (DIPEA, 1.1 mmol) under an argon atmosphere at 0 °C. The solution was stirred for 5 min and bromacetamide (1.1 mmol) was added. After 30 min, the temperature was elevated to 25 °C. The reaction mixture was stirred for additional 18 h and the precipitated product filtered off, washed with water and dried under vacuum. The products were obtained in satisfactory purity without the need for additional purification.

4.3.1. 2-((4-Oxo-3,4-dihydroquinazolin-2-yl)thio)-*N*-phenylacetamide (**9a**): Yield 86%; m.p.: 233.5 – 234.3 °C; HPLC 99% (t_R = 16.51 min); ^1H NMR (400 MHz, DMSO-*d*₆) δ ppm 4.17 (s, 2 H, 9-H), 7.04 (t, J = 7.3 Hz, 1 H, 4'-H), 7.30 (t, J = 7.3 Hz, 2 H, 3'-H), 7.40 (td, J = 8.1, 1.5 Hz, 1 H, 6-H), 7.47 (d, J = 8.1 Hz, 1 H, 8-H), 7.59 (d, J = 7.6 Hz, 2 H, 2'-H), 7.73 (td, J = 7.6, 1.6 Hz, 1 H, 7-H), 8.02 (dd, J = 8.1, 1 Hz, 1 H, 5-H), 10.34 (s, 1 H, NH), 12.68 (s, 1 H, NH, 3-H). ^{13}C NMR (101 MHz, DMSO-*d*₆) δ ppm 35.1 (9-C), 119.1 (2'-C), 119.9 (4a-C), 123.4 (4'-C), 125.6 (5-C), 125.9(8-C), 128.7 (3'-C), 134.6 (7-C), 138.8 (1'-C), 148.2 (8a-C), 155.2 (2-C), 161.0 (4-C), 165.8 (10-C); FTMS (ESI) m/z 312.0797 [M+H]⁺; calcd for C₁₆H₁₃N₃O₂S: 312.0801.

4.3.2. *N*-(4-Methoxyphenyl)-2-((4-oxo-3,4-dihydroquinazolin-2-yl)thio)acetamide (**9b**): Yield 81%; m.p.: 214.1 – 216.9 °C; HPLC 95% (t_R = 16.34 min); ^1H NMR (400 MHz, DMSO-*d*₆) δ ppm 3.70 (s, 3 H), 4.14 (s, 2 H), 6.87 (d, J = 9.0 Hz, 2 H), 7.38-7.42 (m, 1 H), 7.47-7.50 (m, 3 H), 7.74 (td, J = 8.3, 1.5 Hz, 1 H), 8.02 (dd, J = 7.8, 1.5 Hz, 1 H), 10.20 (s, 1 H), 12.66 (s, 1 H). ^{13}C NMR (101 MHz, DMSO-*d*₆) δ ppm 35.0, 55.1, 113.9, 119.9, 120.7, 125.7, 125.8, 126.0, 132.0, 134.6, 148.2, 155.3, 155.3, 161.0, 165.3; FTMS (ESI) m/z 342.0873 [M+H]⁺; calcd for C₁₇H₁₅N₃O₃S: 342.0907.

4.3.3. 2-((4-Oxo-3,4-dihydroquinazolin-2-yl)thio)-*N*-(*p*-tolyl)acetamide (**9c**): Yield 69%; m.p.: 247.9 – 250.1 °C; HPLC 96% (t_R = 17.00 min); ^1H NMR (400 MHz, DMSO-*d*₆) δ ppm 2.23 (s, 3 H), 4.15 (s, 2 H), 7.10 (d, J = 8.1 Hz, 2 H), 7.40 (td, J = 8.0, 1.5 Hz, 1 H), 7.47 (d, J = 8.6 Hz, 3 H), 7.73 (td, J = 8.4, 1.5 Hz, 1 H), 8.02 (dd, J = 7.9, 1.5 Hz, 1 H), 10.35 (s, 1 H), 12.67 (s, 1 H). ^{13}C NMR (101 MHz, DMSO-*d*₆) δ ppm 20.4, 35.1, 119.1,

119.9, 125.7, 125.8, 126.0, 129.1, 132.3, 134.6, 136.4, 148.2, 155.2, 161.0, 165.6; FTMS (ESI) m/z 326.0927 [M+H]⁺; calcd for C₁₇H₁₅N₃O₂S: 326.0958.

4.3.4. N-(4-Fluorophenyl)-2-((4-oxo-3,4-dihydroquinazolin-2-yl)thio)acetamide (9d**):** Yield 68%; m.p.: 243.6 – 244.8 °C; HPLC 97% (*t_R* = 16.62 min); ¹H NMR (400 MHz, DMSO-*d*₆) δ ppm 4.16 (s, 2 H), 7.11-7.17 (m, 2 H), 7.40 (td, *J* = 8.1, 1.5 Hz, 1 H), 7.46 (d, *J* = 8.1 Hz, 1 H), 7.58-7.63 (m, 2 H), 7.73 (td, *J* = 7.6, 1.6 Hz, 1 H), 8.02 (dd, *J* = 8.1, 1.5 Hz, 1 H), 10.40 (s, 1 H), 12.67 (s, 1 H). ¹³C NMR (101 MHz, DMSO-*d*₆) δ ppm 35.0, 115.3 (d, ²*J_{CF}* = 22.0 Hz), 119.9, 120.9 (d, ³*J_{CF}* = 8.0 Hz), 125.7, 125.8, 126.0, 134.6, 135.2 (d, ⁴*J_{CF}* = 2.9 Hz), 148.2, 155.2, 156.8 (d, ¹*J_{CF}* = 239.8 Hz), 161.0, 165.8; FTMS (ESI) m/z 330.0674 [M+H]⁺; calcd for C₁₆H₁₂FN₃O₂S: 330.0707.

4.3.5. N-(4-Chlorophenyl)-2-((4-oxo-3,4-dihydroquinazolin-2-yl)thio)acetamide (9e**):** Yield 81%; m.p.: 262.7 – 264.1 °C; HPLC 93% (*t_R* = 17.21 min); ¹H NMR (400 MHz, DMSO-*d*₆) δ ppm 4.18 (s, 2 H), 7.37 (d, *J* = 8.0, 2 H), 7.41 (td, *J* = 8.1, 1.1 Hz, 1 H), 7.46 (d, *J* = 8 Hz, 1 H), 7.63 (d, *J* = 8.0, 2 H), 7.75 (td, *J* = 8.0, 1.1 Hz, 1 H), 8.03 (dd, *J* = 7.8, 1.5 Hz, 1 H), 10.49 (s, 1 H), 12.68 (s, 1 H). ¹³C NMR (101 MHz, DMSO-*d*₆) δ ppm 35.1, 119.9, 120.7, 125.7, 126.0, 127.0, 128.7, 134.6, 137.9, 140.4, 148.1, 155.3, 161.1, 166.0; FTMS (ESI) m/z 346.0403 [M+H]⁺; calcd for C₁₆H₁₃ClN₃O₂S: 346.0412.

4.3.6. N-(4-bromophenyl)-2-((4-oxo-3,4-dihydroquinazolin-2-yl)thio)acetamide (9f**):** Yield 89%; m.p.: 236.2 – 238.1 °C; HPLC 92% (*t_R* = 17.26 min); ¹H NMR (400 MHz, DMSO-*d*₆) δ ppm 4.17 (s, 2 H), 7.40 (td, *J* = 8.1, 1.5 Hz, 1 H), 7.44 (d, *J* = 8.1 Hz, 1 H), 7.48 (d, *J* = 8.8 Hz, 2 H), 7.57 (d, *J* = 8.8 Hz, 2 H), 7.73 (td, *J* = 7.6, 1.6 Hz, 1 H), 8.02 (dd, *J* = 7.8, 1.5 Hz, 1 H), 10.48 (s, 1 H), 12.67 (s, 1 H). ¹³C NMR (101 MHz, DMSO-*d*₆) δ ppm 35.1, 114.9, 119.8, 121.0, 125.6, 126.0, 131.5, 134.6, 138.2, 148.0, 155.2, 161.0, 166.0; FTMS (ESI) m/z 391.9843 [M+H]⁺; calcd for C₁₆H₁₂BrN₃O₂S: 391.9886.

4.3.7. N-(4-Iodophenyl)-2-((4-oxo-3,4-dihydroquinazolin-2-yl)thio)acetamide (9g**):** Yield 86%; m.p.: 233.5 – 235.5 °C; HPLC 91% (*t_R* = 17.44 min); ¹H NMR (400 MHz, DMSO-*d*₆) δ ppm 4.17 (s, 2 H), 7.39-7.47 (m, 4 H), 7.64 (d, *J* = 7.6 Hz, 2 H), 7.74 (td, *J* = 8.5, 1.5 Hz, 1 H), 8.03 (dd, *J* = 8.1, 1.5 Hz, 1 H), 10.36 (s, 1 H), 12.58 (s, 1 H). ¹³C NMR (101 MHz, DMSO-*d*₆) δ ppm 34.9, 86.6, 119.8, 121.3, 125.5, 125.8, 134.4, 137.2, 138.5, 147.9, 155.1, 160.9, 165.9.; FTMS (ESI) m/z 437.9723 [M+H]⁺; calcd for C₁₆H₁₂IN₃O₂S: 437.9768.

4.3.8. N-(4-Nitrophenyl)-2-((4-oxo-3,4-dihydroquinazolin-2-yl)thio)acetamide (9h**):** Yield 50%; m.p.: 235.8 – 238.1°C; HPLC 95% (*t_R* = 16.75 min); ¹H NMR (400 MHz, DMSO-*d*₆) δ ppm 4.26 (s, 2 H), 7.40-7.44 (m, 2 H), 7.74 (td, *J* = 7.6, 1.6 Hz, 1 H), 7.88 (d, *J* = 9.7 Hz, 2 H), 8.04 (dd, *J* = 7.8, 1.5 Hz, 1 H), 8.25 (d, *J* = 9.7 Hz, 2 H), 11.00 (s, 1 H), 12.73 (s, 1 H). ¹³C NMR (101 MHz, DMSO-*d*₆) δ ppm 35.3, 118.8, 119.9, 125.0, 125.7, 126.1, 134.6, 142.3, 145.0, 148.1, 155.1, 161.0, 167.0; FTMS (ESI) m/z 357.0617 [M+H]⁺; calcd for C₁₆H₁₂N₄O₄S: 357.0652.

4.3.9. 2-((4-Oxo-3,4-dihydroquinazolin-2-yl)thio)-*N*-(4-propylphenyl)acetamide (9i**):** Yield 75%; m.p.: 209.8 – 212.1 °C; HPLC 95% (*t_R* = 17.83 min); ¹H NMR (400 MHz, DMSO-*d*₆) δ ppm 0.87 (t, *J* = 8.1 Hz, 3 H), 1.51-1.60 (m, 2 H), 2.47-2.52 (m, 2 H), 4.19 (s, 2 H), 7.13 (d, *J* = 7.6 Hz, 2 H), 7.42 (t, *J* = 7.6 Hz, 1 H), 7.51 (d, *J* = 6.8 Hz, 3 H), 7.76 (t, *J* = 7.6 Hz, 1 H), 8.05 (d, *J* = 7.8 Hz, 1 H), 10.29 (s, 1 H), 12.70 (s, 1 H). ¹³C NMR

(101 MHz, DMSO-*d*₆) δ ppm 13.5, 24.0, 35.1, 36.6, 119.2, 119.9, 125.7, 125.8, 126.0, 128.5, 134.6, 136.6, 137.2, 148.2, 155.3, 161.0, 165.6; FTMS (ESI) m/z 354.1236 [M+H]⁺; calcd for C₁₉H₁₉N₃O₂S: 354.1271.

4.3.10. 2-((4-Oxo-3,4-dihydroquinazolin-2-yl)thio)-*N*-(4-pentylphenyl)acetamide (**9j**): Yield 88%; m.p.: 218.2 – 219.6 °C; HPLC 94% (*t*_R = 18.52 min); ¹H NMR (400 MHz, DMSO-*d*₆) δ ppm 0.85 (t, *J* = 8.0 Hz, 3 H), 1.20-1.28 (m, 4 H), 1.51-1.57 (m, 2 H), 2.49-2.54 (m, 2 H), 4.17 (s, 2 H), 7.12 (d, *J* = 8.3 Hz, 2 H), 7.42 (t, *J* = 7.9, 1 H), 7.48-7.50 (m, 3 H), 7.75 (td, *J* = 7.6, 1.6 Hz, 1 H), 8.04 (dd, *J* = 7.9, 1.3 Hz, 1 H), 10.27 (s, 1 H), 12.69 (s, 1 H). ¹³C NMR (101 MHz, DMSO-*d*₆) δ ppm 13.8, 21.9, 30.6, 30.8, 34.5, 35.1, 119.2, 119.9, 125.7, 125.8, 126.0, 128.4, 134.6, 136.5, 137.4, 148.2, 155.2, 161.0, 165.6; FTMS (ESI) m/z 382.1546 [M+H]⁺; calcd for C₂₁H₂₃N₃O₂S: 382.1584.

4.3.11. *N*-(Naphthalen-2-yl)-2-((4-oxo-3,4-dihydroquinazolin-2-yl)thio)acetamide (**9k**): Yield 81%; m.p.: 219.3 – 221.5 °C; HPLC 95% (*t*_R = 17.37 min); ¹H NMR (400 MHz, DMSO-*d*₆) δ ppm 4.25 (s, 2 H), 7.36-7.43 (m, 3 H), 7.47 (t, *J* = 7.3 Hz, 2 H), 7.62 (d, *J* = 8.8 Hz, 1 H), 7.72 (t, *J* = 8.2 Hz, 1 H), 7.80 (dd, *J* = 11.1, 8.2 Hz, 1 H), 7.86 (d, *J* = 8.8 Hz, 1 H), 8.03 (d, *J* = 8.1 Hz, 1 H), 8.29 (s, 1 H), 10.57 (s, 1 H), 12.70 (s, 1 H). ¹³C NMR (101 MHz, DMSO-*d*₆) δ ppm 35.2, 115.3, 119.8, 119.9, 124.6, 125.7, 125.8, 126.0, 126.4, 127.3, 127.4, 128.4, 129.8, 133.4, 134.6, 136.5, 148.2, 155.3, 161.1, 166.1; FTMS (ESI) m/z 362.0942 [M+H]⁺; calcd for C₂₀H₁₅N₃O₂S: 362.0958.

4.3.12. (*S*)-2-((4-Oxo-3,4-dihydroquinazolin-2-yl)thio)-*N*-(1,2,3,4-tetrahydronaphthalen-2-yl)acetamide (**9l**): Yield 37%; m.p.: 244.1 – 245.0 °C; HPLC 93% (*t*_R = 17.31 min); ¹H NMR (400 MHz, DMSO-*d*₆) δ ppm 1.67-1.73 (m, 2 H), 1.87-1.91 (m, 2 H), 2.67-2.78 (m, 2 H), 3.95-4.04 (m, 2 H), 4.94-5.00 (m, 1 H), 7.01 (t, *J* = 7.3 Hz, 1 H), 7.08 (d, *J* = 7.1 Hz, 1 H), 7.11-7.17 (m, 2 H), 7.41-7.46 (m, 2 H), 7.77 (t, *J* = 7.7 Hz, 1 H), 8.04 (d, *J* = 7.8 Hz, 1 H), 8.60 (d, *J* = 8.8 Hz, 1 H), 12.66 (s, 1 H). ¹³C NMR (101 MHz, DMSO-*d*₆) δ ppm 19.9, 28.6, 29.6, 33.9, 46.9, 119.9, 125.6, 125.6, 125.8, 125.9, 126.6, 128.0, 128.6, 134.4, 136.9, 137.1, 148.2, 155.3, 161.0, 166.3; FTMS (ESI) m/z 366.1269 [M+H]⁺; calcd for C₂₀H₁₉N₃O₂S: 366.1271.

4.3.13. (*R*)-2-((4-Oxo-3,4-dihydroquinazolin-2-yl)thio)-*N*-(1,2,3,4-tetrahydronaphthalen-2-yl)acetamide (**9m**): Yield 80%; m.p.: 241.2 – 242.7 °C; HPLC 96% (*t*_R = 17.28 min); ¹H NMR (400 MHz, DMSO-*d*₆) δ ppm 1.66-1.72 (m, 2 H), 1.85-1.92 (m, 2 H), 2.64-2.73 (m, 2 H), 3.94-4.03 (m, 2 H), 4.96-5.00 (m, 1 H), 6.98-7.16 (m, 4 H), 7.40-7.44 (m, 2 H), 7.76 (t, *J* = 7.1 Hz, 1 H), 8.03 (d, *J* = 7.8 Hz, 1 H), 8.58 (d, *J* = 8.6 Hz, 1 H), 12.66 (s, 1 H). ¹³C NMR (101 MHz, DMSO-*d*₆) δ ppm 19.9, 28.6, 29.6, 33.9, 46.9, 119.9, 125.6, 125.6, 125.8, 125.9, 126.6, 128.0, 128.6, 134.4, 136.9, 137.1, 148.2, 155.3, 161.0, 166.3.; FTMS (ESI) m/z 366.1268 [M+H]⁺; calcd for C₂₀H₁₉N₃O₂S: 366.1271.

4.3.14. *N*-Cyclohexyl-2-((4-oxo-3,4-dihydroquinazolin-2-yl)thio)acetamide (**9n**): Yield 65%; m.p.: 219.0 – 221.3 °C; HPLC 91% (*t*_R = 16.17 min); ¹H NMR (400 MHz, DMSO-*d*₆) δ ppm 1.08-1.30 (m, 5 H), 1.52 (m, 1 H), 1.65-1.74 (m, 4 H), 3.50-3.60 (m, 1 H, 1'-H), 3.92 (s, 2 H, 9-H), 7.42 (td, *J* = 8.1, 1.5 Hz, 1 H, 6-H), 7.50 (d, *J* = 8.1 Hz, 1 H, 8-H), 7.77 (td, *J* = 7.6, 1.6 Hz, 1 H, 7-H), 8.03 (dd, *J* = 7.8, 1.5 Hz, 1 H, 5-H), 8.13 (d, *J* = 7.6 Hz, 1 H, HN), 12.65 (s, 1 H, NH, 3-H). ¹³C NMR (101 MHz, DMSO-*d*₆) δ ppm 24.3, 25.1, 32.2, 34.1, 47.9, 119.9, 125.6, 125.7, 125.9, 134.5, 148.2, 155.3, 161.0, 165.8; FTMS (ESI) m/z 318.1277 [M+H]⁺; calcd for C₁₆H₁₉N₃O₂S: 318.1271.

4.3.15. *N*-Cyclohexyl-*N*-methyl-2-((4-oxo-3,4-dihydroquinazolin-2-yl)thio)acetamide (9o**):** Yield 52%; m.p.: 184.2 – 185.2 °C; HPLC 97% (t_R = 17.43 min); ^1H NMR (400 MHz, DMSO-*d*₆) δ ppm 1.07-1.11 (m, 2 H), 1.25-1.35 (m, 4 H), 1.43-1.47 (m, 5 H), 1.48-1.57 (m, 4 H), 1.72-1.78 (m, 5 H), 2.74 and 3.01 (s, 2x NCH₃), 3.78 and 4.21 (m, 2x CH), 4.23 and 4.34 (s, 2x CH₂), 7.40-7.48 (m, 4x ArH), 7.74-7.79 (m, 2x ArH), 8.04 (d, J = 8.1, 2x ArH), 12.61 (s, 1 H, 2x HN). ^{13}C NMR (101 MHz, DMSO-*d*₆) δ ppm 24.7, 24.9, 25.1, 25.2, 27.2, 29.1, 29.6, 30.2, 33.1, 34.0, 52.5, 56.1, 119.9, 125.5, 125.6, 125.7, 125.8, 125.9, 126.0, 134.5, 134.6, 148.2, 148.3, 155.2, 155.5, 161.0, 166.3; FTMS (ESI) m/z 332.1419 [M+H]⁺; calcd for C₁₇H₂₀N₃O₂S: 332.1427.

4.3.16. *N*-(2-Methylcyclohexyl)-2-((4-oxo-3,4-dihydroquinazolin-2-yl)thio)acetamide (9p**):** Yield 55%; m.p.: 230.2 – 232.8 °C; HPLC 91% (t_R = 17.03 and 17.17 min); ^1H NMR (400 MHz, DMSO-*d*₆) δ ppm 0.81 (J = 6.6 Hz, 3 H), 0.93-1.02 (m, 1 H), 1.10-1.39 (m, 4 H), 1.59 (d, J = 11.2 Hz, 1 H), 1.69 (q, J = 13 Hz, 2 H), 3.23-3.29 (m, 1 H), 3.89-4.01 (m, 2 H), 7.42 (t, J = 7.5 Hz, 1 H), 7.50 (d, J = 8.1 Hz, 1 H), 7.77 (t, J = 7.6 Hz, 1 H), 8.04 (d, J = 8.1 Hz, 2 H), 12.66 (s, 1 H). ^{13}C NMR (101 MHz, DMSO-*d*₆) δ ppm 19.0, 25.0, 25.3, 32.7, 33.8, 34.1, 37.2, 49.2, 53.8, 119.9, 125.6, 125.8, 126.0, 134.5, 148.3, 155.4, 161.0, 166.1; FTMS (ESI) m/z 332.1414 [M+H]⁺; calcd for C₁₇H₂₁N₃O₂S: 332.1427.

4.3.17. *N*-(3-Methylcyclohexyl)-2-((4-oxo-3,4-dihydroquinazolin-2-yl)thio)acetamide (9q**):** Yield 35%; m.p.: 219.2 – 223.2 °C; HPLC 94% (t_R = 17.24 and 17.47 min); ^1H NMR (400 MHz, DMSO-*d*₆) δ ppm 0.71-0.90 (m, 7 H), 1.00-1.10 (m, 1 H), 1.20-1.29 (m, 2 H), 1.35-1.51 (m, 2 H), 1.58 (d, J = 12.5 Hz, 1 H), 1.75 (d, J = 11.7 Hz, 2 H), 3.52-3.54 (m, 1 H), 3.91 (s, 2 H), 7.42 (t, J = 8.1, 1 H), 7.50 (d, J = 8.1 Hz, 1 H), 7.77 (t, J = 7.7 Hz, 1 H), 8.04 (d, J = 8.1 Hz, 1 H), 8.12 (d, J = 7.1 Hz, 1 H), 12.64 (s, 1 H). ^{13}C NMR (101 MHz, DMSO-*d*₆) δ ppm 22.2, 24.4, 31.3, 31.9, 33.8, 34.2, 41.2, 48.3, 120.0, 125.6, 125.8, 126.0, 134.4, 148.3, 155.3, 161.0, 165.9; FTMS (ESI) m/z 332.1415 [M+H]⁺; calcd for C₁₇H₂₁N₃O₂S: 332.1427.

4.3.18. *N*-(4-Methylcyclohexyl)-2-((4-oxo-3,4-dihydroquinazolin-2-yl)thio)acetamide (9r**):** Yield 45%; m.p.: 199.2 – 200.8 °C; HPLC 90% (t_R = 17.23 min); ^1H NMR (400 MHz, DMSO-*d*₆) δ ppm 0.80 (d, J = 6.6 Hz, 3 H), 0.84 (d, J = 6.6 Hz, 1 H), 0.89-0.99 (m, 1 H), 1.14-1.23 (m, 4 H), 1.39-1.48 (m, 6 H), 1.55-1.65 (m, 3 H), 1.77 (d, J = 11.0 Hz, 1 H), 3.5 (m, 1 H), 4.2 (s, 2 H), 7.3-7.4 (m, 3 H), 7.4 (t, J = 7.3 Hz, 2 H), 7.6 (d, J = 8.8 Hz, 1 H), 7.7 (t, J = 8.2 Hz, 1 H), 7.8 (dd, J = 11.1, 8.2 Hz, 1 H), 7.9 (d, J = 8.8 Hz, 1 H), 8.0 (d, J = 8.1 Hz, 1 H), 8.3 (s, 1 H), 10.6 (s, 1 H), 12.7 (s, 1 H). ^{13}C NMR (101 MHz, DMSO-*d*₆) δ ppm 35.2, 115.3, 119.8, 119.9, 124.6, 125.7, 125.8, 126.0, 126.4, 127.3, 127.4, 128.4, 129.8, 133.4, 134.6, 136.5, 148.2, 155.3, 161.1, 166.1; FTMS (ESI) m/z 332.1414 [M+H]⁺; calcd for C₁₇H₂₁N₃O₂S: 332.1427.

4.3.19. *N*-(*trans*-4-Methylcyclohexyl)-2-((4-oxo-3,4-dihydroquinazolin-2-yl)thio)acetamide (9s**):** Yield 59%; m.p.: 223.4 – 225.8 °C; HPLC 91% (t_R = 17.29 min); ^1H NMR (400 MHz, DMSO-*d*₆) δ ppm 0.85 (d, J = 6.6 Hz, 3 H), 0.92-0.99 (m, 2 H), 1.13-1.23 (m, 2 H), 1.26-1.35 (m, 1 H), 1.65 (d, J = 11.7 Hz, 2 H), 1.76 (d, J = 11.0 Hz, 2 H), 3.47-3.50 (m, 1 H), 3.91 (s, 2 H), 7.42 (t, J = 8.1 Hz, 1 H), 7.49 (d, J = 8.1 Hz, 1 H), 7.77 (td, J = 7.7, 1.5 Hz, 1 H), 8.03 (dd, J = 8.1, 1.5 Hz, 1 H), 8.11 (d, J = 7.1 Hz, 1 H), 12.65 (s, 1 H). ^{13}C NMR (101 MHz, DMSO-*d*₆) δ ppm 22.0, 31.3, 32.1, 33.4, 34.1,

48.2, 119.9, 125.6, 125.8, 125.9, 134.5, 148.3, 155.3, 161.0, 165.9; FTMS (ESI) m/z 332.1433 [M+H]⁺; calcd for C₁₇H₂₁N₃O₂S: 332.1427.

4.3.20. *N*-Cyclopentyl-2-((4-oxo-3,4-dihydroquinazolin-2-yl)thio)acetamide (**9t**): Yield 60%; m.p.: 214.5 – 242.9 °C; HPLC 98% (*t_R* = 16.38 min); ¹H NMR (400 MHz, DMSO-*d*₆) δ ppm 1.38-1.41 (m, 2 H), 1.47-1.51 (m, 2 H), 1.57-1.64 (m, 2 H), 1.73-1.81 (m, 2 H), 3.90 (s, 2 H), 3.95-4.03 (m, 1 H), 7.41 (td, *J* = 8.1, 1.5 Hz, 1 H), 7.48 (d, *J* = 8.1 Hz, 1 H), 7.76 (td, *J* = 8.4, 1.5 Hz, 1 H), 8.02 (dd, *J* = 8.1, 1.5 Hz, 1 H), 8.20 (d, *J* = 7.1 Hz, 1 H), 12.64 (s, 1 H). ¹³C NMR (101 MHz, DMSO-*d*₆) δ ppm 23.3, 32.1, 34.0, 50.6, 119.9, 125.6, 125.7, 125.9, 134.5, 148.2, 155.3, 161.0, 166.2; FTMS (ESI) m/z 304.1119 [M+H]⁺; calcd for C₁₅H₁₇N₃O₂S: 304.1114.

4.3.21. *N*-Cycloheptyl-2-((4-oxo-3,4-dihydroquinazolin-2-yl)thio)acetamide (**9u**): Yield 76%; m.p.: 223.0 – 223.3 °C; HPLC 97% (*t_R* = 17.26 min); ¹H NMR (400 MHz, DMSO-*d*₆) δ ppm 1.33-1.55 (m, 10 H), 1.75-1.16 (m, 2 H), 3.72-3.75 (m, 1 H), 3.91 (s, 2 H), 7.42 (td, *J* = 8.0, 1.2 Hz, 1 H), 7.49 (d, *J* = 8.1 Hz, 1 H), 7.77 (td, *J* = 8.4, 1.5 Hz, 1 H), 8.01 (dd, *J* = 7.8, 1.5 Hz, 1 H), 8.16 (d, *J* = 7.8 Hz, 1 H), 12.65 (s, 1 H). ¹³C NMR (101 MHz, DMSO-*d*₆) δ ppm 23.6, 27.7, 34.0, 50.0, 119.9, 125.6, 125.7, 125.9, 134.5, 148.2, 155.3, 161.0, 165.5; FTMS (ESI) m/z 332.1432 [M+H]⁺; calcd for C₁₇H₂₁N₃O₂S: 332.1427.

4.3.22. *N*-Benzyl-2-((4-oxo-3,4-dihydroquinazolin-2-yl)thio)acetamide (**9v**): Yield 41%; m.p.: 188.8 – 191.6 °C; HPLC 96% (*t_R* = 16.32 min); ¹H NMR (400 MHz, DMSO-*d*₆) δ ppm 4.03 (s, 2 H), 4.31 (d, *J* = 6.1 Hz, 2 H), 7.18-7.26 (m, 5 H), 7.41-7.48 (m, 2 H), 7.77 (td, *J* = 7.7, 1.5 Hz, 1 H), 8.04 (dd, *J* = 7.8, 1.5 Hz, 1 H), 8.71 (t, *J* = 5.7 Hz, 1 H), 12.64 (s, 1 H). ¹³C NMR (101 MHz, DMSO-*d*₆) δ ppm 33.7, 42.4, 119.9, 125.6, 125.9, 126.6, 126.9, 128.1, 134.5, 139.0, 148.2, 155.1, 161.0, 166.9; FTMS (ESI) m/z 326.0924 [M+H]⁺; calcd for C₁₇H₁₅N₃O₂S: 326.0958.

4.3.23. *N*-(Cyclohexylmethyl)-2-((4-oxo-3,4-dihydroquinazolin-2-yl)thio)acetamide (**9w**): Yield 46%; m.p.: 231.0 – 231.9 °C; HPLC 97% (*t_R* = 17.20 min); ¹H NMR (400 MHz, DMSO-*d*₆) δ ppm 0.78-0.87 (m, 2 H), 1.05-1.10 (m, 3 H), 1.36-1.40 (m, 1 H), 1.57-1.64 (m, 5 H), 2.93 (t, *J* = 6.4 Hz, 2 H), 3.93 (s, 2 H), 7.42 (td, *J* = 8.1, 1.5 Hz, 1 H), 7.50 (d, *J* = 8.1 Hz, 1 H), 7.76 (td, *J* = 7.7, 1.5 Hz, 1 H), 8.03 (dd, *J* = 7.8, 1.2 Hz, 1 H), 8.15 (t, *J* = 7.8 Hz, 1 H), 12.64 (s, 1 H). ¹³C NMR (101 MHz, DMSO-*d*₆) δ ppm 25.2, 25.8, 30.2, 33.8, 37.4, 45.1, 119.9, 125.6, 125.8, 125.9, 134.4, 148.2, 155.2, 161.0, 166.7; FTMS (ESI) m/z 332.1432 [M+H]⁺; calcd for C₁₇H₂₁N₃O₂S: 332.1427.

4.3.24. (*S*)-*N*-(1-Cyclohexylethyl)-2-((4-oxo-3,4-dihydroquinazolin-2-yl)thio)acetamide (**9x**): Yield 59%; m.p.: 232.5 – 236.7 °C; HPLC 91% (*t_R* = 17.42 min); ¹H NMR (400 MHz, DMSO-*d*₆) δ ppm 0.84-1.13 (m, 7 H), 1.01 (d, *J* = 6.8 Hz, 3 H), 1.22-1.26 (m, 1 H), 1.54-1.69 (m, 6 H), 3.58-3.67 (m, 1 H), 3.89 (d, *J* = 14.9 Hz, 1 H), 3.98 (d, *J* = 14.9 Hz, 1 H), 7.42 (t, *J* = 7.5 Hz, 1 H), 7.51 (d, *J* = 8.1 Hz, 1 H), 7.77 (t, *J* = 7.1 Hz, 1 H), 7.97 (d, *J* = 7.8 Hz, 1 H), 8.04 (d, *J* = 8.6 Hz, 1 H), 12.65 (s, 1 H). ¹³C NMR (101 MHz, DMSO-*d*₆) δ ppm 17.5, 18.4, 25.6, 25.8, 28.5, 28.7, 34.0, 42.4, 49.0, 56.0, 119.5, 119.9, 125.6, 125.8, 125.9, 134.5, 148.2, 155.3, 161.0, 166.1; FTMS (ESI) m/z 346.1577 [M+H]⁺; calcd for C₁₈H₂₃N₃O₂S: 346.1584.

4.3.25. (*R*)-*N*-(1-Cyclohexylethyl)-2-((4-oxo-3,4-dihydroquinazolin-2-yl)thio)acetamide (**9y**): Yield 82%, m.p.: 217.2 – 217.9 °C; HPLC 91% (*t_R* = 17.81); ¹H NMR (400 MHz, DMSO-*d*₆) δ ppm 0.83-0.95 (m, 2 H), 1.00 (d, *J* = 6.8 Hz, 3 H), 1.03-

1.16 (m, 2 H), 1.23-1.29 (m, 1 H), 1.53-1.69 (m, 5 H), 3.57-3.64 (m, 1 H), 3.89 (d, $J=14.9$ Hz, 1 H), 3.98 (d, $J=14.9$ Hz, 1 H), 7.42 (t, $J=7.5$ Hz, 1 H), 7.50 (d, $J=8.1$ Hz, 1 H), 7.77 (t, $J=7.6$ Hz, 1 H), 7.97 (d, $J=7.8$ Hz, 1 H), 8.04 (d, $J=8.6$ Hz, 1 H), 12.66 (s, 1 H). ^{13}C NMR (101 MHz, DMSO- d_6) δ ppm 17.5, 25.6, 25.8, 28.5, 28.7, 34.0, 42.4, 49.0, 119.9, 125.6, 125.8, 125.9, 134.5, 148.2, 155.3, 161.0, 166.0; FTMS (ESI) m/z 346.1606 [M+H] $^+$; calcd for C₁₈H₂₃N₃O₂S: 346.1584.

4.3.26. 2-((2-Oxo-2-(piperidin-1-yl)ethyl)thio)quinazolin-4(3*H*)-one (**9z**): Yield 72%; m.p.: 118.5 – 121.0 °C; HPLC 98% ($t_{\text{R}}=16.34$ min); ^1H NMR (400 MHz, DMSO- d_6) δ ppm 1.46 (m, 2 H), 1.62 (m, 4 H), 3.55 (m, 2 H), 3.51-3.56 (m, 2 H), 4.29 (s, 2 H), 7.42 (t, $J=7.5$ Hz, 1 H), 7.50 (d, $J=8.1$ Hz, 1 H), 7.76 (t, $J=7.2$ Hz, 1 H), 8.04 (d, $J=7.6$ Hz, 1 H), 12.62 (s, 1H). ^{13}C NMR (101 MHz, DMSO- d_6) δ ppm 23.8, 25.2, 26.0, 33.3, 42.7, 46.6, 119.9, 125.6, 125.8, 126.0, 134.5, 148.2, 155.4, 161.0, 165.0; FTMS (ESI) m/z 304.1117 [M+H] $^+$; calcd for C₁₅H₁₇N₃O₂S: 304.1140.

4.4 *Mycobacterium tuberculosis* inhibition assay

The measurement of the minimum inhibitory concentration (MIC) for each tested compound was performed in 96-well U-bottom polystyrene microplates. Isoniazid (positive control) and the compound solutions were prepared at 1 mg/mL concentration in dimethylsulfoxide (DMSO). They were diluted in Middlebrook 7H9 medium containing 10% ADC (albumin, dextrose, catalase) to a concentration between 10 and 20 µg/mL of each compound containing 5% DMSO. Serial two-fold dilutions of each drug in 100 µL of Middlebrook 7H9 medium containing 10% ADC were prepared directly in 96-well plates at concentration ranges of 10.0 to 0.02 µg/mL, or 0.02 to 0.0004 µg/mL. Growth controls containing no antibiotics, and sterile controls without inoculation, were included. The MIC was determined for *M. tuberculosis* H37Rv and for the clinical isolates CDCT10 (1009/09), CDCT16 (630/08), CDCT27 (0128/09) and CDCT28 (1051/10). Mycobacterium strains were grown in Middlebrook 7H9 containing 10% OADC (oleic acid, albumin, dextrose and catalase) and 0.05% Tween 80. The cells were vortexed with sterile glass beads (4 mm) for 5 min to disrupt any clumps and were allowed to settle for 20 min. The supernatant was measured spectrophotometrically at an absorbance of 600 nm. The Mtb suspensions were divided into aliquots and stored at –20 °C. Each

suspension was appropriately diluted in Middlebrook 7H9 broth containing 10% ADC to achieve an optical density at 600 nm of 0.006, and 100 µL was added to each well of the plate except the sterile controls. A 2.5% DMSO final concentration was maintained in each well. The plates were covered, sealed with parafilm, and incubated at 37 °C. After 7 days of incubation, 60 µL of 0.01% resazurin solution was added to each well, and the samples were incubated for an addition 48 h at 37 °C [16, 17]. A change in color from blue to pink indicated bacterial growth, and the MIC was defined as the lowest drug concentration that prevented the color change. Three tests were performed independently, and the MIC values reported here were observed in at least two experiments, or they were the highest values observed among the three assays.

4.5 Cytotoxicity investigation

Cellular viability determination after incubation with the test compounds was performed by using two different methods: the neutral red uptake assay [19] and the MTT method [10]. Briefly, HepG2, HaCat, and Vero cells were grown in DMEM media (Dulbecco's Modified Eagle Medium) supplemented with 10% inactivated fetal bovine serum and 1% antibiotic (penicillin–streptomycin). Cells were seeded at 2×10^3 (HepG2 or HaCat) or 1×10^3 cells/well (Vero) in a 96-well microtiter plate and incubated for 24 h. The medium was carefully aspirated and replaced with 90 µL DMEM, and 10 µL of the different treatment drugs, resulting in a final concentration of 10 µg/mL (DMSO 2%, v/v). Test compounds were incubated with the cell lines for 72 h at 37 °C under 5% CO₂. For the MTT assay, the cultures were incubated with MTT reagent (1 mg/mL) for 3 h. The formazan crystals were dried in room temperature for at least 24 h and dissolved in DMSO. The absorbance was measured at 595 nm (Spectra Max M2e, Molecular Devices,

USA). The precipitated purple formazan crystals were directly proportional to the number of live cells with active mitochondria.

For the neutral red assay, after 72 h of incubation with the compounds, cells were washed with PBS before the addition of 250 µL of neutral red dye solution (25 µg/mL, Sigma) prepared in serum-free medium. The plate was incubated for additional 3 h at 37 °C under 5% CO₂. After incubation, cells were washed with PBS followed by incubation with 100 µL of a desorb solution (CH₃COOH/EtOH/H₂O, 1:50:49) for 30 min with gentle shaking to extract neutral red from the viable cells. The absorbance was analyzed at 540 nm using a microtiter plate reader. The percentage of cell viability for treated groups was reported considering the control wells (DMSO 2%-treated) as 100% of cell viability: cell viability (%) = (absorbance of treated wells/absorbance of control wells) x 100. Data were expressed as mean of cell viability ± standard error of mean of three independent experiments performed in triplicate. The statistical analysis was accomplished by one-way analysis of variance, followed by Bonferroni's post-test, using GraphPad Prism 5.0 software (San Diego, CA, USA). Differences were considered significant at the 95% level of confidence.

4.6 Treatment and Zebrafish embryo maintenance

Zebrafish embryos (AB strain) were obtained from natural mating of adult *Danio rerio* bred and maintained in an automated re-circulating tank system (Tecniplast, Italy) [21]. After spawning, viable embryos were collected and maintained in sterile petri dishes, kept in an incubator with light-dark cycle of 14–10 h and controlled temperature (28 °C) [21]. At 2 hpf (hours post-fertilization) embryos were treated with different concentrations (3.0, 15.0 and 20.0 µM) of 3,4-dihydroquinazolin-4-ones **9n**, **9p-s**, **9u** and **9w** until 5 dpf (days post-fertilization). All compounds were diluted in 100% DMSO for

stock solutions and diluted in fish water (Reverse Osmosis equilibrated with Instant Ocean Salt) to final concentrations of 3.0, 15.0 and 20.0 μM (diluted in 1% DMSO). Since compounds were diluted first in DMSO, there were two control groups for each treatment: one with fish water only and the other with 1% DMSO. Survival and hatching efficiency were monitored daily under a stereomicroscope (Nikon, Melville, USA). All protocols were approved by the Institutional Animal Care Committee from Pontifical Catholic University of Rio Grande do Sul (CEUA-PUCRS, permit number 7249).

4.6.1 Morphological evaluation

Morphological evaluation larvae were monitored daily and registered at 2 and 5 dpf under a stereomicroscope (3 \times) ($n = 30$). The body length (μm), ocular distance (μm) and surface area of the eyes (μm^2) was measured after photographic registration using the software NIS-Elements D 3.2 for Windows, supplied by Nikon Instruments Inc. (Melville, USA). The body length was considered as the distance from the center of an eye to the tip of the tail bud. The ocular distance was assumed to be the distance between the inner edge between the two eyes, and the size of the eyes was assumed as the surface area of the eyes [22].

4.6.2 Cardiotoxicity and cardiac evaluation

Animals were analyzed for heartbeat rate at 2 and 5 dpf under a stereomicroscope ($n = 30$). Treated larvae and controls were placed in petri dishes with mineral water and their heart rate was monitored for 60 s. For all procedures, temperature was kept stable at 28 °C [23].

4.6.3 Neurotoxicity and exploratory behavior evaluation.

Five-day-old larvae were placed individually in a 24-well plate filled with 3 mL of water or respective solution treatment for exploratory performance analysis during a 5 min session following 1 min acclimation [25]. The performance was video-recorded for automated analysis using EthoVision XT software (version 11.5, Noldus), which is able to track the swimming activity of the animals at a rate of 15 positions per second. Total distance travelled (cm) was considered the parameter of exploration of a new environment [22].

4.6.4 Statistical analysis for Zebrafish assays

Survival and hatching rate throughout the five days of experimental treatment was analyzed by Kaplan-Meier test. Data of heartbeat rate, morphological evaluation and exploratory behavior were evaluated using one-way ANOVA followed by post-hoc Tukey's test.

Acknowledgments

This work was supported by FAPERGS-CAPES-CNPq [grant number 465318/2014-2] to C. V. Bizarro, L. A. Basso, D. S. Santos and P. Machado. C. D. Bonan, C. V. Bizarro, L. A. Basso, D. S. Santos and P. Machado are Research Career Awardees of the National Research Council of Brazil (CNPq). The fellowships from BNDES (F. S. Macchi, K. Pissinate, A. D. Villela, V. Rodrigues-Junior, A. S. Dada), CAPES (B. L. Abbadi, F. T. Subtil), CNPq (N. Sperotto, T. F. Freitas), and FAPERGS (A. F. Borsoi) are also acknowledged.

References

1. M. Pai, M.A. Behr, D. Dowdy, K. Dheda, M. Divangahi, C.C. Boehme, A. Ginsberg, S. Swaminathan, M. Spigelman, H. Getahun, D. Menzies, M. Raviglione. *Tuberculosis*. Nat Rev Dis Primers 2 (2016) 16076. doi: 10.1038/nrdp.2016.76
2. Global tuberculosis report 2016, World Health Organization. Available from: <http://www.who.int/tb/publications/2016/en/>, (accessed in October 2017).
3. A. Koul, E. Arnoult, N. Lounis, J. Guillemont, K. Andries. The challenge of new drug discovery for tuberculosis. *Nature* 469 (2011) 483. doi:10.1038/nature09657.
4. World Health Organization. Global Tuberculosis Control: Surveillance, Planning, Financing. WHO Report 2003. Available from: http://apps.who.int/iris/bitstream/10665/63835/14/WHO_CDS_TB_2003.316.pdf, (accessed in October 2017).
5. S. Tiberi, R. Buchanan, J.A. Caminero, R. Centis, M.A. Arbex, M.A. Salazar-Lezama, J. Potter, G.B. Migliori. The challenge of the new tuberculosis drugs. *Press Medicale* 46 (2017) 41–51. <http://dx.doi.org/10.1016/j.lpm.2017.01.016>
6. Global tuberculosis report 2015, World Health Organization. Available from: <http://www.who.int/tb/publications/2015/en/>, (accessed in October 2017).
7. R.S. Wallis, M. Maeurer, P. Mwaba, J. Chakaya, R. Rustomjee, G.B. Migliori, B. Marais, M. Schito, G. Churchyard, S. Swaminathan, M. Hoelscher, A. Zumla. Tuberculosis-advances in development of new drugs, treatment regimens, host-directed therapies, and biomarkers. *Lancet Infect Dis* 16 (2016) 34. [http://dx.doi.org/10.1016/S1473-3099\(16\)00070-0](http://dx.doi.org/10.1016/S1473-3099(16)00070-0)
8. G.V. Bloomberg, P.M. Keller, D. Stucki, A. Trauner, S. Borrell, T. Latshang, M.

- Coscolla, T. Rothe, R. Hömke, C. Ritter, J. Feldmann, B. Schulthess, S. Gagneux, E.C. Böttger. Acquired Resistance to Bedaquiline and Delamanid in Therapy for Tuberculosis. *N Engl J Med* 373 (2015)1986.
9. K. Pissinate, A.D. Villela, V. Rodrigues-Junior, B.C. Giacobbo, E.S. Grams, B.L. Abbadi, R.V. Trindade, L. Roesler Nery, C.D. Bonan, D.F. Back, M.M. Campos, L.A. Basso, D.S. Santos, P. Machado. 2-(Quinolin-4-yloxy)acetamides Are Active against Drug-Susceptible and Drug-Resistant *Mycobacterium tuberculosis* Strains. *ACS Med Chem Lett* 7 (2016) 35.
10. B.C. Giacobbo, K. Pissinate, V. Rodrigues-Junior, A.D. Villela, E.S. Grams, B.L. Abbadi, F.T. Subtil, N. Sperotto, R.V. Trindade, D.F. Back, M.M. Campos, L.A. Basso, P. Machado, D.S. Santos. New insights into the SAR and drug combination synergy of 2-(quinolin-4-yloxy)acetamides against *Mycobacterium tuberculosis*. *Eur J Med Chem* 126 (2017) 491.
11. F.T. Subtil, A.D. Villela, B.L. Abbadi, V.S. Rodrigues-Junior, C.V. Bizarro, L.F.S.M. Timmers, O.N. de Souza, K. Pissinate, P. Machado, A. López-Gavín, G. Tudó, J. González-Martín, L.A. Basso, D.S. Santos. Activity of 2-(quinolin-4-yloxy)acetamides in *Mycobacterium tuberculosis* clinical isolates and identification of their molecular target by whole genome sequencing. *Int J Antimicrob Agents* pii:S0924-8579 (2017). doi: 10.1016/j.ijantimicag.2017.08.023.
12. N. Phummarin, H. I. Boshoff, P.S. Tsang, J. Dalton, S. Wiles, C.E. Barry 3rd, B.R, Copp. SAR and identification of 2-(quinolin-4-yloxy)acetamides as *Mycobacterium tuberculosis* cytochrome bc₁ inhibitors. *Med Chem Commun* 7 (2016) 2122. doi: 10.1039/c6md00236f
13. J. Rybníkář, A. Vocat, C. Sala, P. Busso, F. Pojer, A. Benjak, S.T. Cole.

- Lansoprazole is an antituberculous prodrug targeting cytochrome bc1. *Nat Commun* 6 (2015).
14. G.S. Pedgaonkar, J.P. Sridevi, V.U. Jeankumar, S. Saxena, P.B. Devi, J. Renuka, P. Yogeeshwari, D. Sriram. Development of 2-(4-oxoquinazolin-3(4H)-yl)acetamide derivatives as novel enoyl-acyl carrier protein reductase (InhA) inhibitors for the treatment of tuberculosis. *Eur J Med Chem* 86 (2014) 613. <http://dx.doi.org/10.1016/j.ejmech.2014.09.028>
15. R.S.N. Munuganti, E. Leblanc, P. Axerio-Cilieis, C. Labriere, K. Frewin, K. Singh, M.D. Hassona, N.A. Lack, H. Li, F. Ban, E. Tomlinson Guns, R. Young, P.S. Rennie, A. Cherkasov. Targeting the Binding Function 3 (BF3) Site of the Androgen Receptor Through Virtual Screening. 2. Development of 2-((2-phenoxyethyl) thio)-1 H -benzimidazole Derivatives. *J Med Chem* 56 (2013) 1136. doi: 10.1021/jm3015712.
16. Ballell L, Bates RH, Young RJ, Alvarez-Gomez D, Alvarez-Ruiz E, Barroso V, et al. Fueling open-source drug discovery: 177 small-molecule leads against tuberculosis. *ChemMedChem* 8(2013) 313. doi: 10.1002/cmdc.201200428.
17. J. Palomino, A. Martin, M. Camacho, H. Guerra, J. Swings, F. Portaels. Resazurin Microtiter Assay Plate : Simple and Inexpensive Method for Detection of Drug Resistance in *Mycobacterium tuberculosis* Resazurin Microtiter Assay Plate : Simple and Inexpensive Method for Detection of Drug Resistance in *Mycobacterium tuberculosis*. *Antimicrobail Agents Chemother* 46 (2002) 2720.
18. E.L. White, C. Maddox, N.M. Nebane, N.A. Tower, S. McKellip, A. Manuvakhova, L. Reddy, M. Sosa, L. Rasmussen, K. Whig, S. Ananthan, S. Lun, W. Bishai, W. S. Weiner, F. Schoenen, A. Dutta, J. Aubé. Discovery and Development of Highly Potent Inhibitors of *Mycobacterium tuberculosis* Growth

- In Vitro. Probe Reports from the NIH Molecular Libraries Program 50 (2013).
19. G. Repetto, A. del Peso, J.L. Zurita. Neutral red uptake assay for the estimation of cell viability/cytotoxicity. Nat Protoc 3 (2008) 1125. doi: 10.1038/nprot.2008.75.
 20. Tuberculosis Antimicrobial Acquisition & Coordinating Facility (TAACF): Description of TAACF Assays.
 21. M. Westerfield. The Zebrafish Book: A guide for the laboratory use of zebrafish (*Danio rerio*). 4th ed. University of Oregon Press; 2000. Available at: https://zfin.org/zf_info/zfbook/zfbk.html (accessed in October 2017).
 22. S. Altenhofen, D.D. Nabinger, M.T. Wiprich, T.C.B. Pereira, M.R. Bogo, C.D. Bonan. Tebuconazole alters morphological, behavioral and neurochemical parameters in larvae and adult zebrafish (*Danio rerio*). Chemosphere 180 (2017) 483. doi: 10.1016/j.chemosphere.2017.04.029
 23. L.K.B. Martinelli, M. Rotta, A.D. Villela, V.S. Rodrigues-Junior, B.L. Abbadi, R.V. Trindade, G.O. Petersen, G.M. Danesi, L.R. Nery, I. Pauli, M.M. Campos, C.D. Bonan, O.N. de Souza, L.A. Basso, D.S. Santos. Functional, thermodynamics, structural and biological studies of in silico-identified inhibitors of *Mycobacterium tuberculosis* enoyl- ACP(CoA) reductase enzyme. Nat Publ Gr 24 (2017). doi: 10.1038/srep46696.
 24. J. Avorn. Approval of a Tuberculosis Drug Based on a Paradoxical Surrogate Measure. JAMA 309 (2013) 1349. doi: 10.1001/jama.2013.623.
 25. R.M. Colwill, R. Creton. Imaging escape and avoidance behavior in zebrafish larvae. Rev Neurosci 22 (2011) 63. doi: 10.1515/RNS.2011.008.

Supporting Information

1*H*-Benzo[*d*]imidazoles and 3,4-dihydroquinazolin-4-ones: design, synthesis and antitubercular activity

Fernanda Souza Macchi, Kenia Pissinate, Anne Drumond Villela, Bruno Lopes Abbadi, Valnês Rodrigues-Junior, Débora Dreher Nabinger, Stefani Altenhofen, Nathalia Sperotto, Adílio da Silva Dadda, Fernanda Teixeira Subtil, Talita Freitas de Freitas, Ana Paula Erhart Rauber, Ana Flávia Borsoi, Carla Denise Bonan, Cristiano Valim Bizarro, Luiz Augusto Basso, Diógenes Santiago Santos, Pablo Machado*

TABLE OF CONTENTS

- 1.** ^1H NMR and ^{13}C NMR spectra of synthesized compounds
- 2.** Determination of stability of the 3,4-dihydroquinazolin-4-ones **9n**, **9p-s**, **9u**, and **9w** in aqueous media

1. ^1H NMR and ^{13}C NMR spectra of synthesized compounds

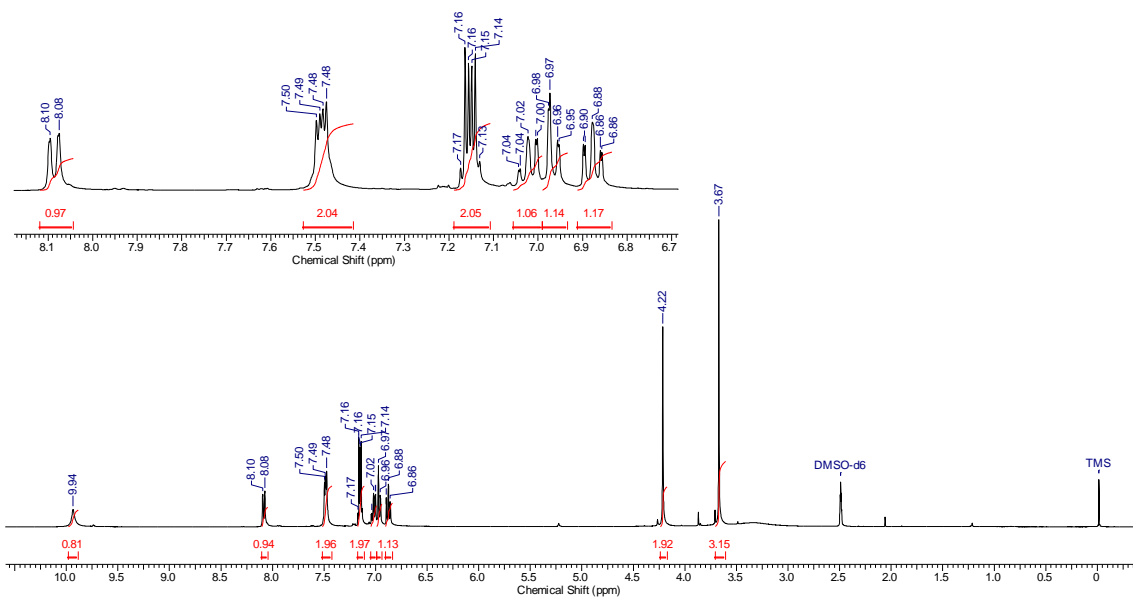


Figure S1. ^1H RMN spectrum of 2-((1*H*-Benzo[*d*]imidazol-2-yl)thio)-*N*-(2-methoxyphenyl)acetamide (**6a**) in DMSO-*d*₆

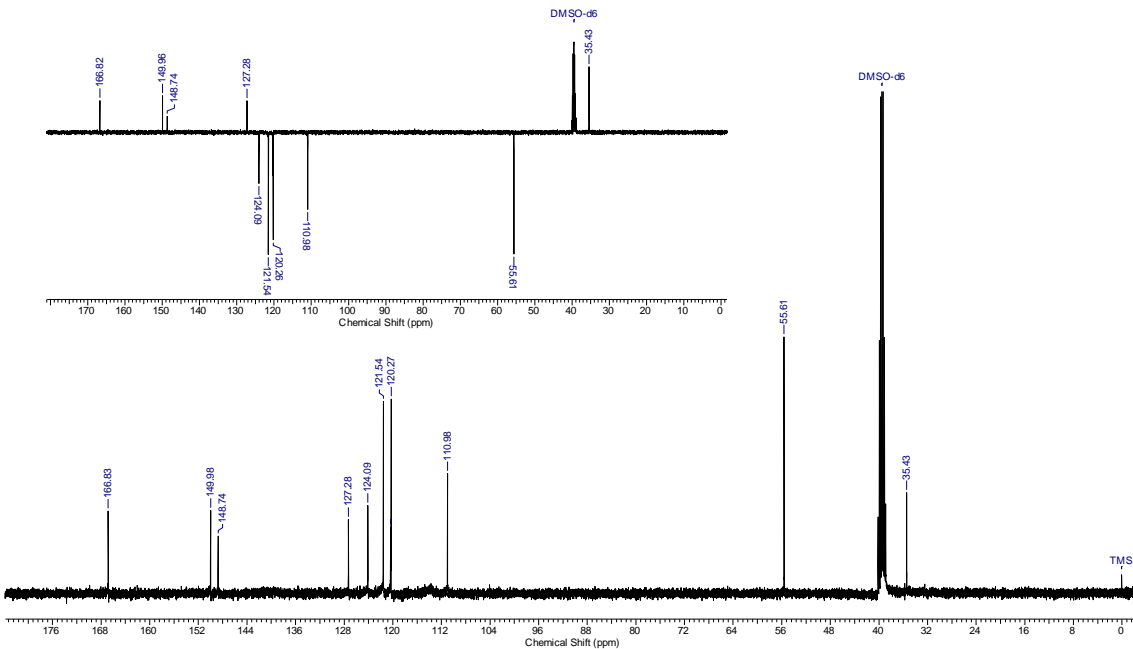


Figure S2. ^{13}C RMN spectrum of 2-((1*H*-Benzo[*d*]imidazol-2-yl)thio)-*N*-(2-methoxyphenyl)acetamide (**6a**) in DMSO-*d*₆.

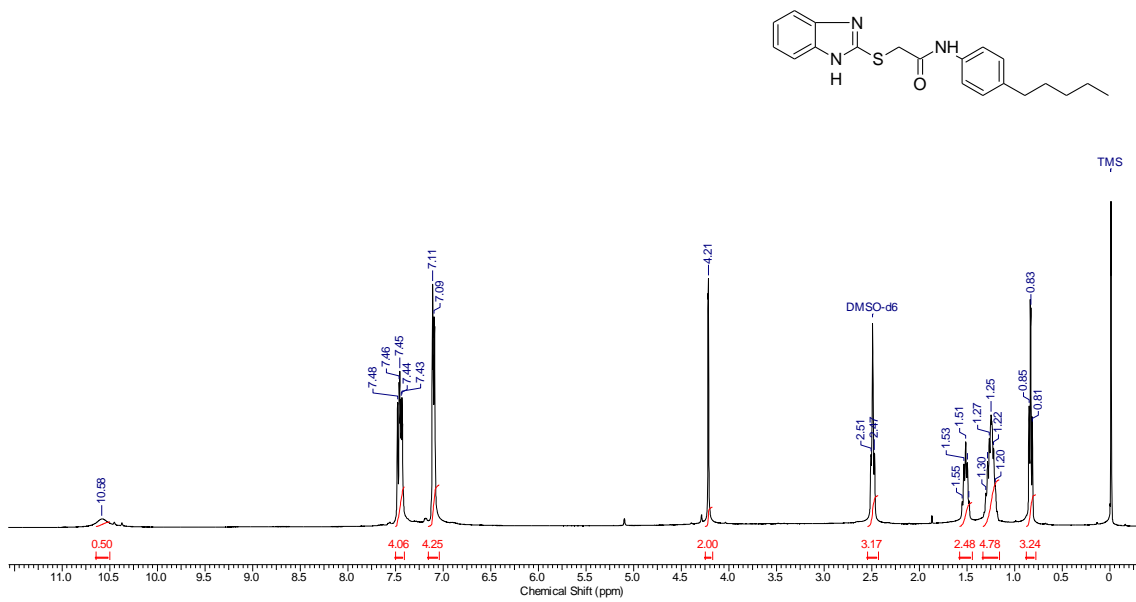


Figure S3. ^1H RMN spectrum of 2-((1*H*-Benzodimidazol-2-yl)thio)-*N*-(4-pentylphenyl)acetamide (**6b**) in $\text{DMSO}-d_6$

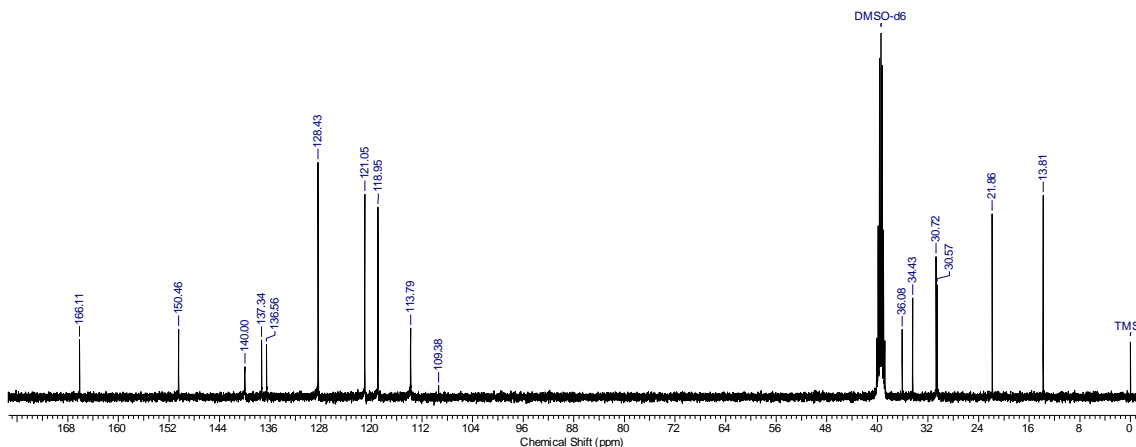


Figure S4. ^{13}C RMN spectrum of 2-((1*H*-Benzodimidazol-2-yl)thio)-*N*-(4-pentylphenyl)acetamide (**6b**) in $\text{DMSO}-d_6$.

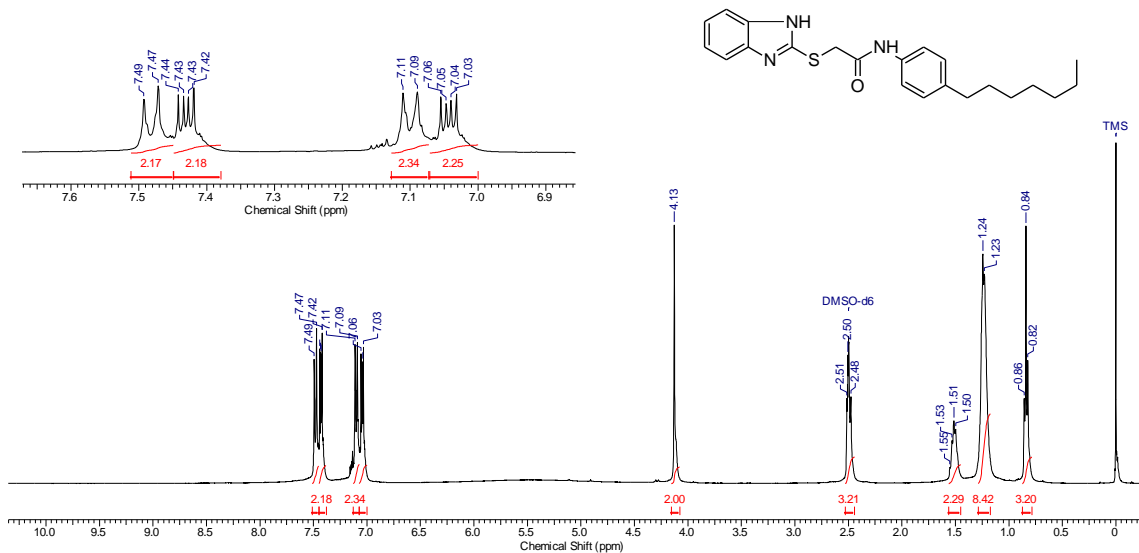


Figure S5. ¹H RMN spectrum of 2-((1*H*-Benzo[*d*]imidazol-2-yl)thio)-*N*-(4-heptylphenyl)acetamide (**6c**) in DMSO-*d*₆

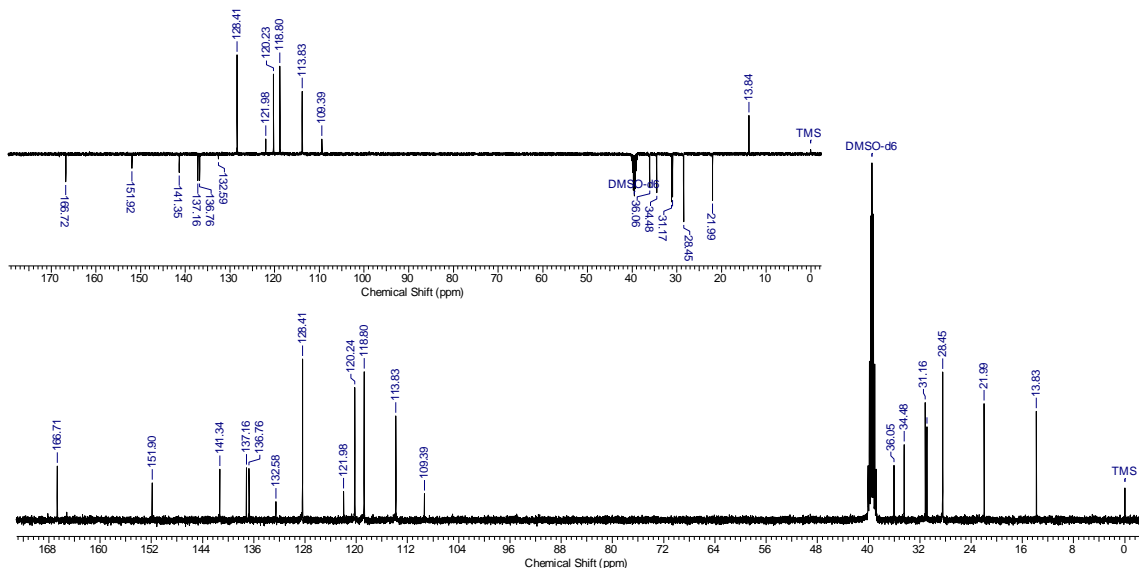


Figure S6. ¹³C RMN spectrum of 2-((1*H*-Benzo[*d*]imidazol-2-yl)thio)-*N*-(4-heptylphenyl)acetamide (**6c**) in DMSO-*d*₆.

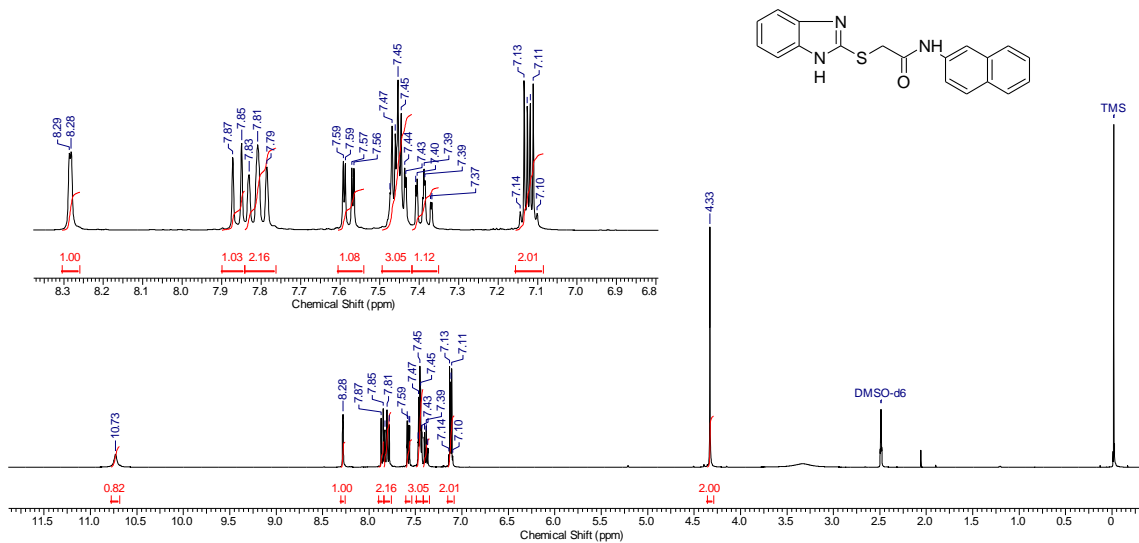


Figure S7. ¹H RMN spectrum of 2-((1*H*-benzo[*d*]imidazol-2-yl)thio)-*N*-(naphthalen-2-yl)acetamide (**6d**) in DMSO-*d*₆

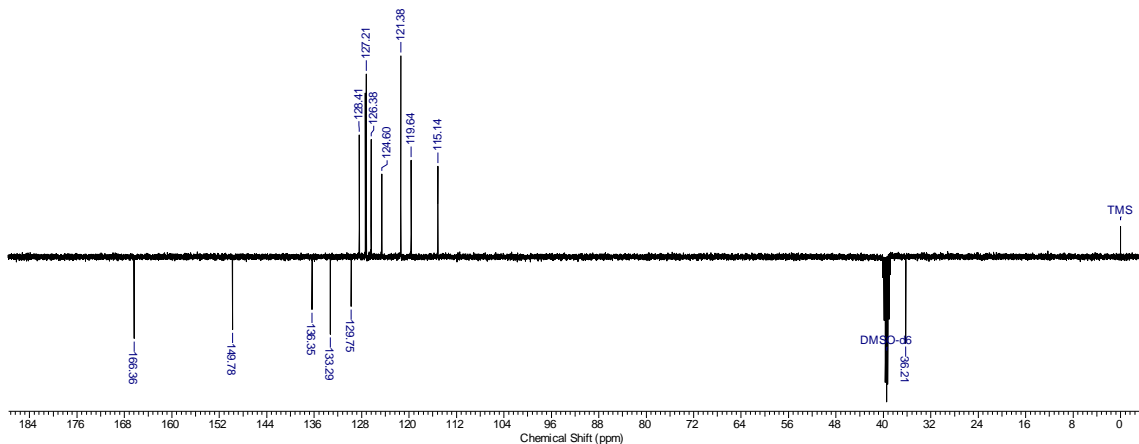


Figure S8. ¹³C RMN spectrum of 2-((1*H*-benzo[*d*]imidazol-2-yl)thio)-*N*-(naphthalen-2-yl)acetamide (**6d**) in DMSO-*d*₆.

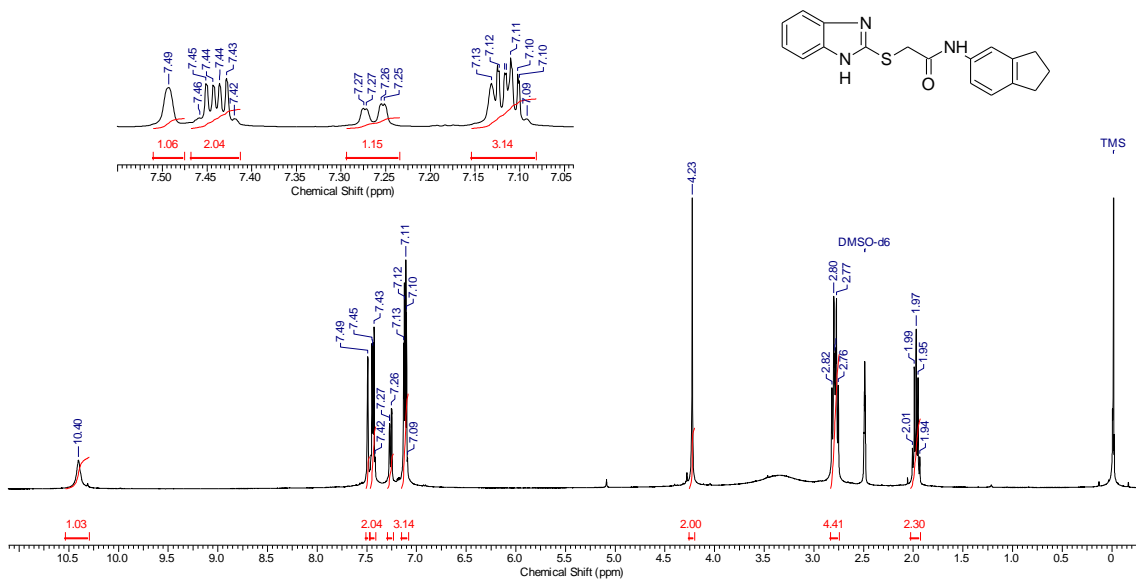


Figure S9. ^1H RMN spectrum of 2-((1*H*-Benzo[*d*]imidazol-2-yl)thio)-*N*-(2,3-dihydro-1*H*-inden-5-yl)acetamide (**6e**) in DMSO-*d*₆.

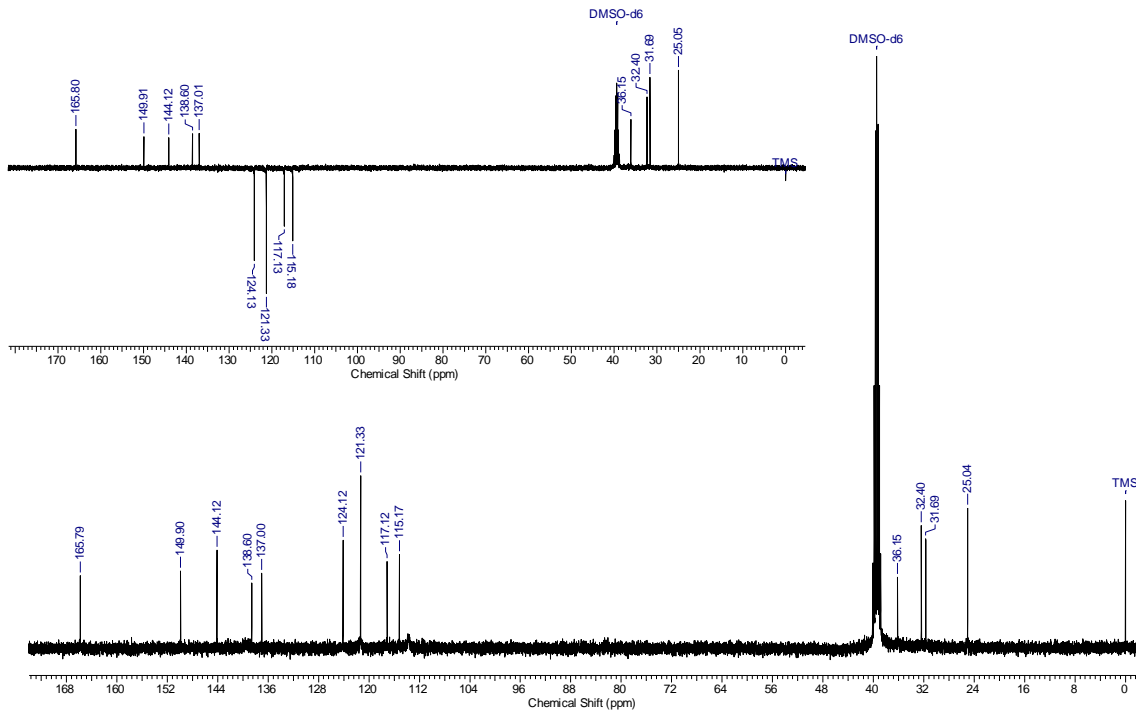


Figure S10. ^{13}C RMN spectrum of 2-((1*H*-Benzo[*d*]imidazol-2-yl)thio)-*N*-(2,3-dihydro-1*H*-inden-5-yl)acetamide (**6e**) in DMSO-*d*₆.

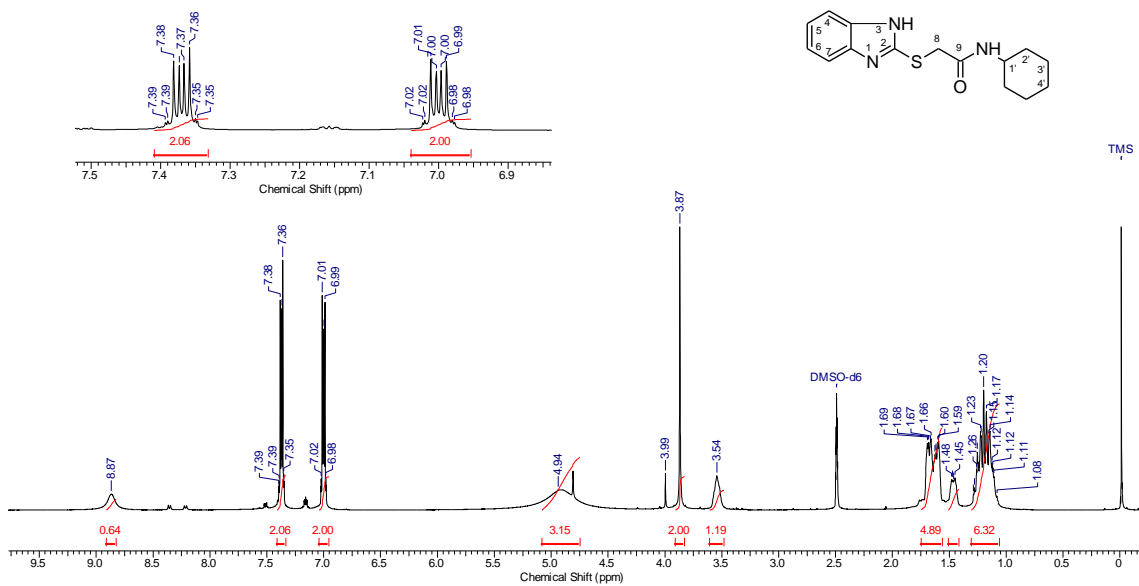


Figure S11. ^1H RMN spectrum of 2-((1*H*-Benzo[*d*]imidazol-2-yl)thio)-*N*-cyclohexylacetamide (**6f**) in DMSO-*d*₆

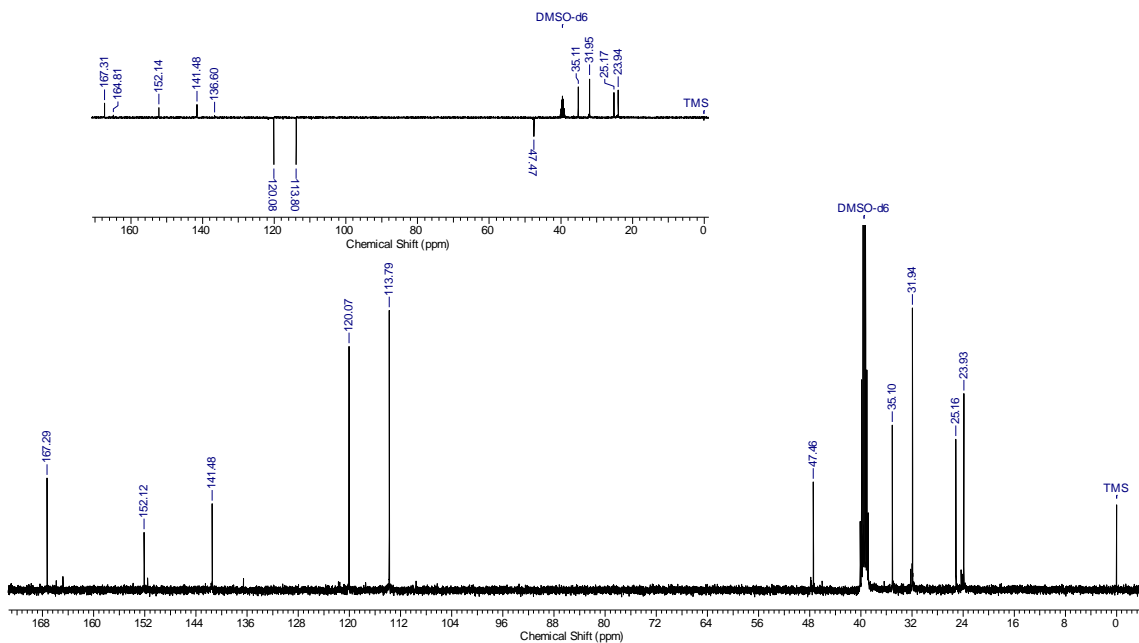


Figure S12. ^{13}C RMN spectrum 2-((1*H*-Benzo[*d*]imidazol-2-yl)thio)-*N*-cyclohexylacetamide (**6f**) in DMSO-*d*₆.

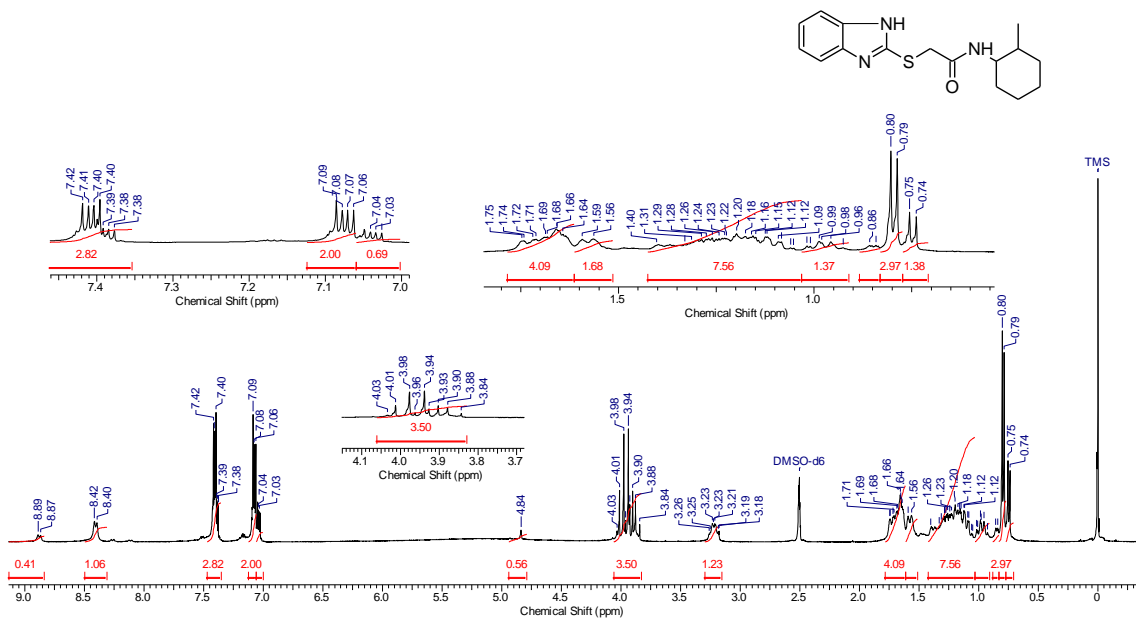


Figure S13. ^1H RMN spectrum of 2-((1*H*-Benzo[*d*]imidazol-2-yl)thio)-*N*-(2-methylcyclohexyl)acetamide (**6g**) in DMSO-*d*₆

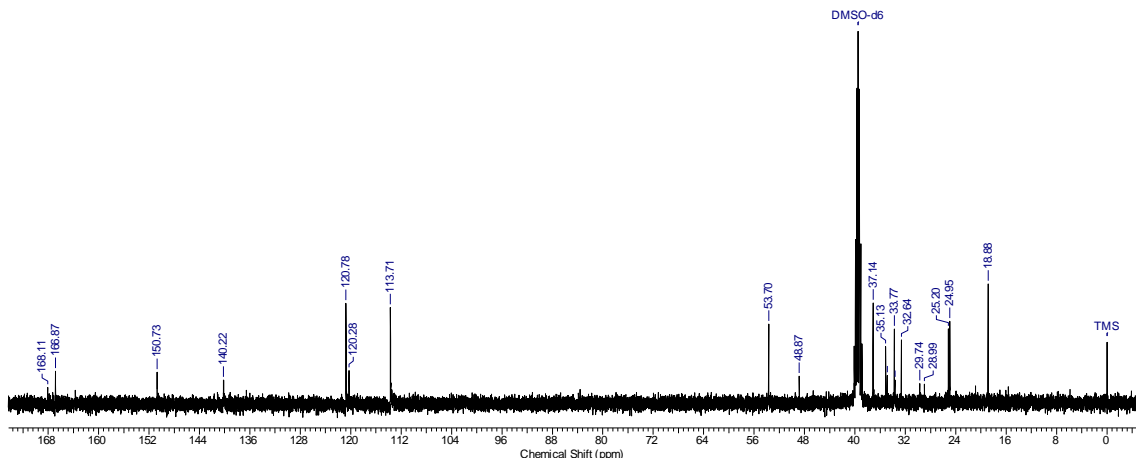


Figure S14. ^{13}C RMN spectrum of 2-((1*H*-Benzo[*d*]imidazol-2-yl)thio)-*N*-(2-methylcyclohexyl)acetamide (**6g**) in DMSO-*d*₆.

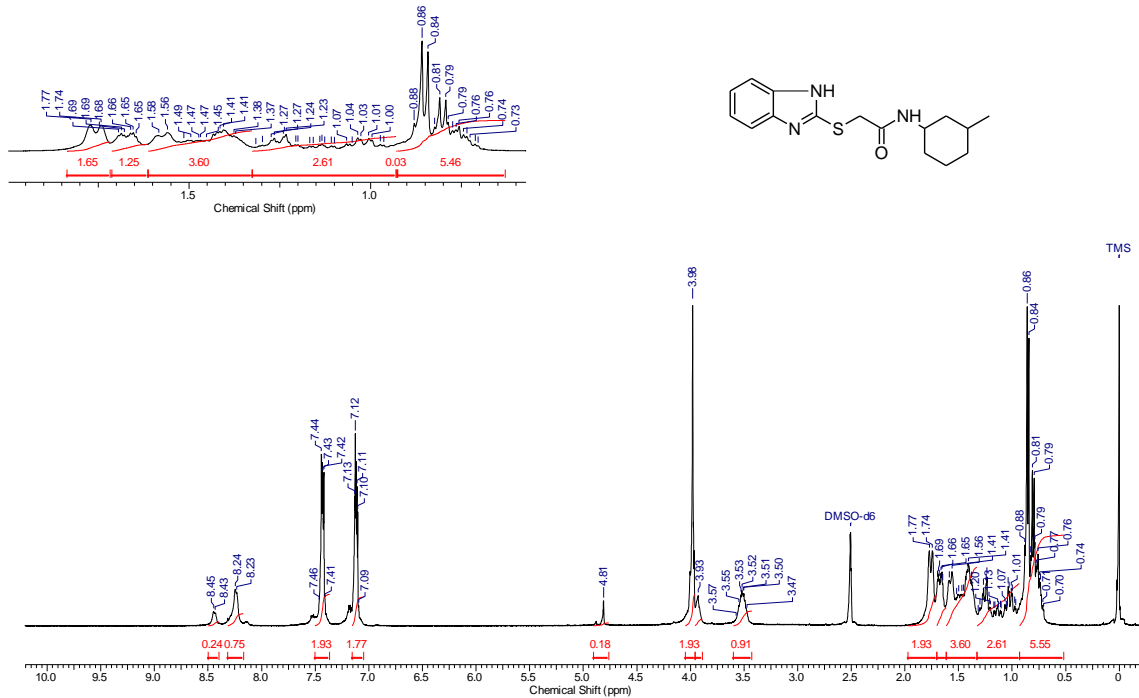


Figure S15. ¹H RMN spectrum of 2-((1*H*-Benzo[*d*]imidazol-2-yl)thio)-*N*-(3-methylcyclohexyl)acetamide (**6h**) in DMSO-*d*₆

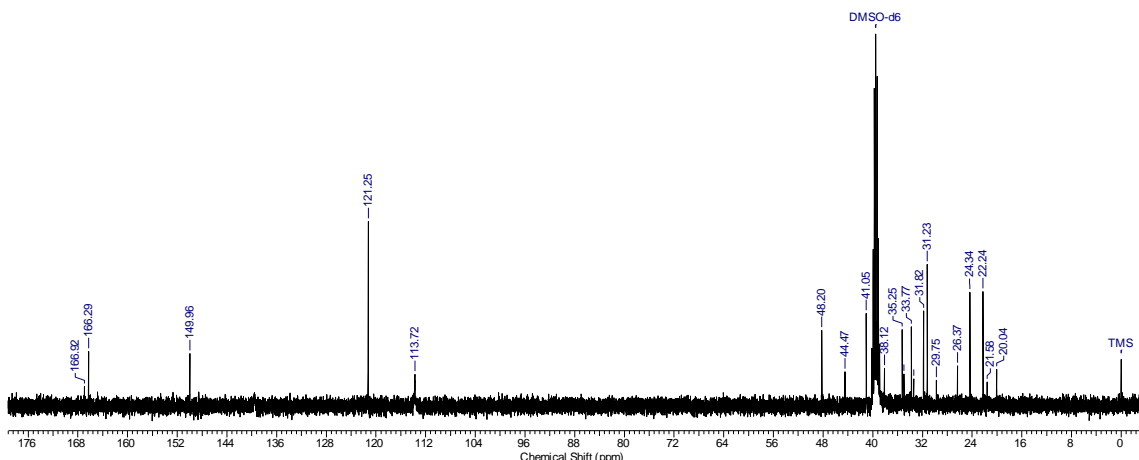


Figure S16. ¹³C RMN spectrum of 2-((1*H*-Benzo[*d*]imidazol-2-yl)thio)-*N*-(3-methylcyclohexyl)acetamide (**6h**) in DMSO-*d*₆.

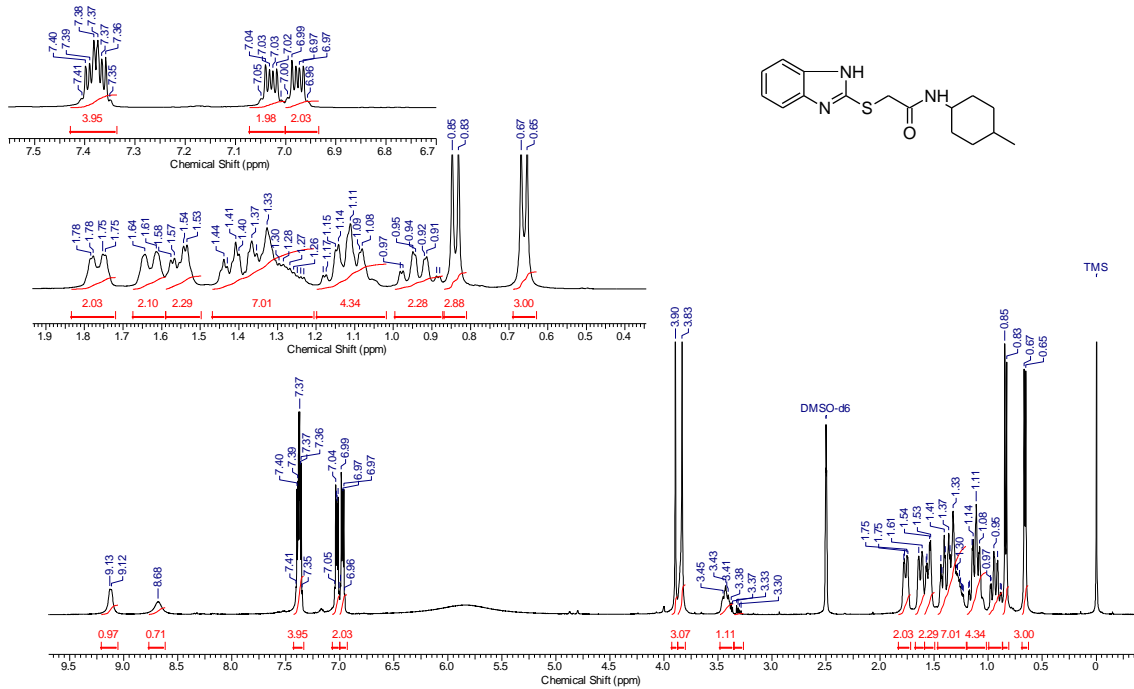


Figure S17. ^1H RMN spectrum of 2-((1*H*-Benzo[*d*]imidazol-2-yl)thio)-*N*-(4-methylcyclohexyl)acetamide (**6i**) in DMSO-*d*₆

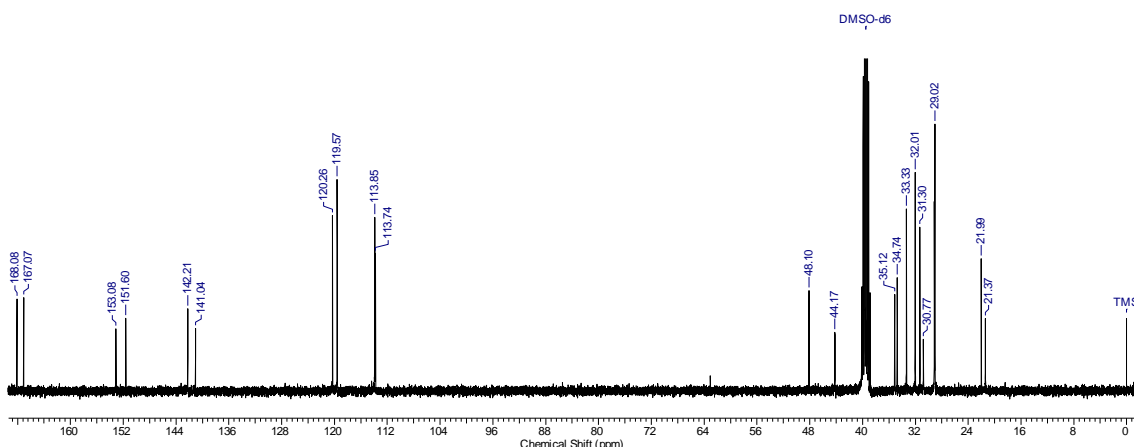


Figure S18. ^{13}C RMN spectrum of 2-((1*H*-Benzo[*d*]imidazol-2-yl)thio)-*N*-(4-methylcyclohexyl)acetamide (**6i**) in DMSO-*d*₆.

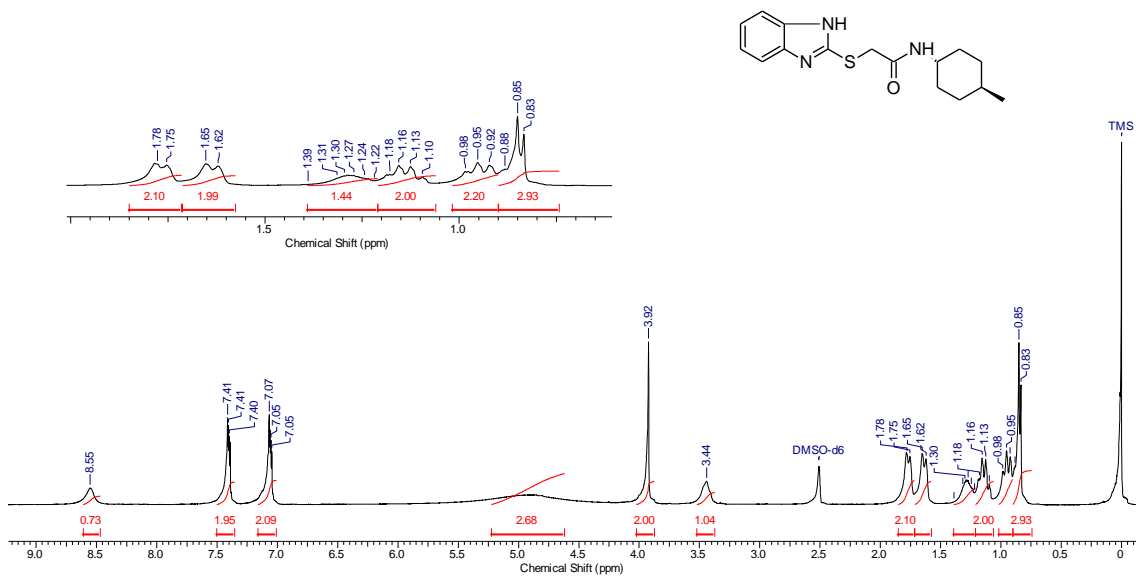


Figure S19. ¹H RMN spectrum of 2-((1*H*-Benzo[*d*]imidazol-2-yl)thio)-*N*-(*trans*-4-methylcyclohexyl)acetamide (**6j**) in DMSO-*d*₆.

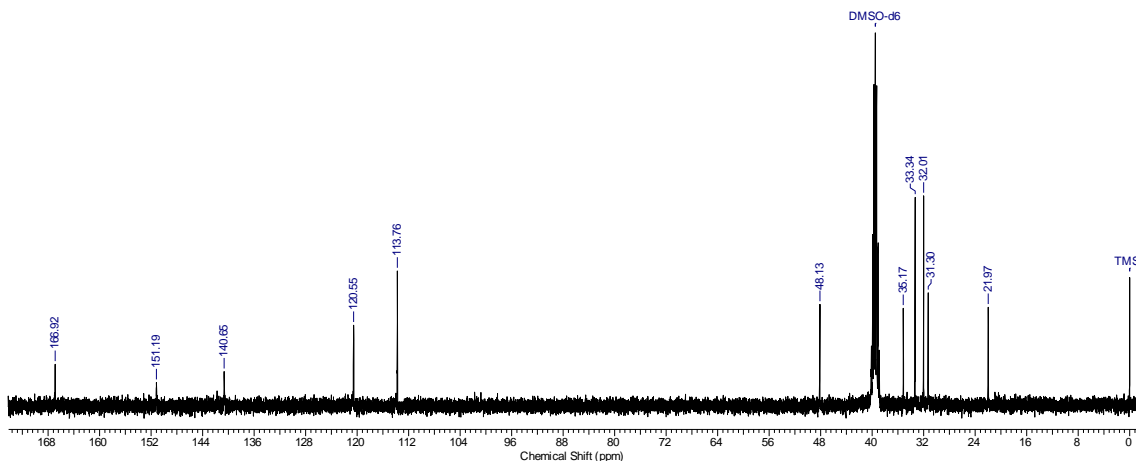


Figure S20. ¹³C RMN spectrum of 2-((1*H*-Benzo[*d*]imidazol-2-yl)thio)-*N*-(*trans*-4-methylcyclohexyl)acetamide (**6j**) in DMSO-*d*₆.

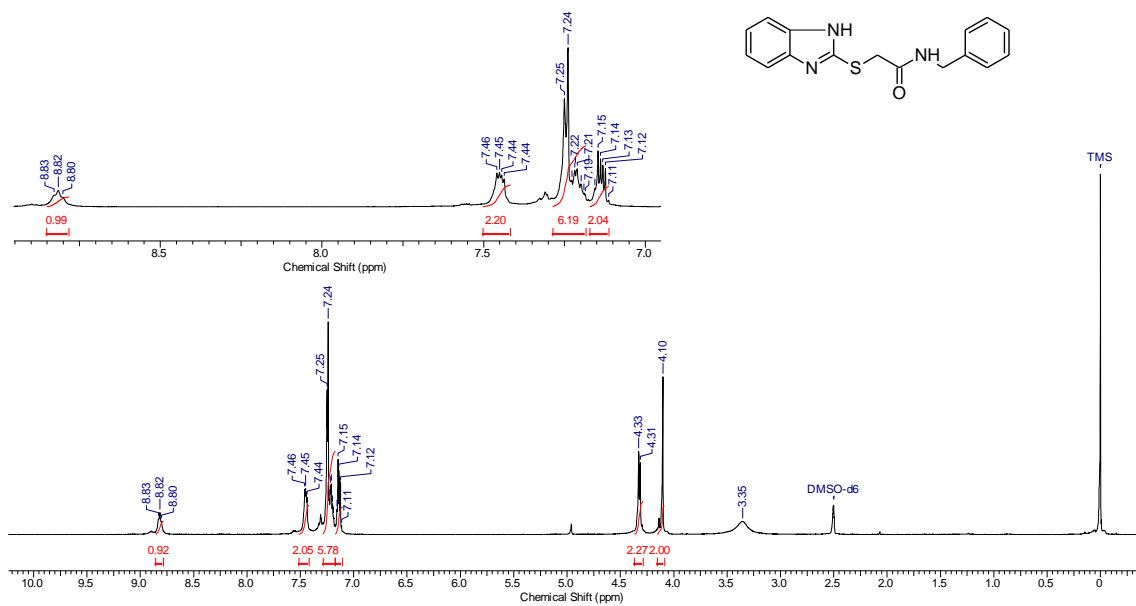
6k

Figure S21. ^1H RMN spectrum of 2-((1*H*-Benzo[*d*]imidazol-2-yl)thio)-*N*-benzylacetamide (**6k**) in DMSO-*d*₆.

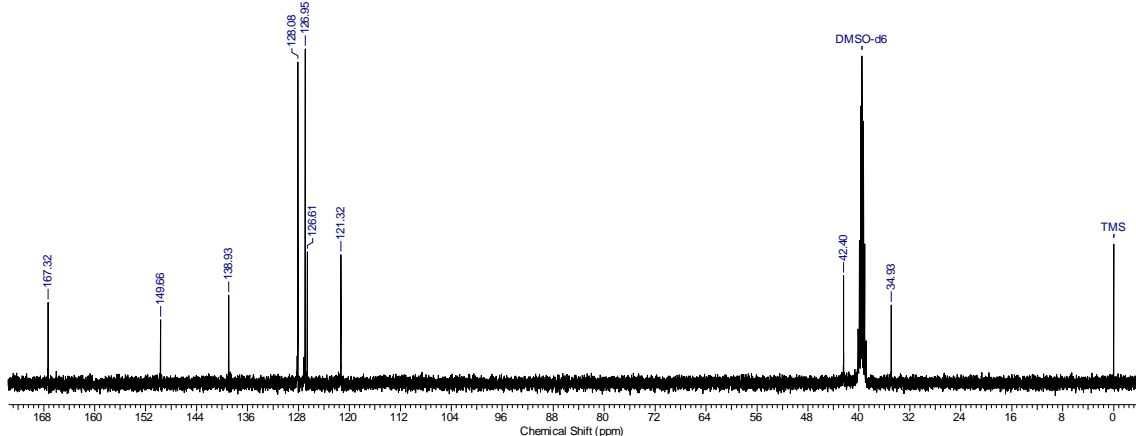


Figure S22. ^{13}C RMN spectrum 2-((1*H*-Benzo[*d*]imidazol-2-yl)thio)-*N*-benzylacetamide (**6k**) in DMSO-*d*₆.

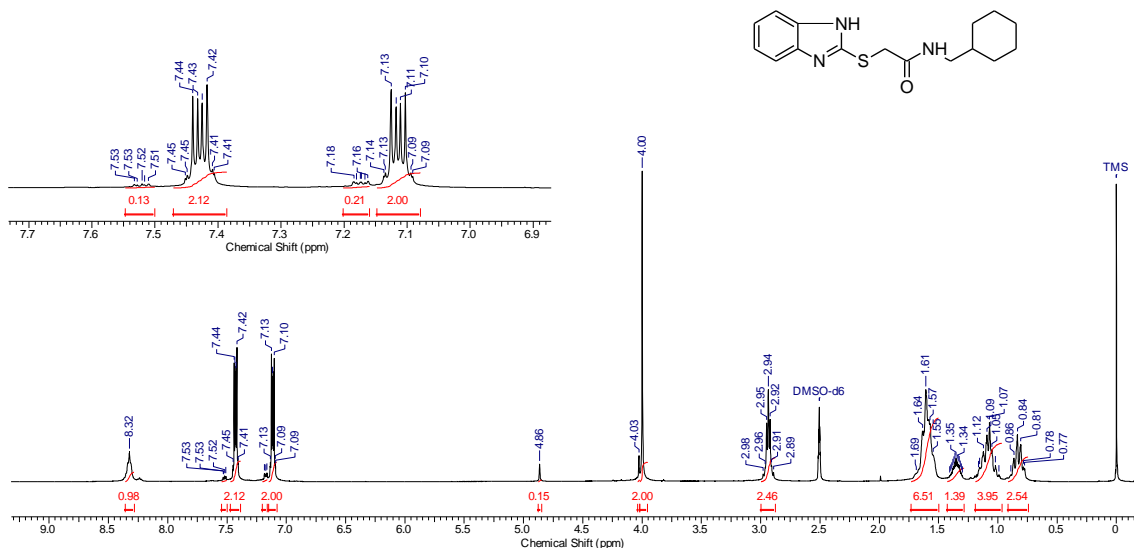


Figure S23. ^1H RMN spectrum of 2-((1*H*-Benzo[*d*]imidazol-2-yl)thio)-*N*-(cyclohexylmethyl)acetamide (**6l**) in DMSO-*d*₆

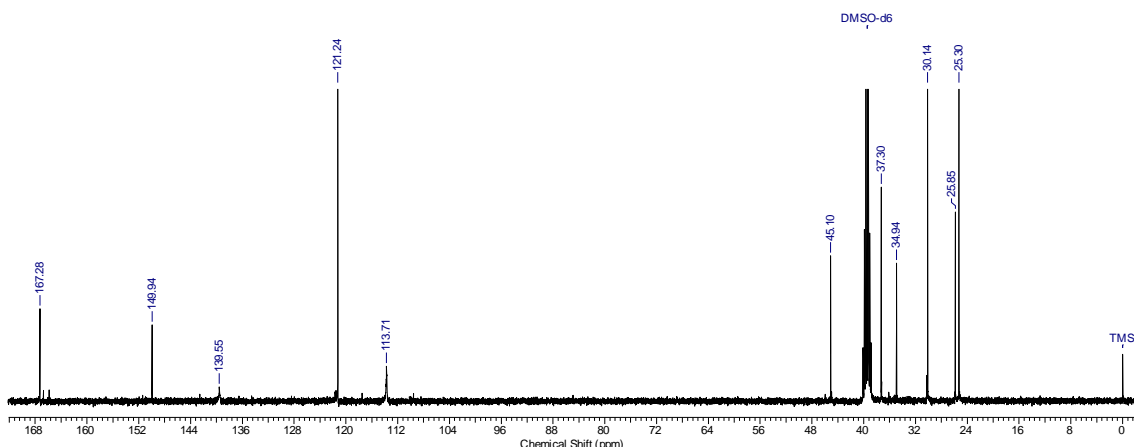


Figure S24. ^{13}C RMN spectrum 2-((1*H*-Benzo[*d*]imidazol-2-yl)thio)-*N*-(cyclohexylmethyl)acetamide (**6l**) in DMSO-*d*₆.

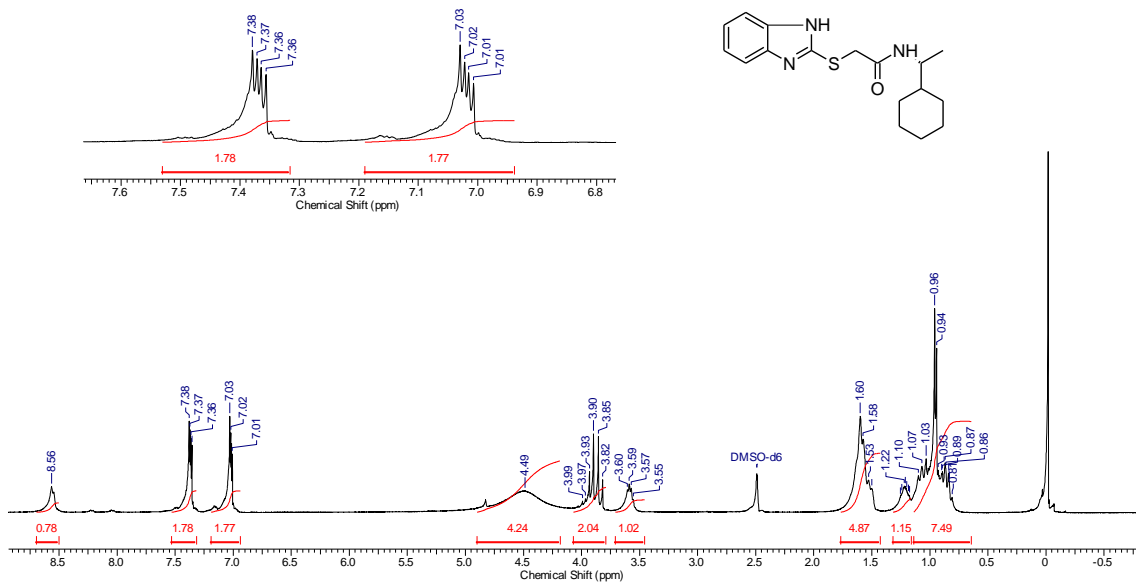


Figure S25. ^1H RMN spectrum of (*S*)-2-((1*H*-Benzo[*d*]imidazol-2-yl)thio)-*N*-(1-cyclohexylethyl)acetamide (**6m**) in DMSO-*d*₆.

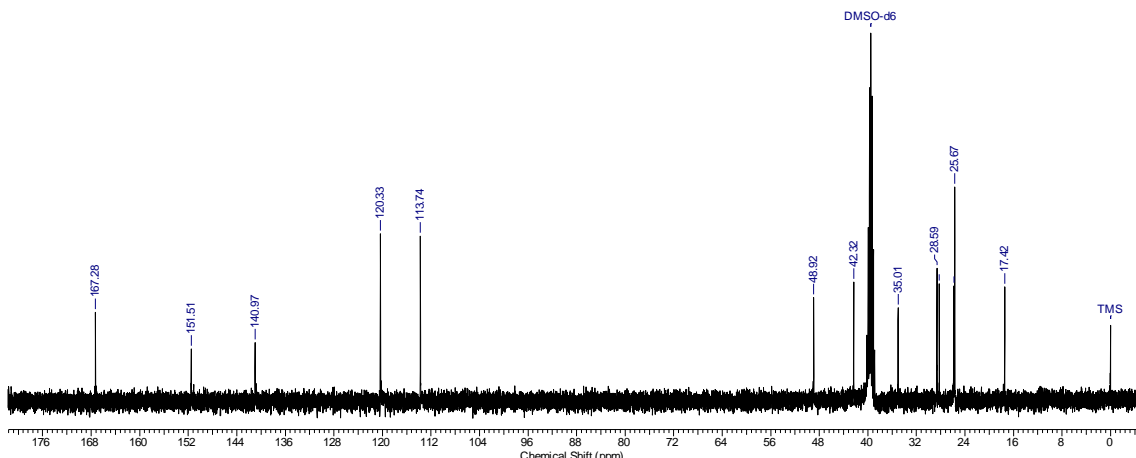


Figure S26. ^{13}C RMN spectrum (*S*)-2-((1*H*-Benzo[*d*]imidazol-2-yl)thio)-*N*-(1-cyclohexylethyl)acetamide (**6m**) in DMSO-*d*₆.

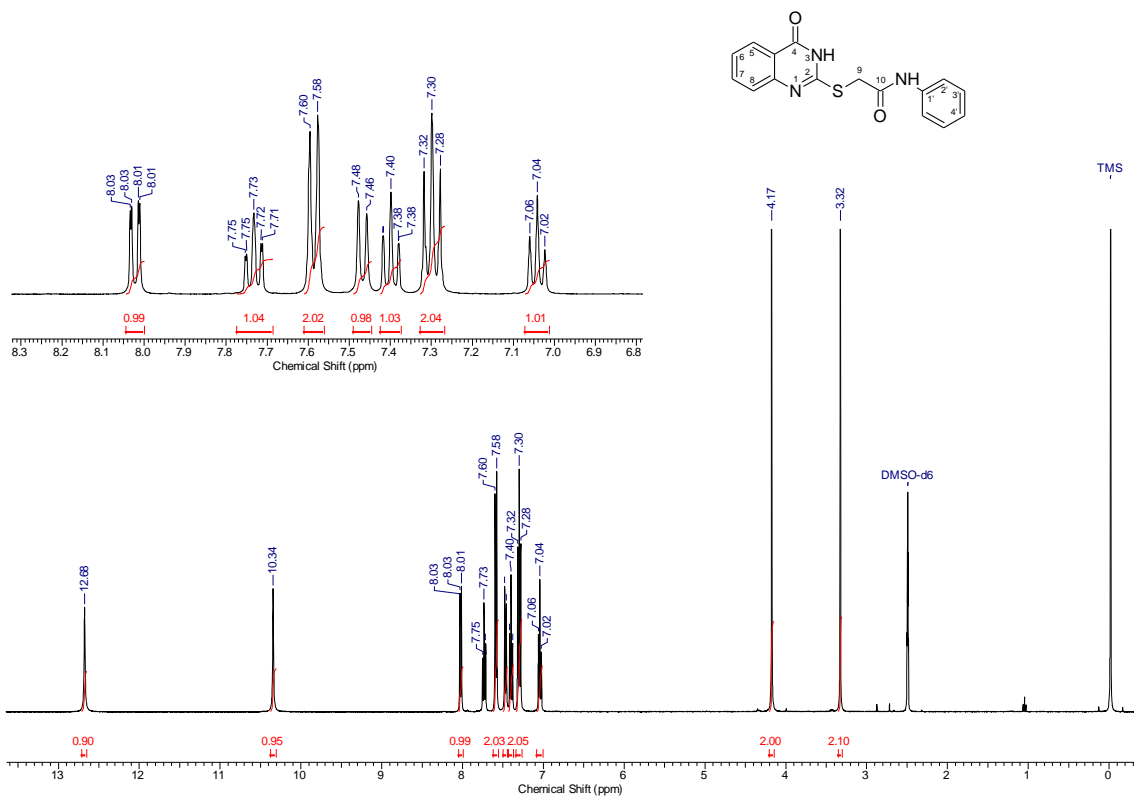


Figure S27. ^1H RMN spectrum of 2-((4-Oxo-3,4-dihydroquinazolin-2-yl)thio)-*N*-phenylacetamide (**9a**) in $\text{DMSO}-d_6$.

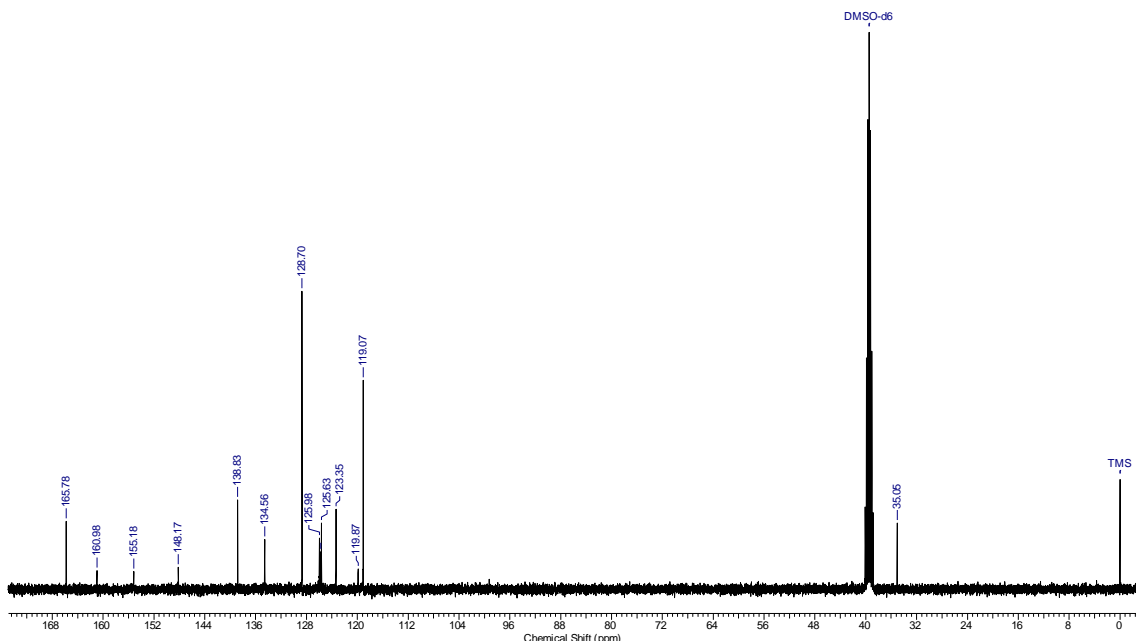


Figure S28. ^{13}C RMN spectrum of 2-((4-Oxo-3,4-dihydroquinazolin-2-yl)thio)-*N*-phenylacetamide (**9a**) in $\text{DMSO}-d_6$.

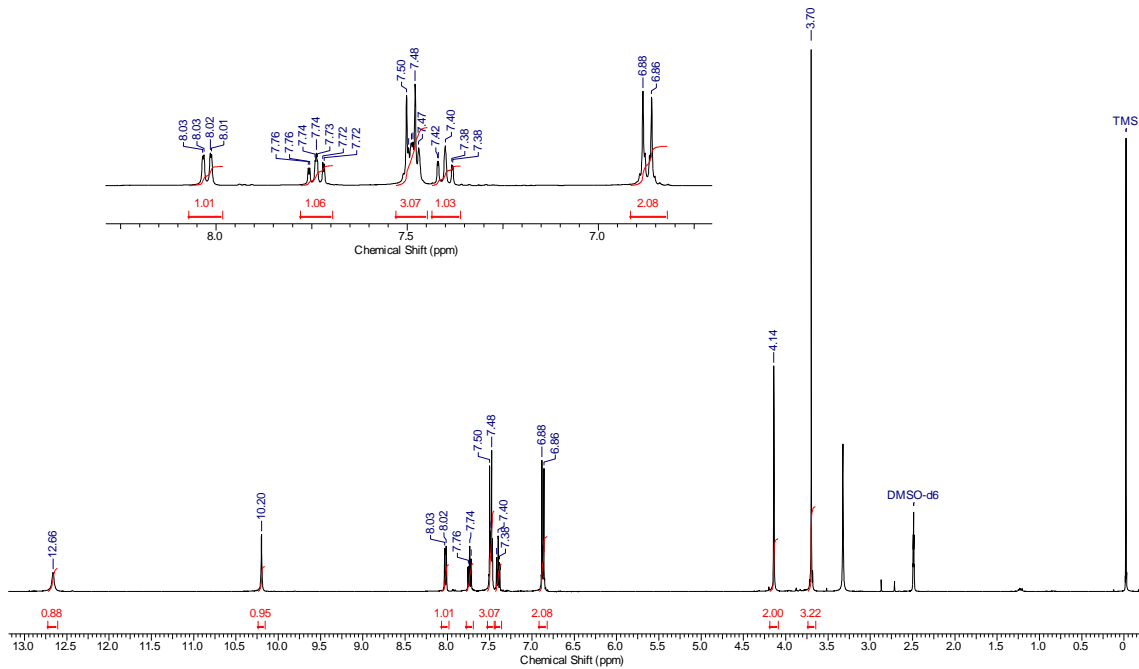
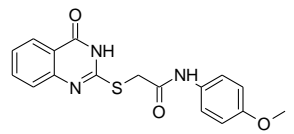


Figure S29. ^1H RMN spectrum of *N*-(4-Methoxyphenyl)-2-((4-oxo-3,4-dihydroquinazolin-2-yl)thio)acetamide (**9b**) in $\text{DMSO}-d_6$

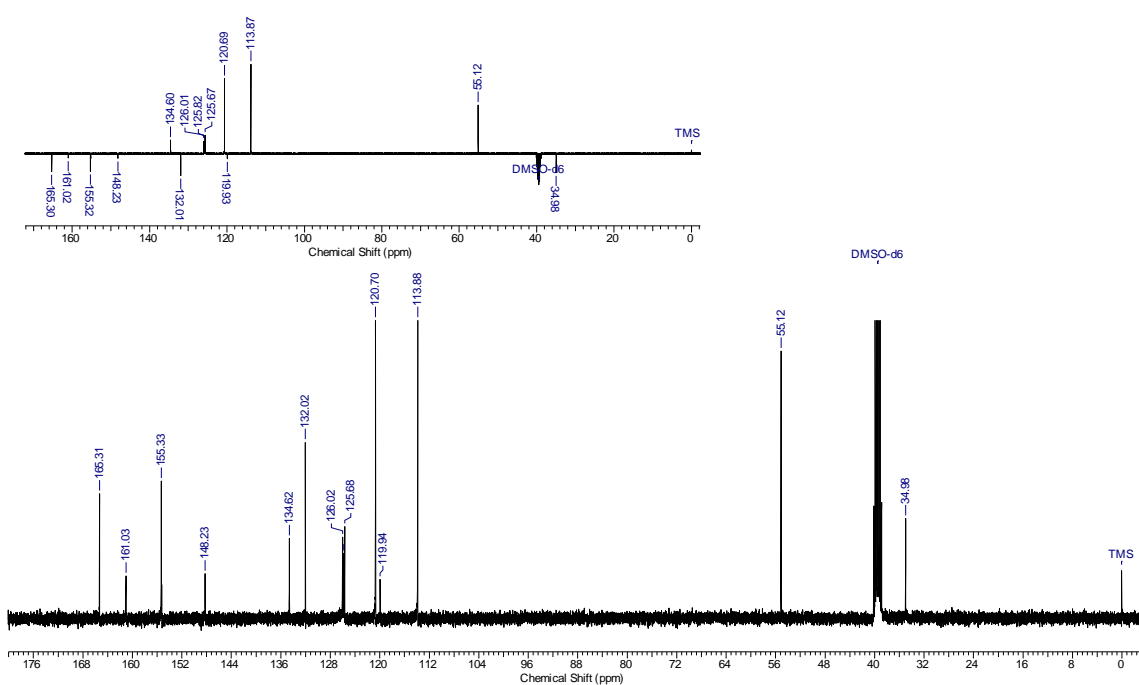


Figure S30. ^{13}C RMN spectrum of *N*-(4-Methoxyphenyl)-2-((4-oxo-3,4-dihydroquinazolin-2-yl)thio)acetamide (**9b**) in $\text{DMSO}-d_6$.

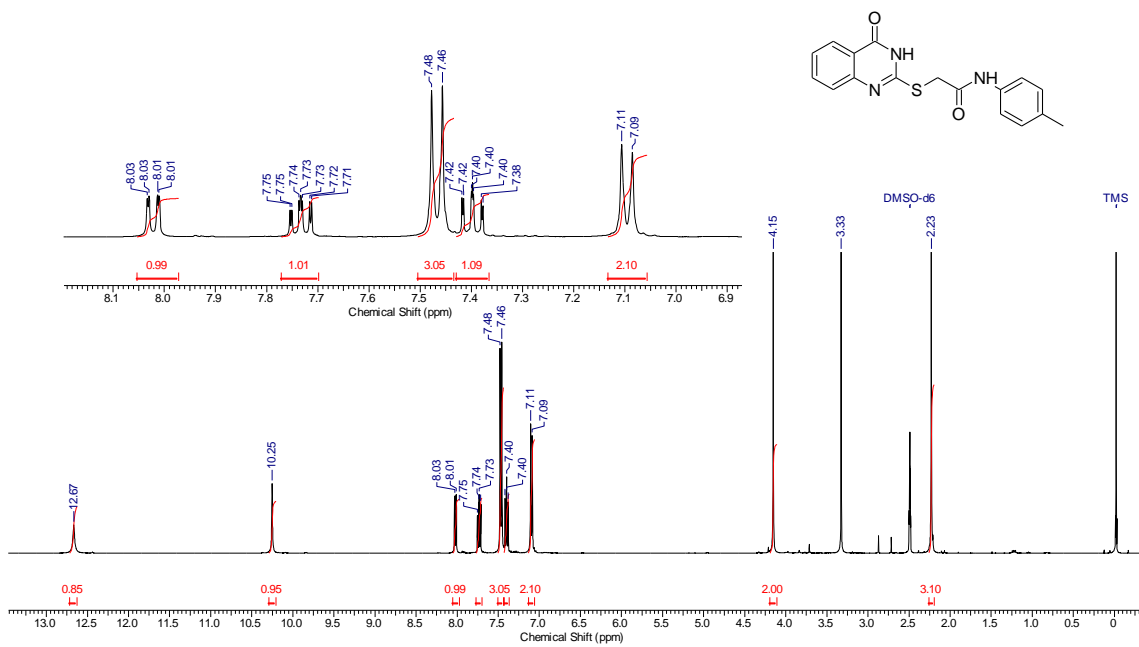


Figure S31. ^1H RMN spectrum of 2-((4-Oxo-3,4-dihydroquinazolin-2-yl)thio)-N-(*p*-tolyl)acetamide (**9c**) in $\text{DMSO}-d_6$.

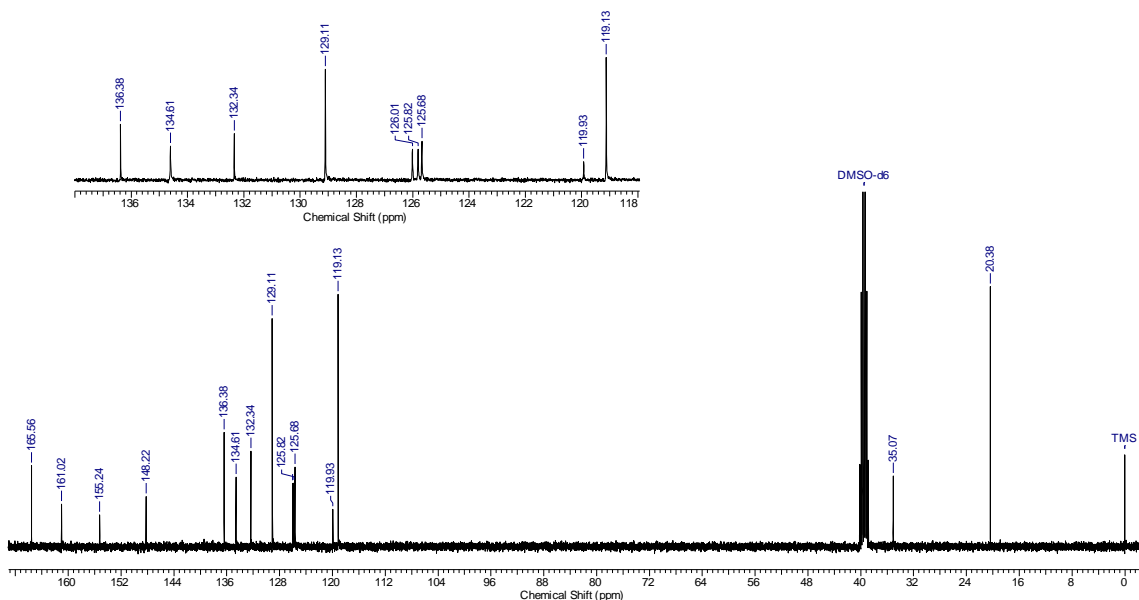


Figure S32. ^{13}C RMN spectrum of 2-((4-Oxo-3,4-dihydroquinazolin-2-yl)thio)-N-(*p*-tolyl)acetamide (**9c**) in $\text{DMSO}-d_6$.

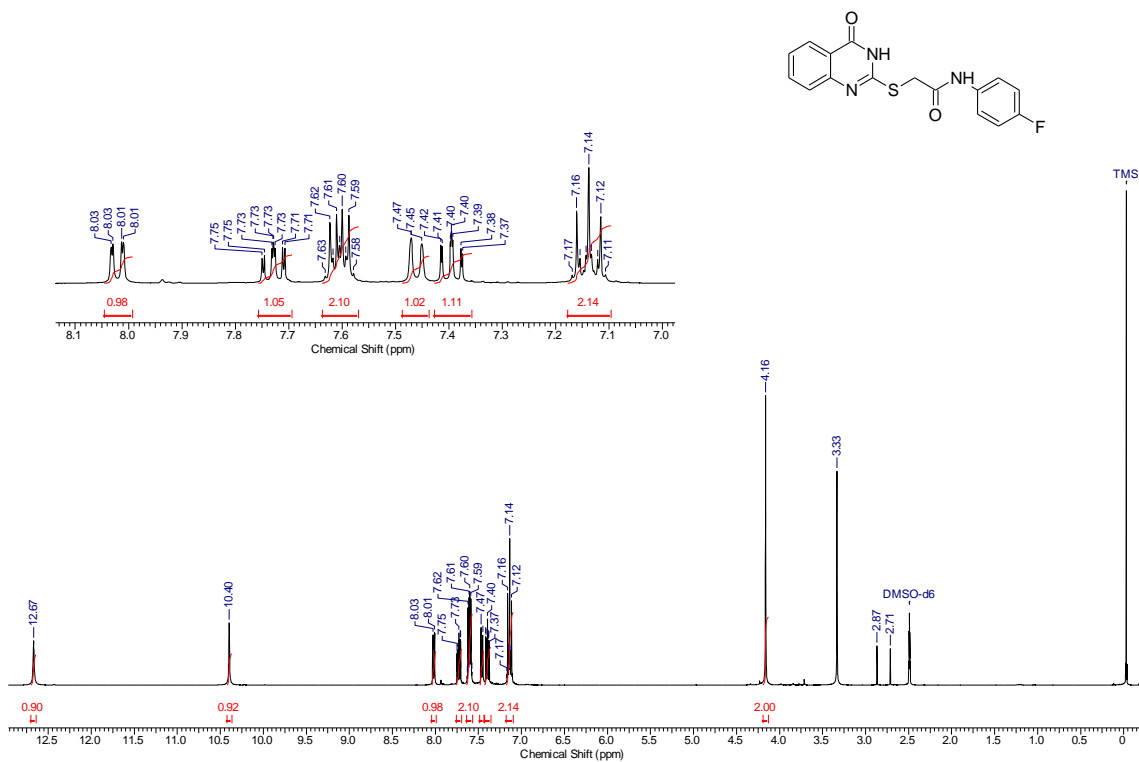


Figure S33. ^1H RMN spectrum of *N*-(4-Fluorophenyl)-2-((4-oxo-3,4-dihydroquinazolin-2-yl)thio)acetamide (**9d**) in $\text{DMSO}-d_6$.

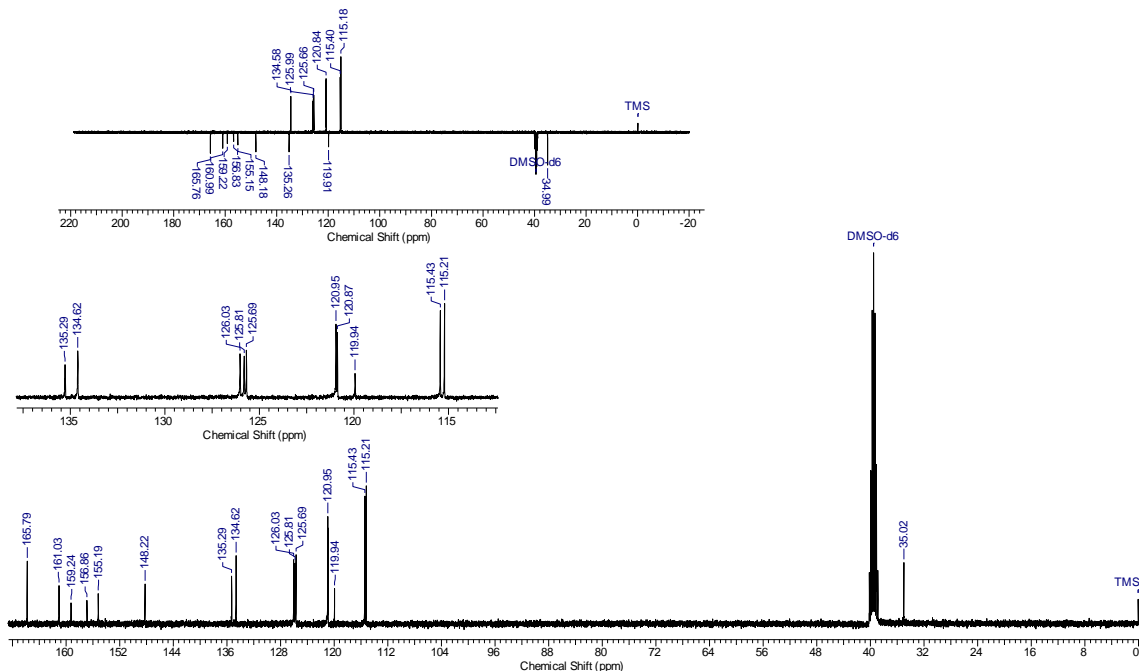


Figure S34. ^{13}C RMN spectrum of *N*-(4-Fluorophenyl)-2-((4-oxo-3,4-dihydroquinazolin-2-yl)thio)acetamide (**9d**) in $\text{DMSO}-d_6$.

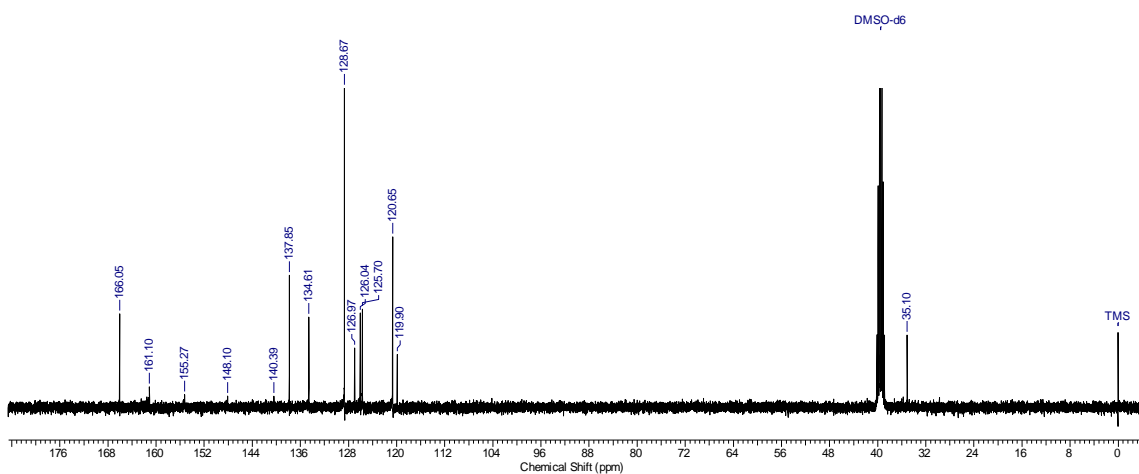
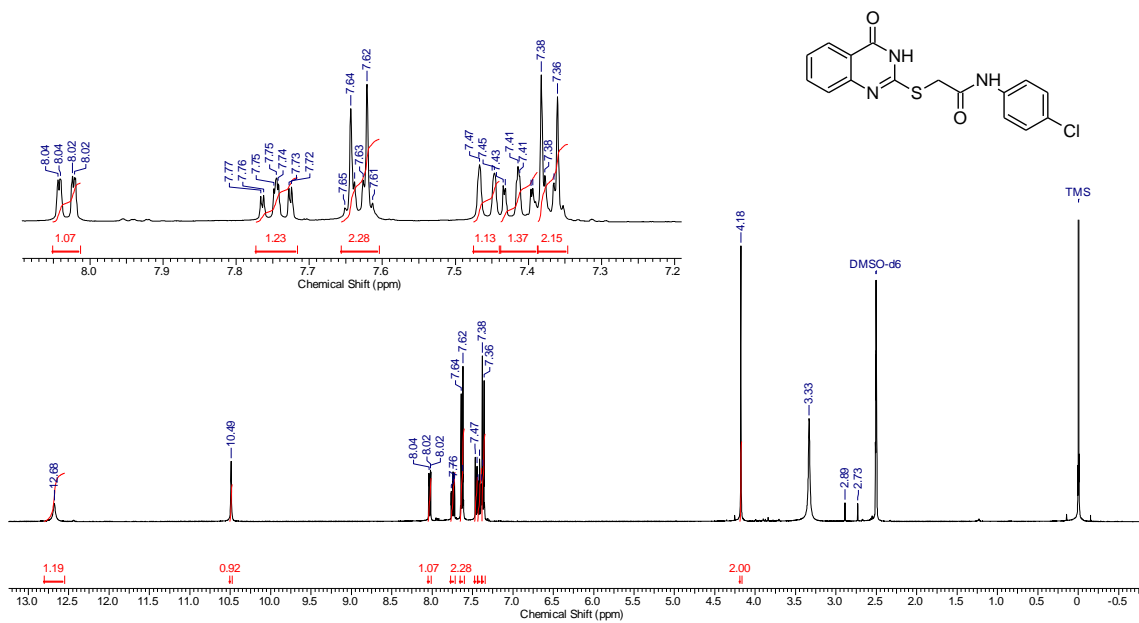


Figure S36. ^{13}C RMN spectrum of *N*-(4-Chlorophenyl)-2-((4-oxo-3,4-dihydroquinazolin-2-yl)thio)acetamide (**9e**) in $\text{DMSO}-d_6$.

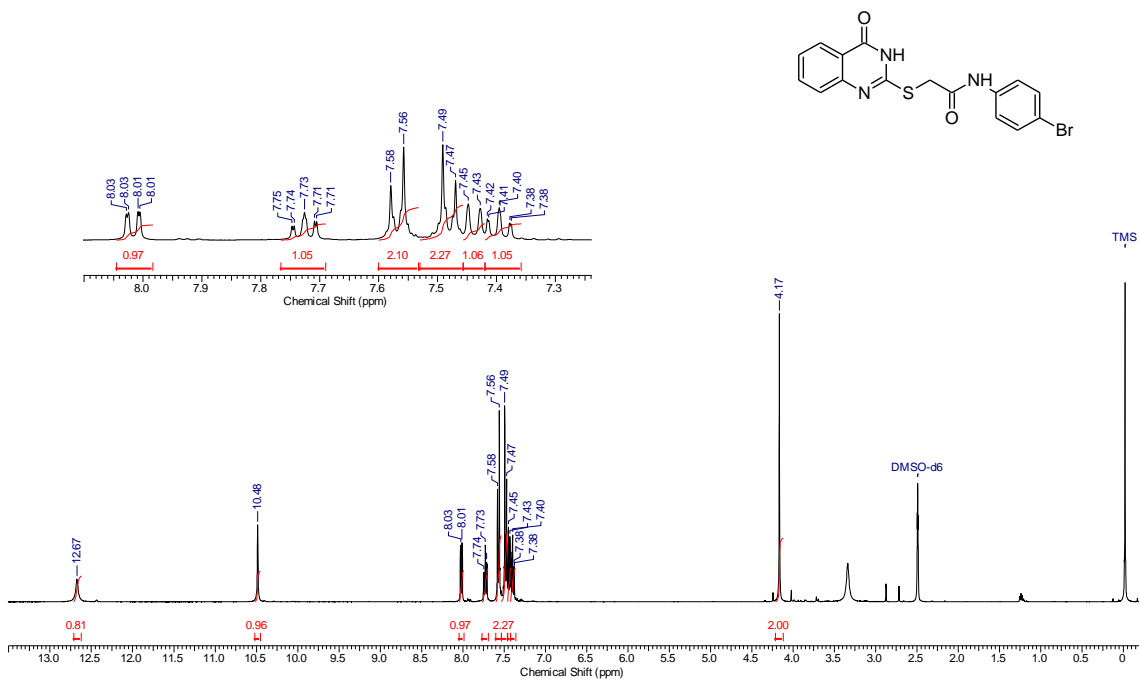


Figure S37. ^1H RMN spectrum *N*-(4-bromophenyl)-2-((4-oxo-3,4-dihydroquinazolin-2-yl)thio)acetamide (**9f**) in $\text{DMSO}-d_6$.

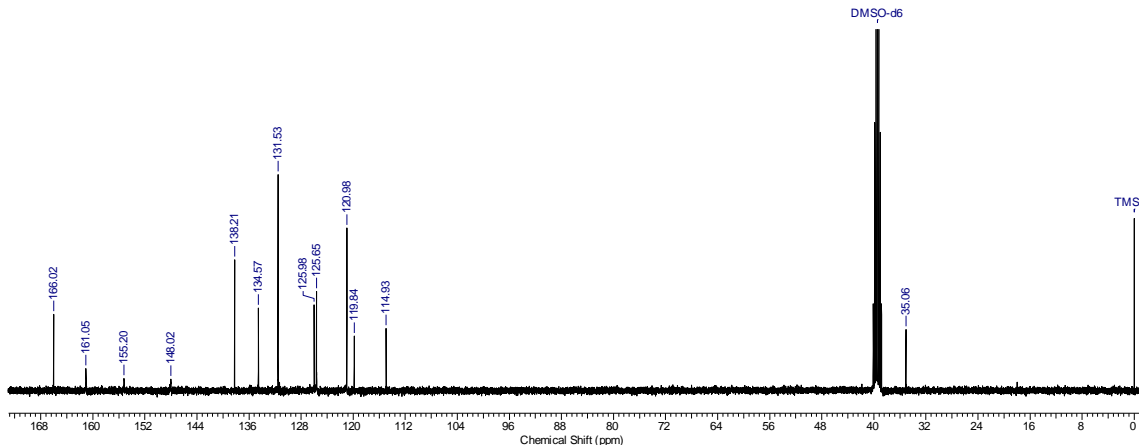


Figure S38. ^{13}C RMN spectrum of *N*-(4-bromophenyl)-2-((4-oxo-3,4-dihydroquinazolin-2-yl)thio)acetamide (**9f**) in $\text{DMSO}-d_6$.

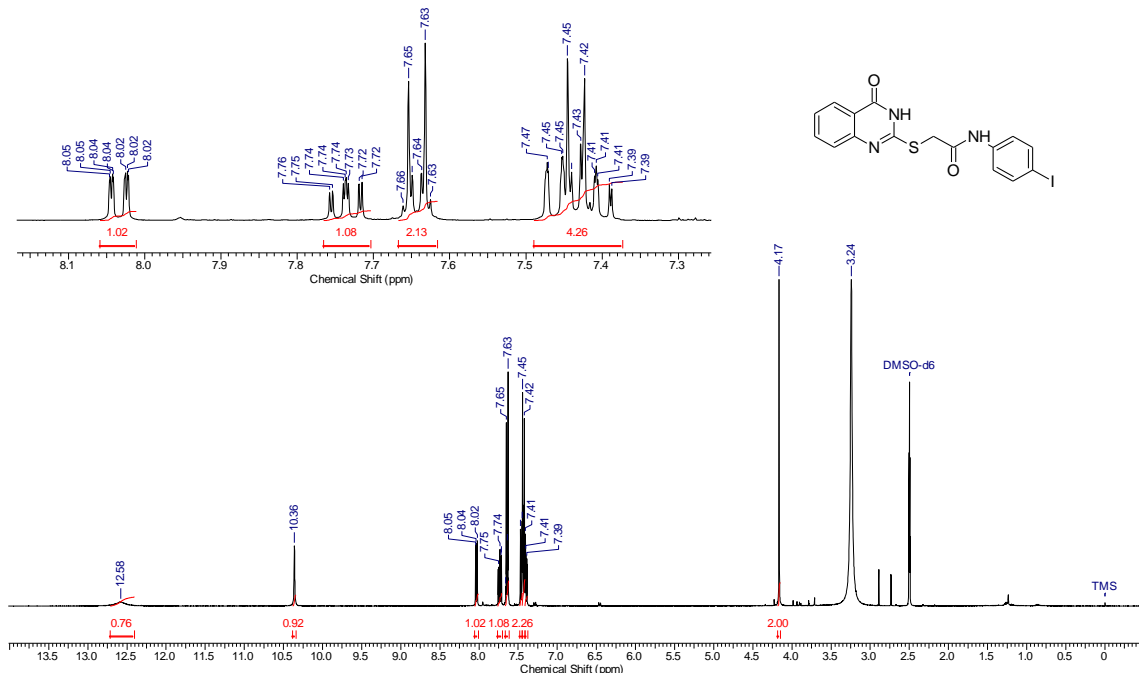


Figure S39. ¹H RMN spectrum *N*-(4-Iodophenyl)-2-((4-oxo-3,4-dihydroquinazolin-2-yl)thio)acetamide (**9g**) in DMSO-*d*₆.

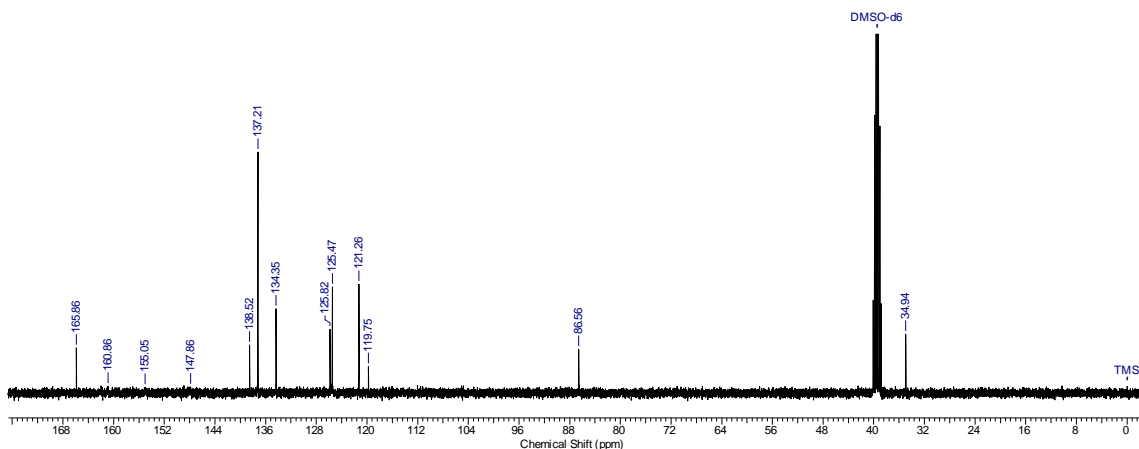


Figure S40. ¹³C RMN spectrum of *N*-(4-Iodophenyl)-2-((4-oxo-3,4-dihydroquinazolin-2-yl)thio)acetamide (**9g**) in DMSO-*d*₆.

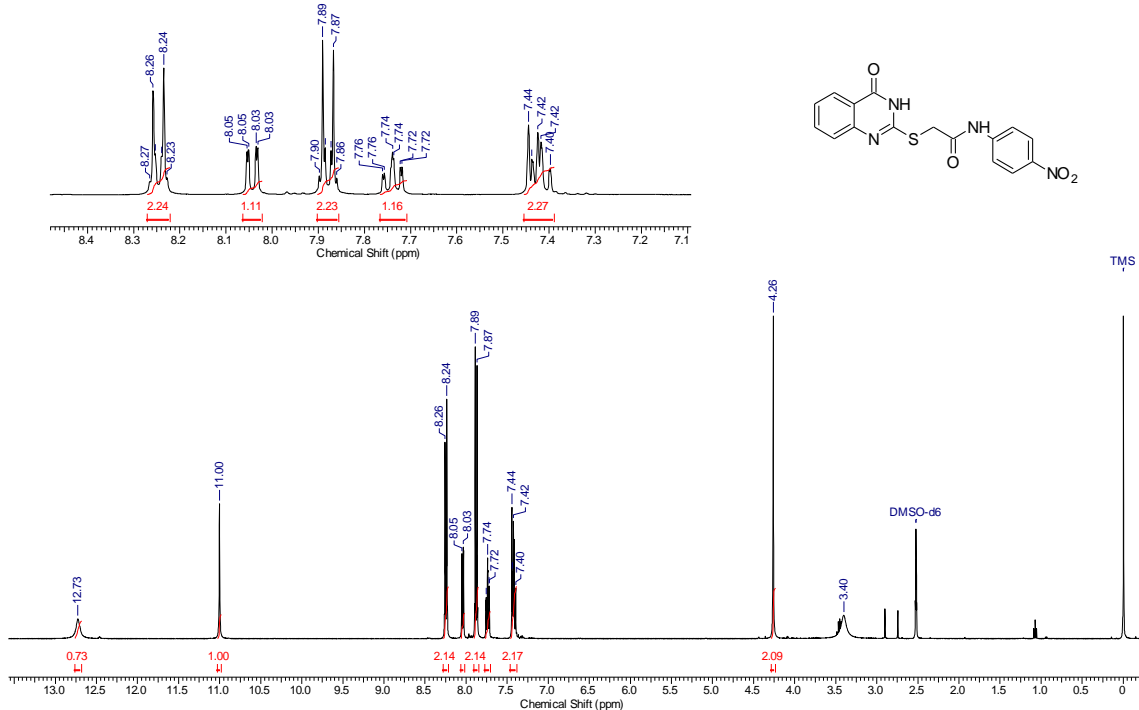


Figure S41. ^1H RMN spectrum N -(4-Nitrophenyl)-2-((4-oxo-3,4-dihydroquinazolin-2-yl)thio)acetamide (**9h**) in $\text{DMSO}-d_6$.

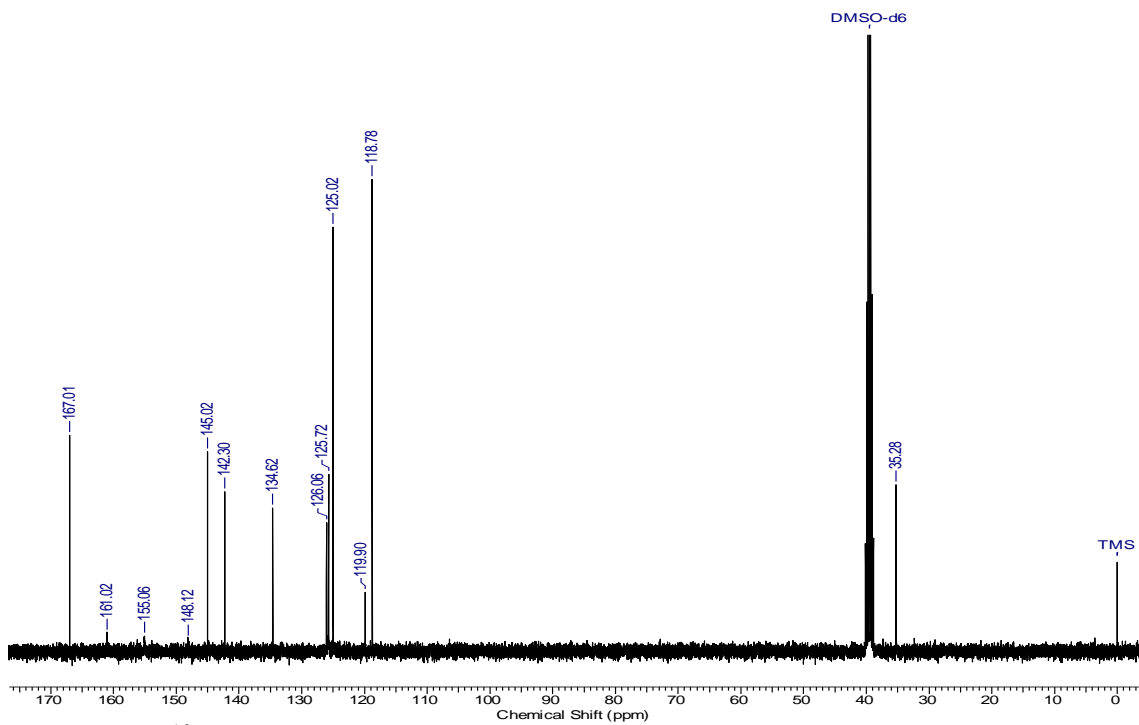


Figure S42. ^{13}C RMN spectrum of N -(4-Nitrophenyl)-2-((4-oxo-3,4-dihydroquinazolin-2-yl)thio)acetamide (**9h**) in $\text{DMSO}-d_6$.

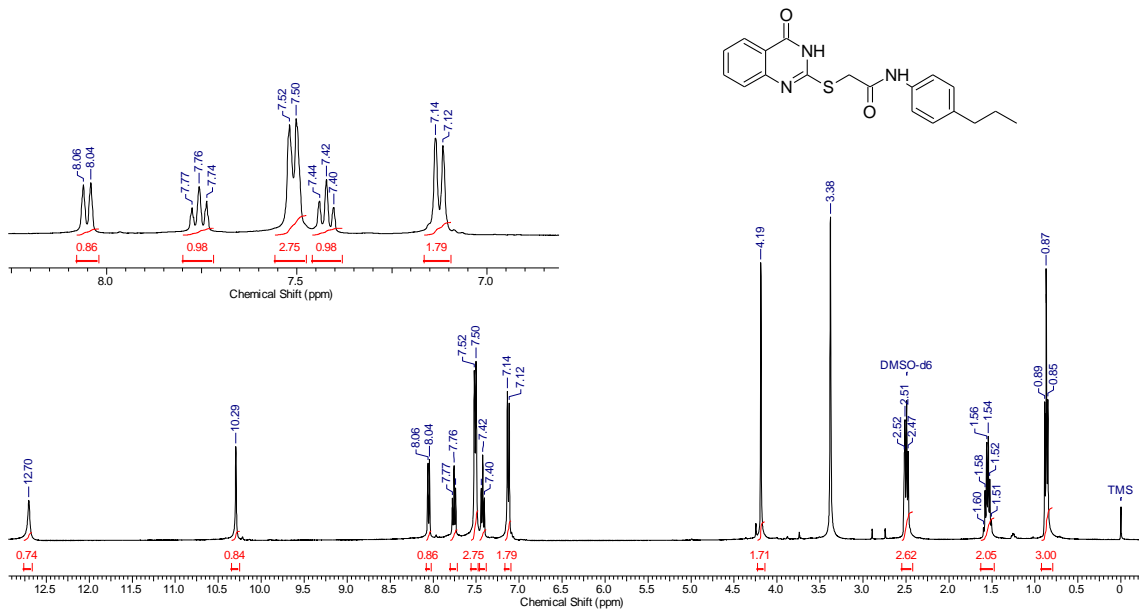


Figure S43. ^1H RMN spectrum of 2-((4-Oxo-3,4-dihydroquinazolin-2-yl)thio)-*N*-(4-propylphenyl)acetamide (**9i**) in $\text{DMSO}-d_6$.

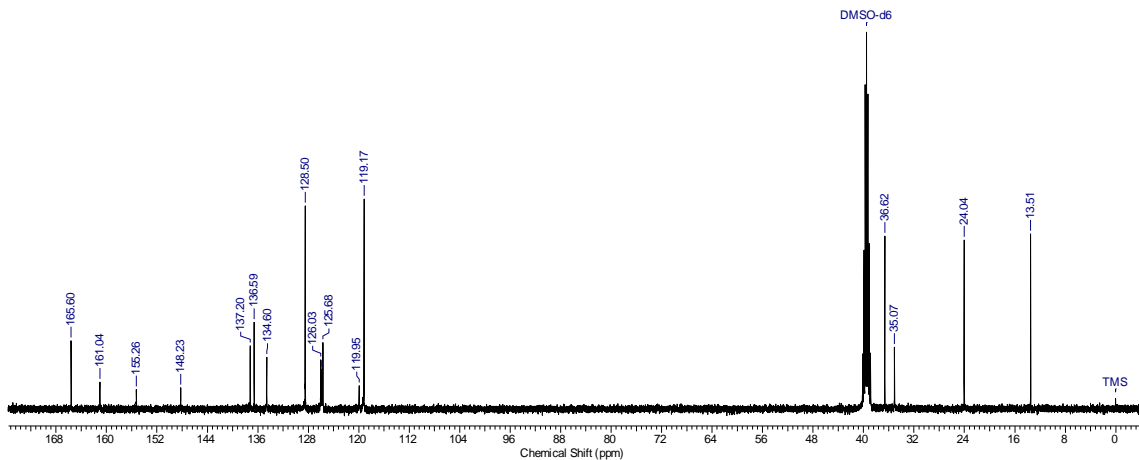


Figure S44. ^{13}C RMN spectrum of 2-((4-Oxo-3,4-dihydroquinazolin-2-yl)thio)-*N*-(4-propylphenyl)acetamide (**9i**) in DMSO-*d*₆.

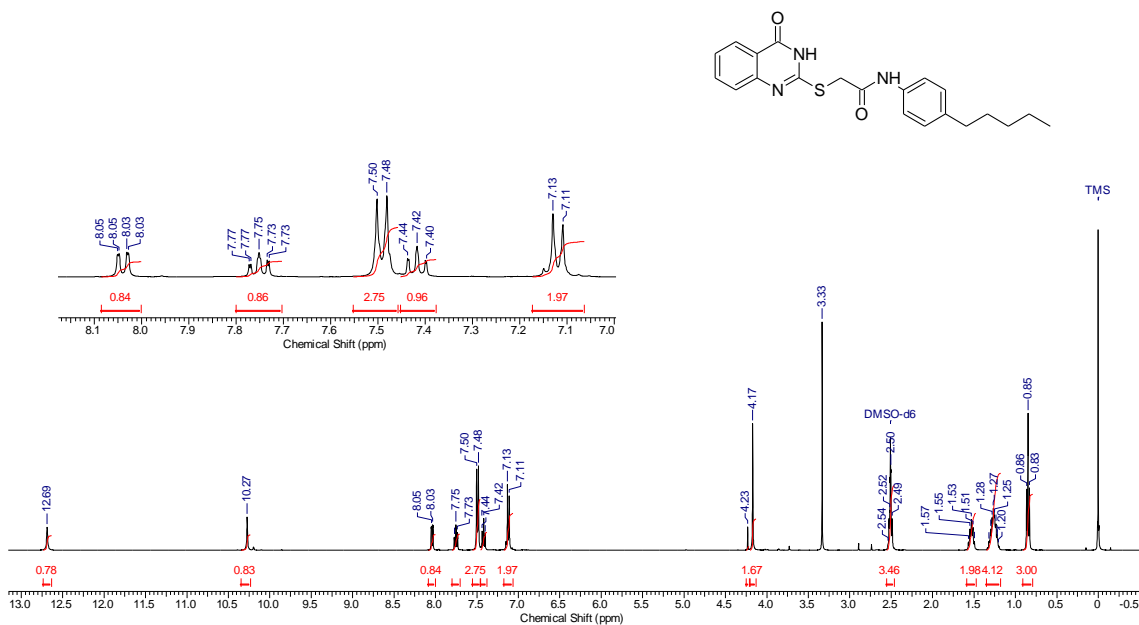


Figure S45. ¹H RMN spectrum of 2-((4-Oxo-3,4-dihydroquinazolin-2-yl)thio)-*N*-(4-pentylphenyl)acetamide (**9j**) in DMSO-*d*₆.

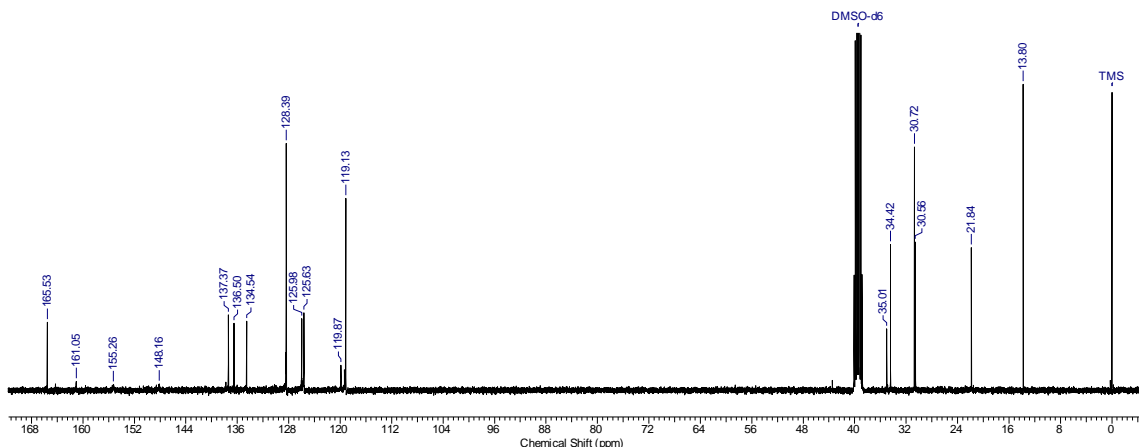


Figure S46. ¹³C RMN spectrum of 2-((4-Oxo-3,4-dihydroquinazolin-2-yl)thio)-*N*-(4-pentylphenyl)acetamide (**9j**) in DMSO-*d*₆.

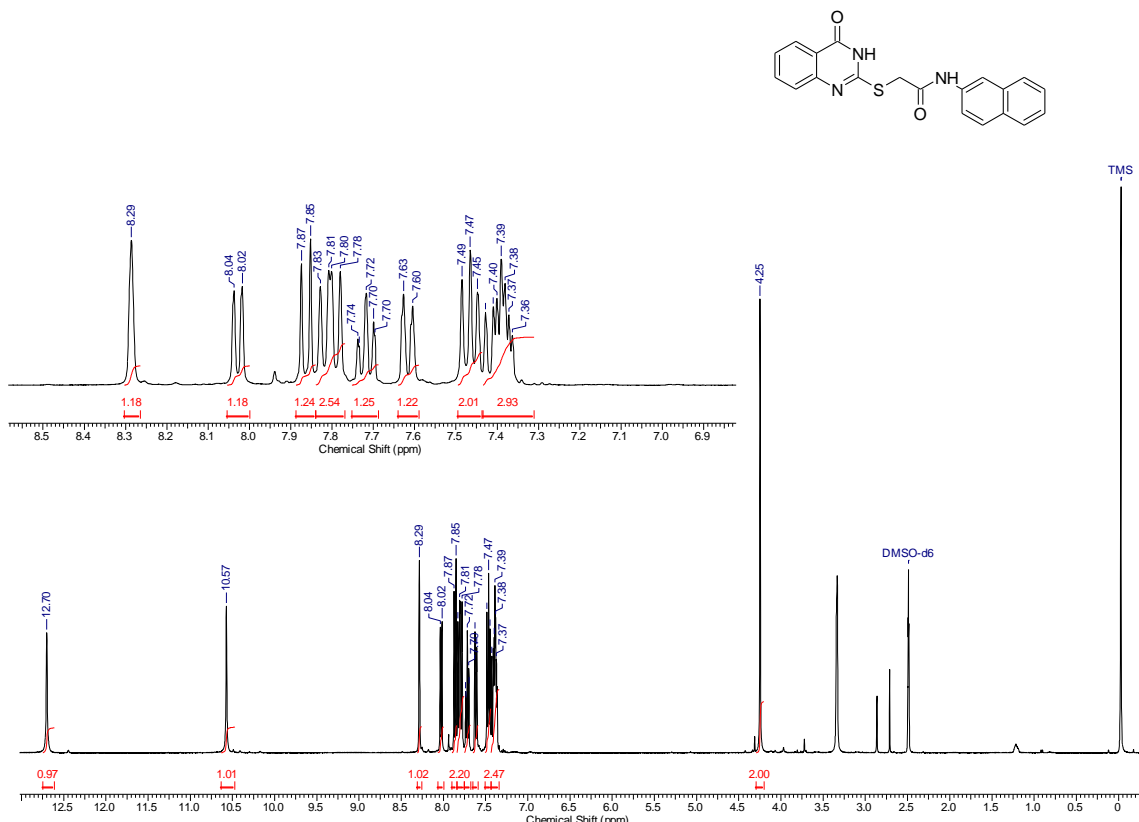
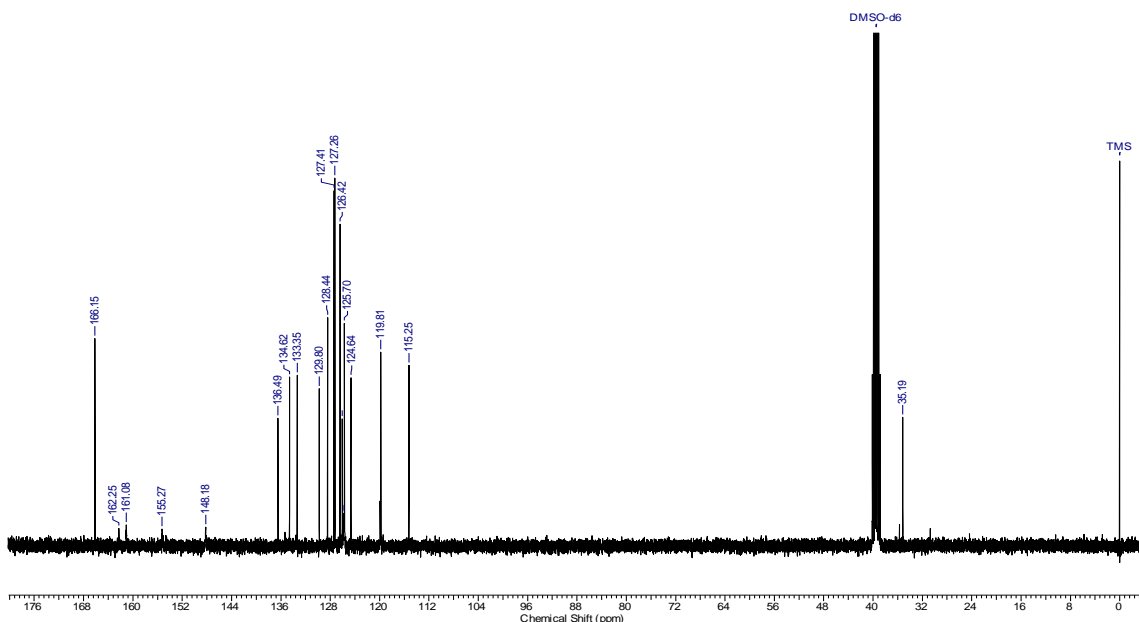


Figure S47. ¹H RMN spectrum of *N*-(Naphthalen-2-yl)-2-((4-oxo-3,4-dihydroquinazolin-2-yl)thio)acetamide (**9k**) in DMSO-*d*₆.



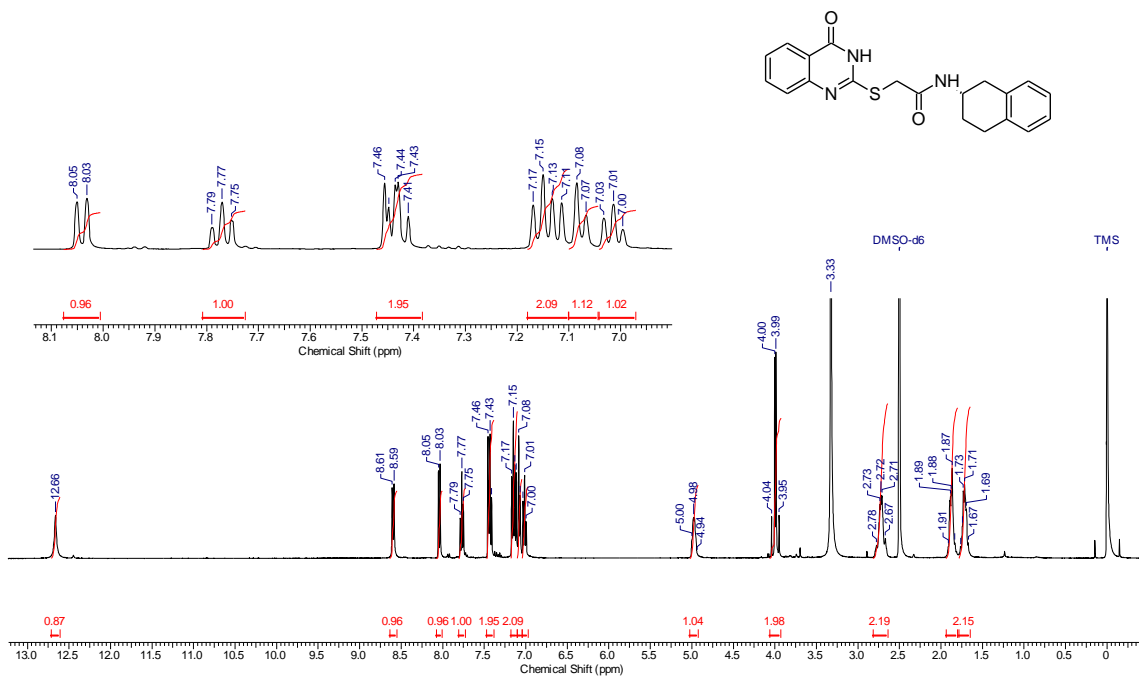


Figure S49. ^1H RMN spectrum of (*S*)-2-((4-Oxo-3,4-dihydroquinazolin-2-yl)thio)-*N*-(1,2,3,4-tetrahydronaphthalen-2-yl)acetamide (**9I**) in DMSO-*d*₆.

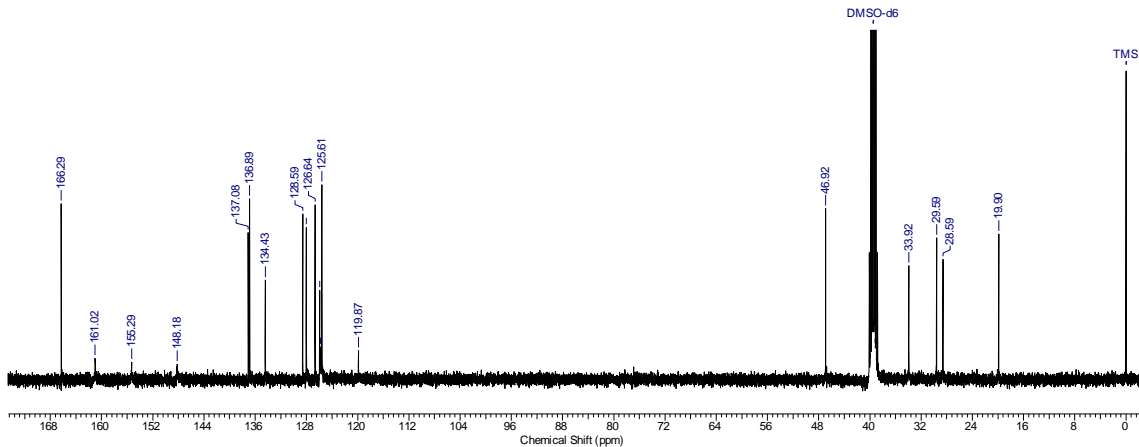


Figure S50. ^{13}C RMN spectrum of (*S*)-2-((4-Oxo-3,4-dihydroquinazolin-2-yl)thio)-*N*-(1,2,3,4-tetrahydronaphthalen-2-yl)acetamide (**9I**) in DMSO-*d*₆.

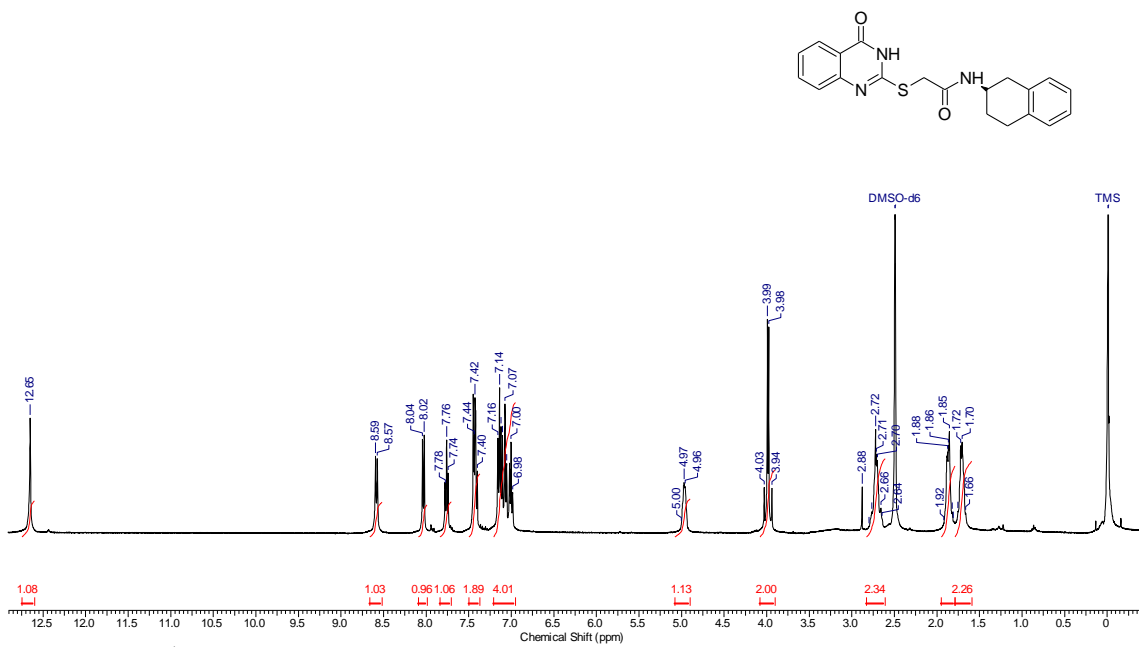


Figure S51. ^1H RMN spectrum of (*R*)-2-((4-Oxo-3,4-dihydroquinazolin-2-yl)thio)-*N*-(1,2,3,4-tetrahydronaphthalen-2-yl)acetamide (**9m**) in $\text{DMSO}-d_6$.

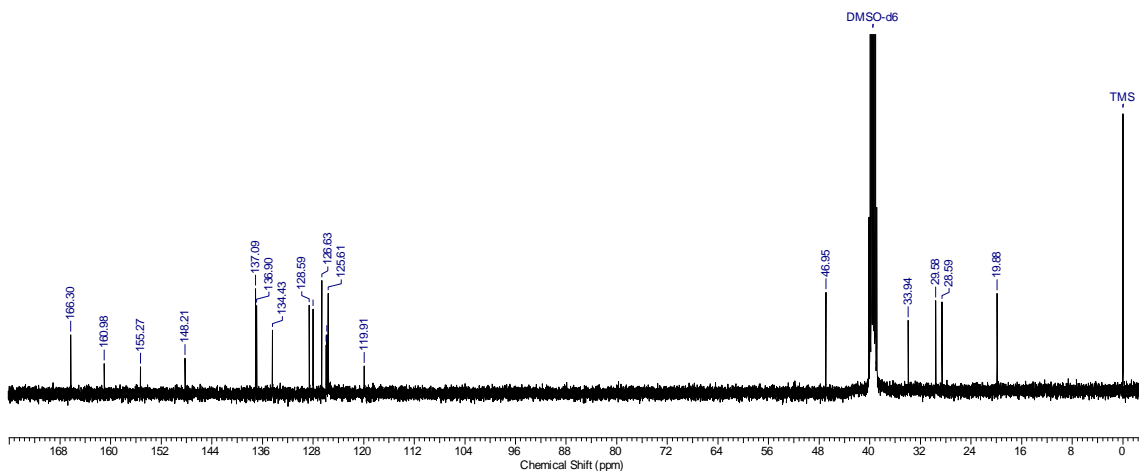


Figure S52. ^{13}C RMN spectrum of (*R*)-2-((4-Oxo-3,4-dihydroquinazolin-2-yl)thio)-*N*-(1,2,3,4-tetrahydronaphthalen-2-yl)acetamide (**9m**) in $\text{DMSO}-d_6$.

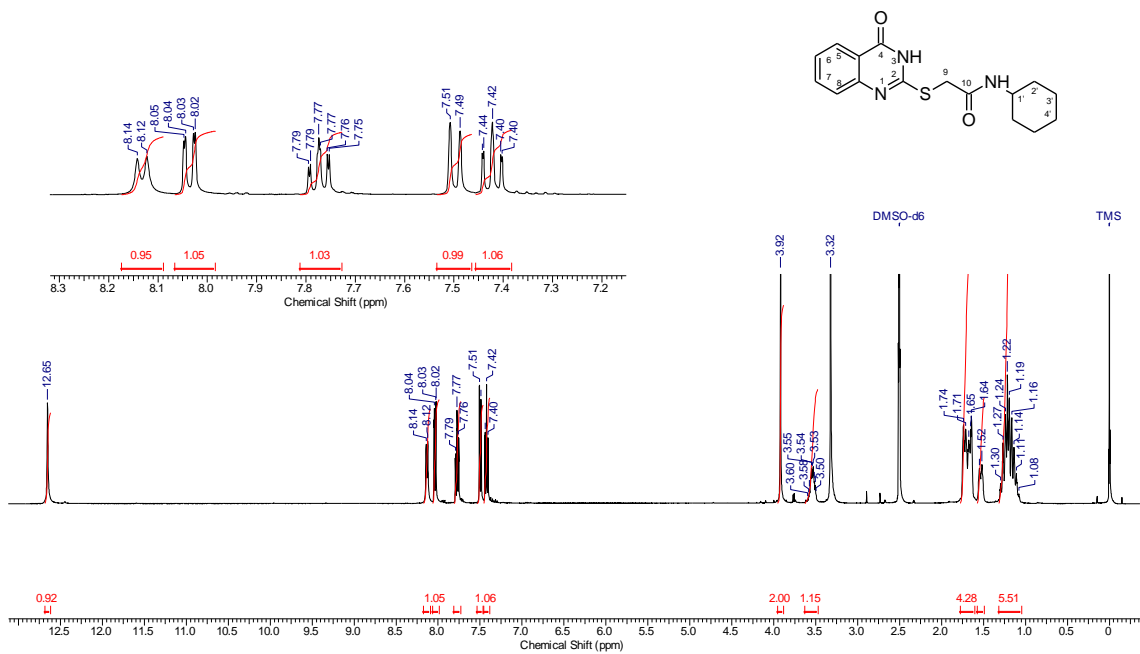


Figure S53. ^1H RMN spectrum of *N*-Cyclohexyl-2-((4-oxo-3,4-dihydroquinazolin-2-yl)thio)acetamide (**9n**) in $\text{DMSO}-d_6$.

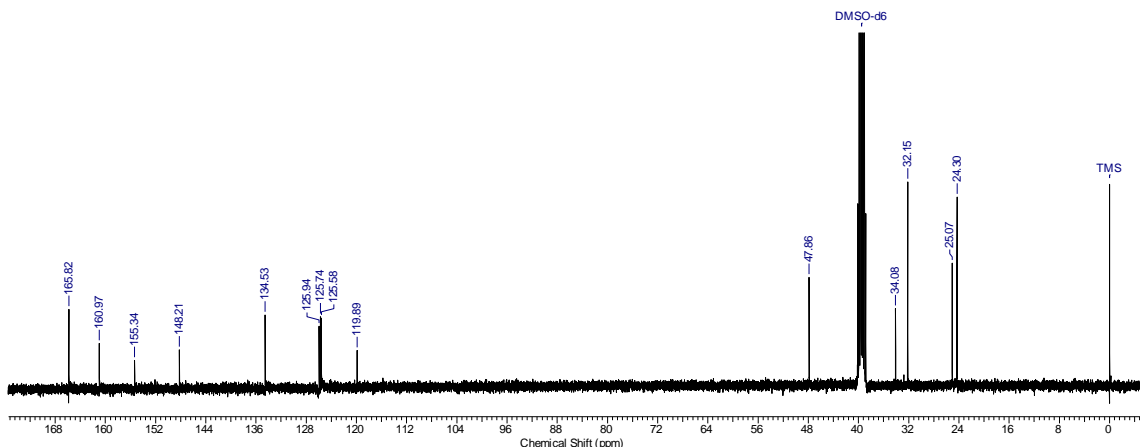


Figure S54. ^{13}C RMN spectrum of *N*-Cyclohexyl-2-((4-oxo-3,4-dihydroquinazolin-2-yl)thio)acetamide (**9n**) in $\text{DMSO}-d_6$.

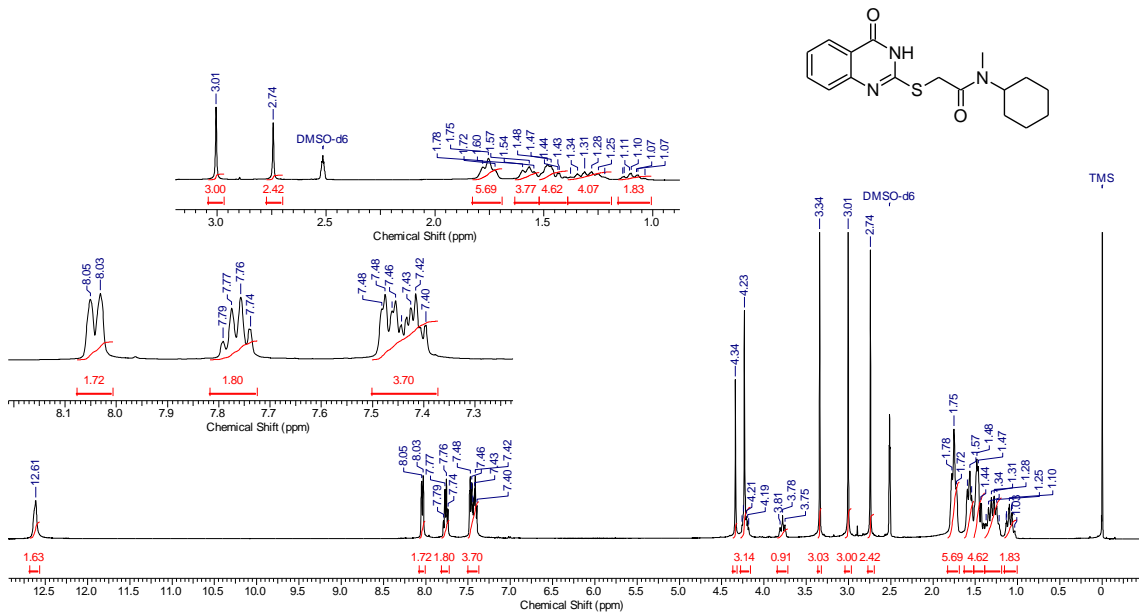


Figure S55. ^1H RMN spectrum of *N*-Cyclohexyl-*N*-methyl-2-((4-oxo-3,4-dihydroquinazolin-2-yl)thio)acetamide (**9o**) in $\text{DMSO}-d_6$.

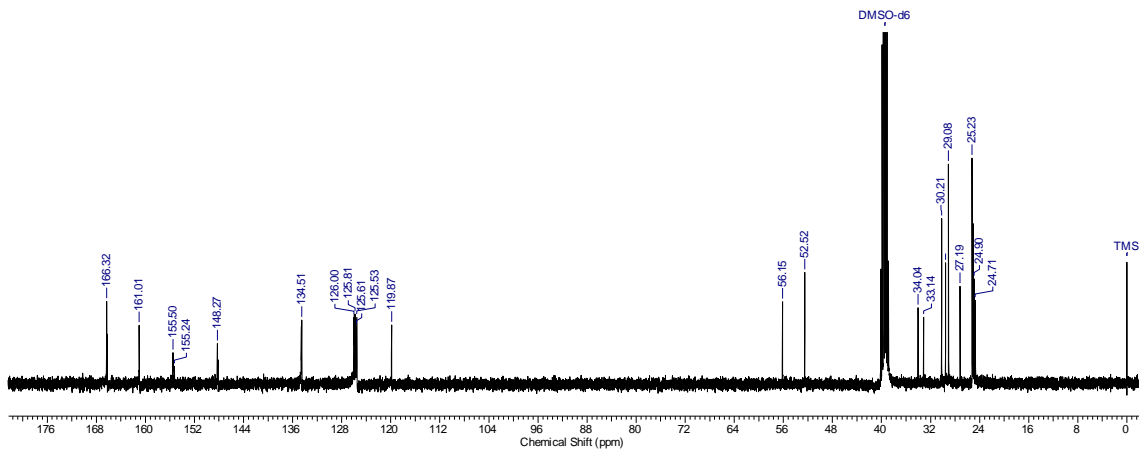


Figure S56. ^{13}C RMN spectrum of *N*-Cyclohexyl-*N*-methyl-2-((4-oxo-3,4-dihydroquinazolin-2-yl)thio)acetamide (**9o**) in DMSO- d_6 .

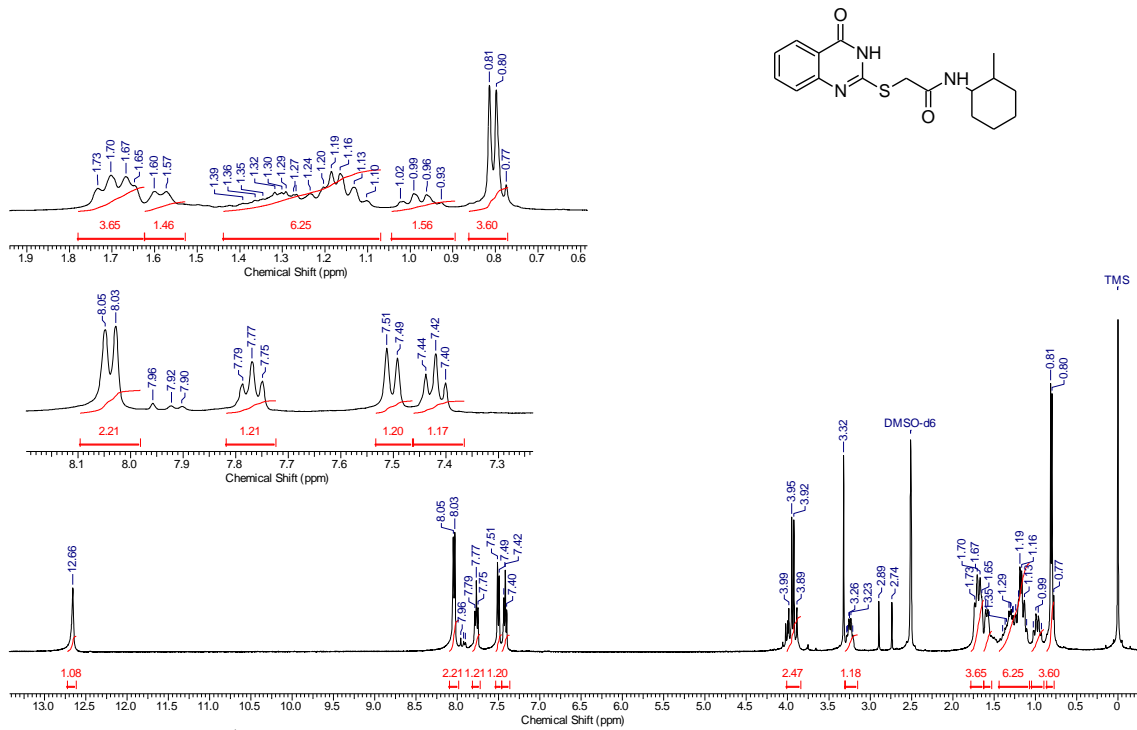


Figure S57. ¹H RMN spectrum of *N*-(2-Methylcyclohexyl)-2-((4-oxo-3,4-dihydroquinazolin-2-yl)thio)acetamide (**9p**) in DMSO-d₆.

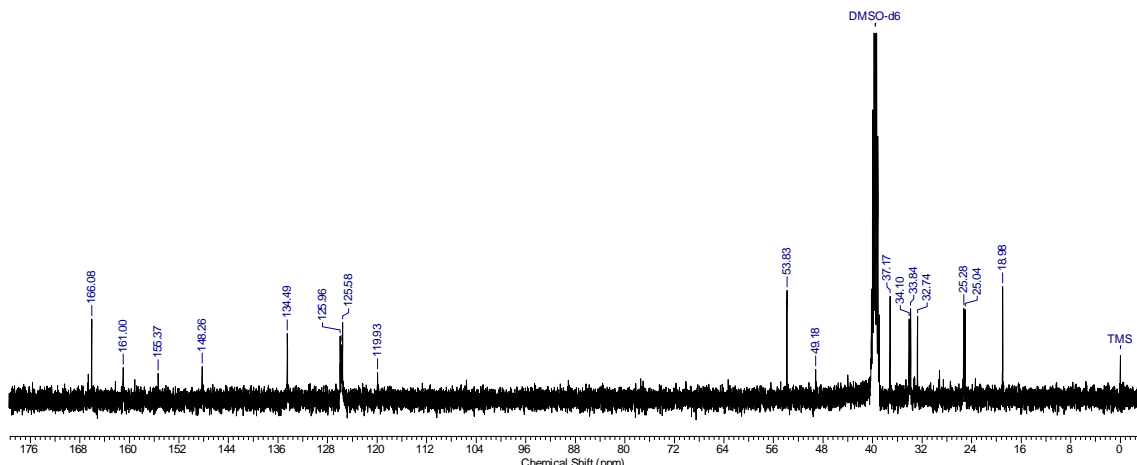


Figure S58. ¹³C RMN spectrum of *N*-(2-Methylcyclohexyl)-2-((4-oxo-3,4-dihydroquinazolin-2-yl)thio)acetamide (**9p**) in DMSO-d₆.

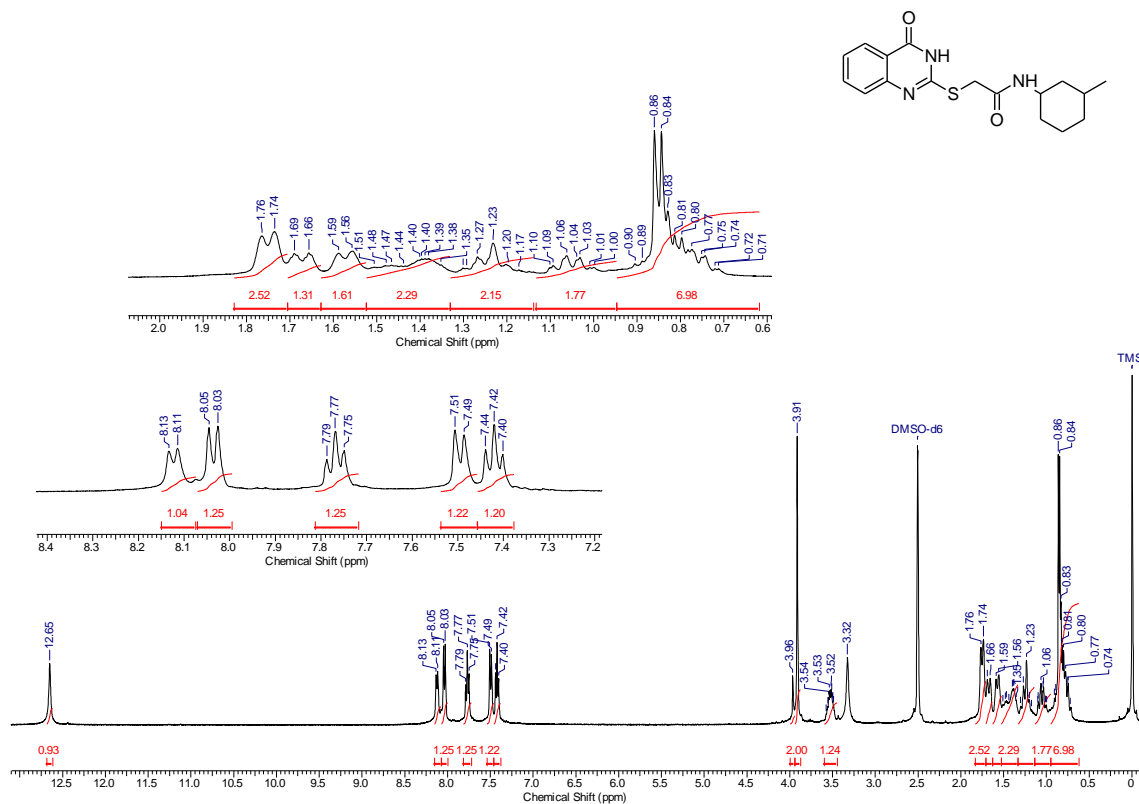


Figure S59. ^1H RMN spectrum of *N*-(3-Methylcyclohexyl)-2-((4-oxo-3,4-dihydroquinazolin-2-yl)thio)acetamide (**9q**) in $\text{DMSO}-d_6$.

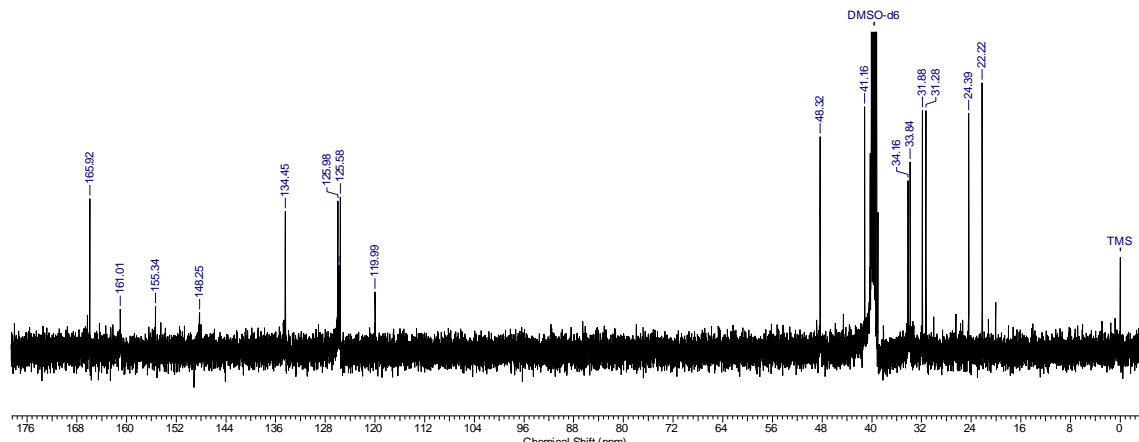


Figure S60. ^{13}C RMN spectrum of *N*-(3-Methylcyclohexyl)-2-((4-oxo-3,4-dihydroquinazolin-2-yl)thio)acetamide (**9q**) in $\text{DMSO}-d_6$.

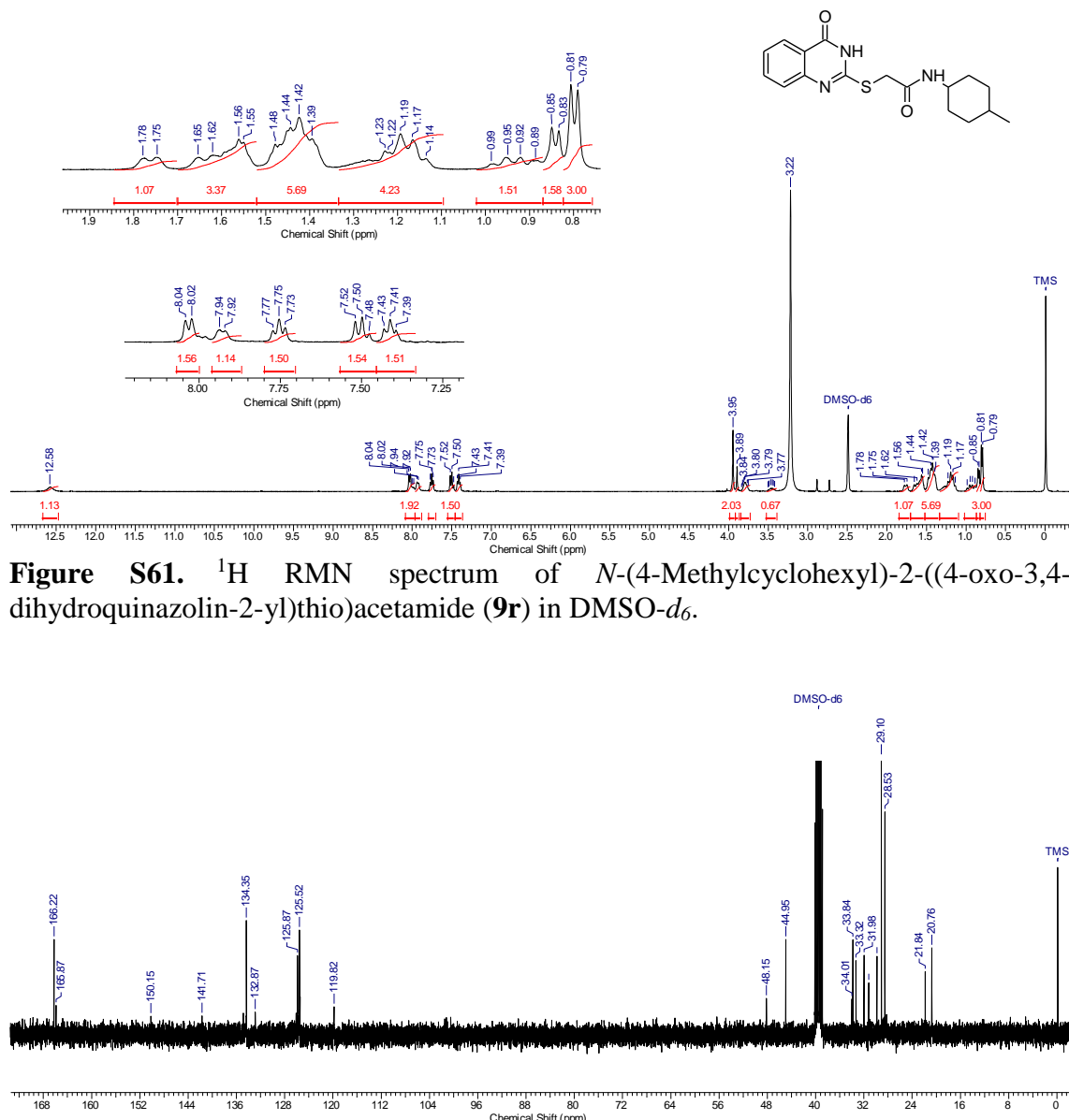


Figure S62. ^{13}C RMN spectrum of *N*-(4-Methylcyclohexyl)-2-((4-oxo-3,4-dihydroquinazolin-2-yl)thio)acetamide (**9r**) in $\text{DMSO}-d_6$.

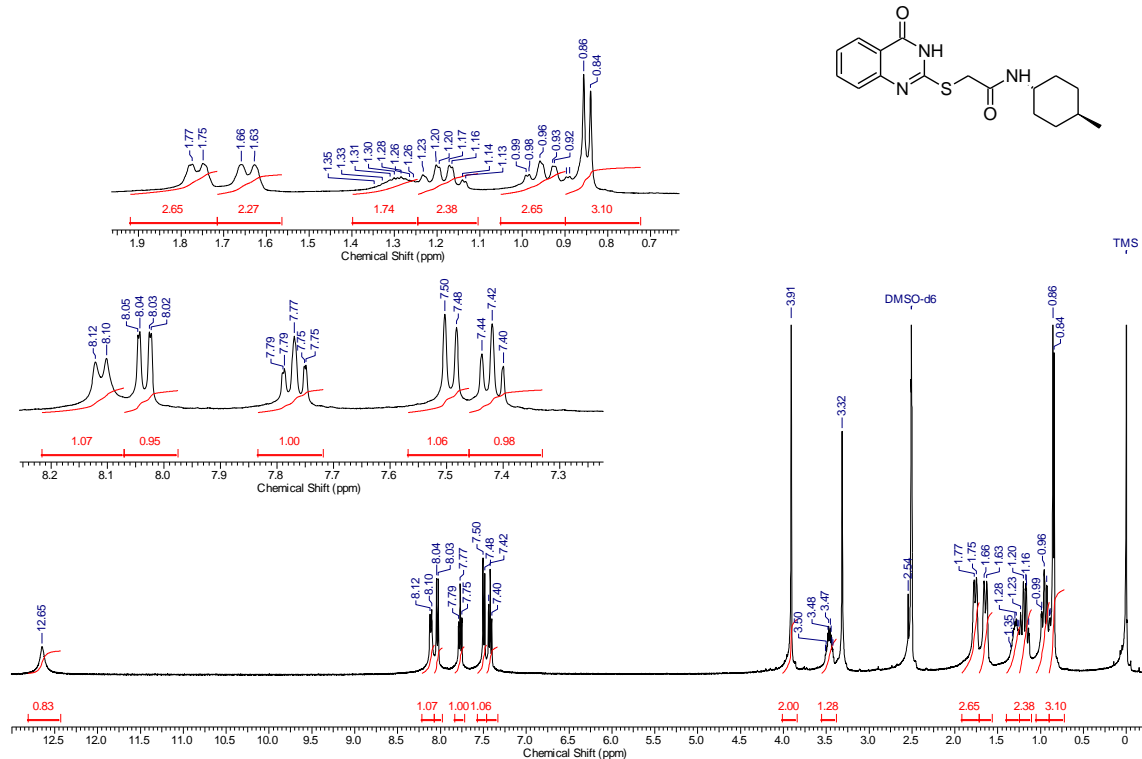


Figure S63. ¹H RMN spectrum of *N*-(*trans*-4-Methylcyclohexyl)-2-((4-oxo-3,4-dihydroquinazolin-2-yl)thio)acetamide (**9s**) in DMSO-*d*₆.

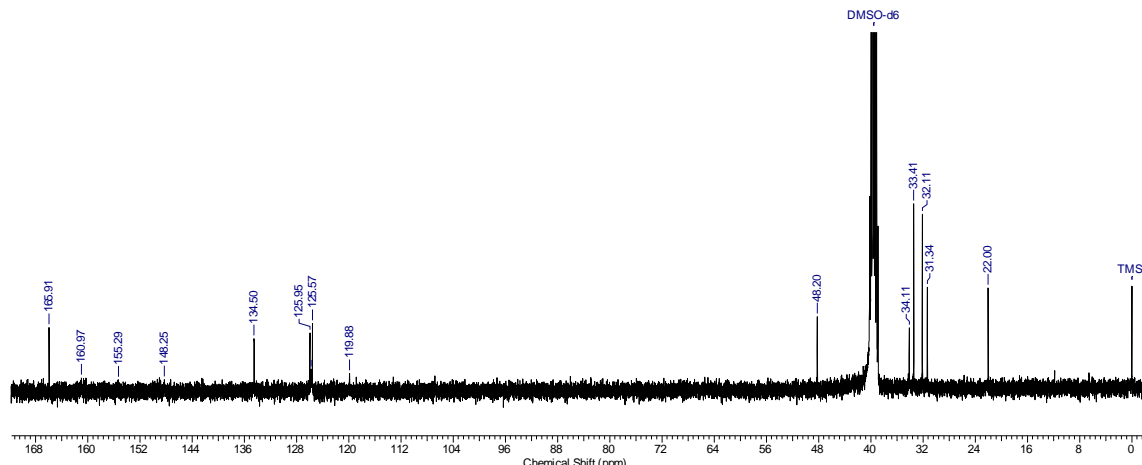


Figure S64. ¹³C RMN spectrum of *N*-(4-*trans*-Methylcyclohexyl)-2-((4-oxo-3,4-dihydroquinazolin-2-yl)thio)acetamide (**9s**) in DMSO-*d*₆.

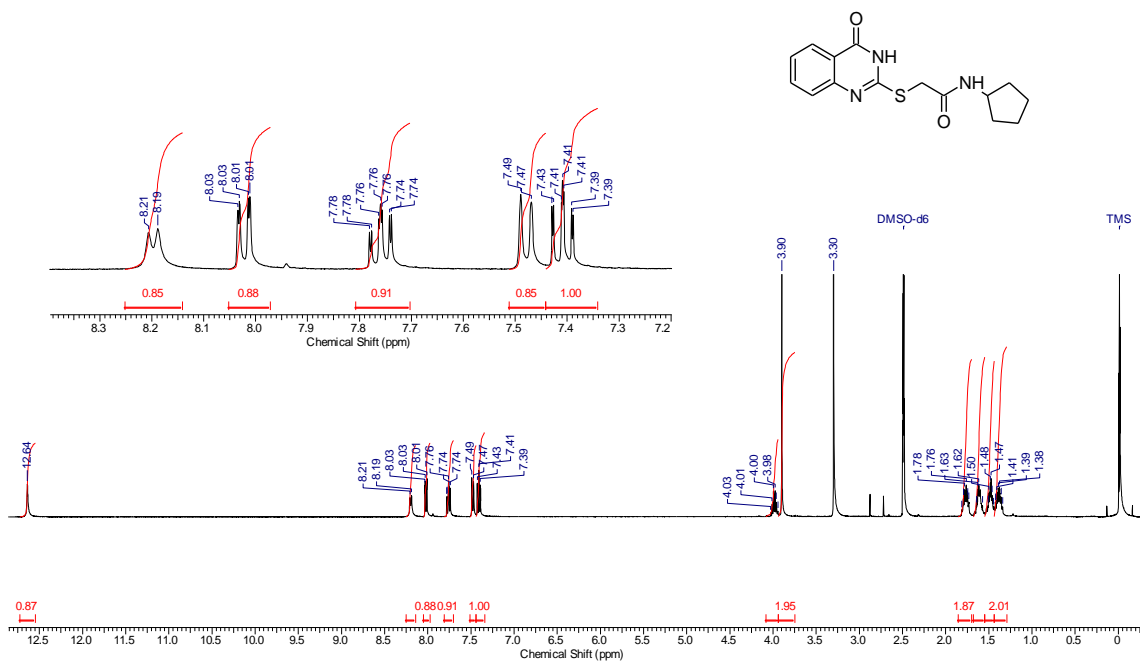


Figure S65. ^1H RMN spectrum of *N*-Cyclopentyl-2-((4-oxo-3,4-dihydroquinazolin-2-yl)thio)acetamide (**9t**) in $\text{DMSO}-d_6$.

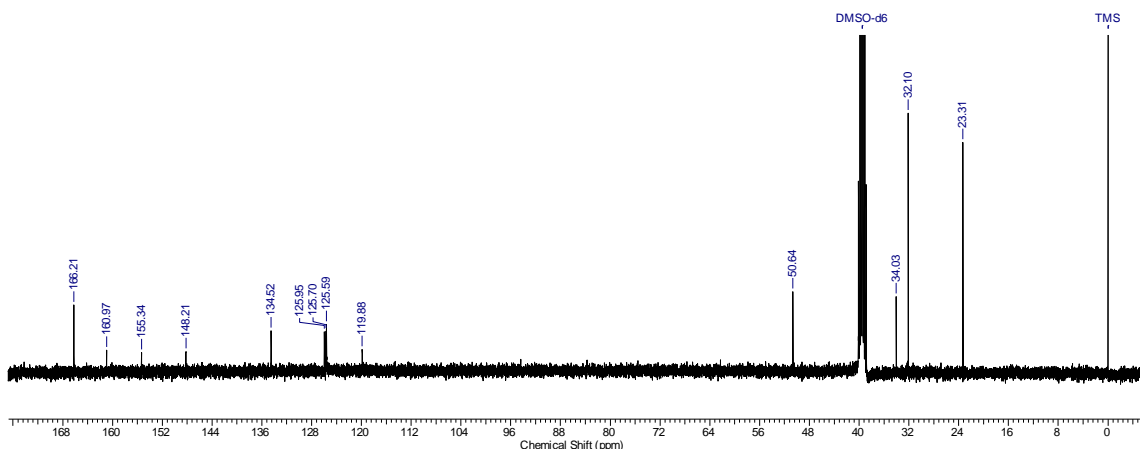


Figure S66. ^{13}C RMN spectrum of *N*-Cyclopentyl-2-((4-oxo-3,4-dihydroquinazolin-2-yl)thio)acetamide (**9t**) in $\text{DMSO}-d_6$.

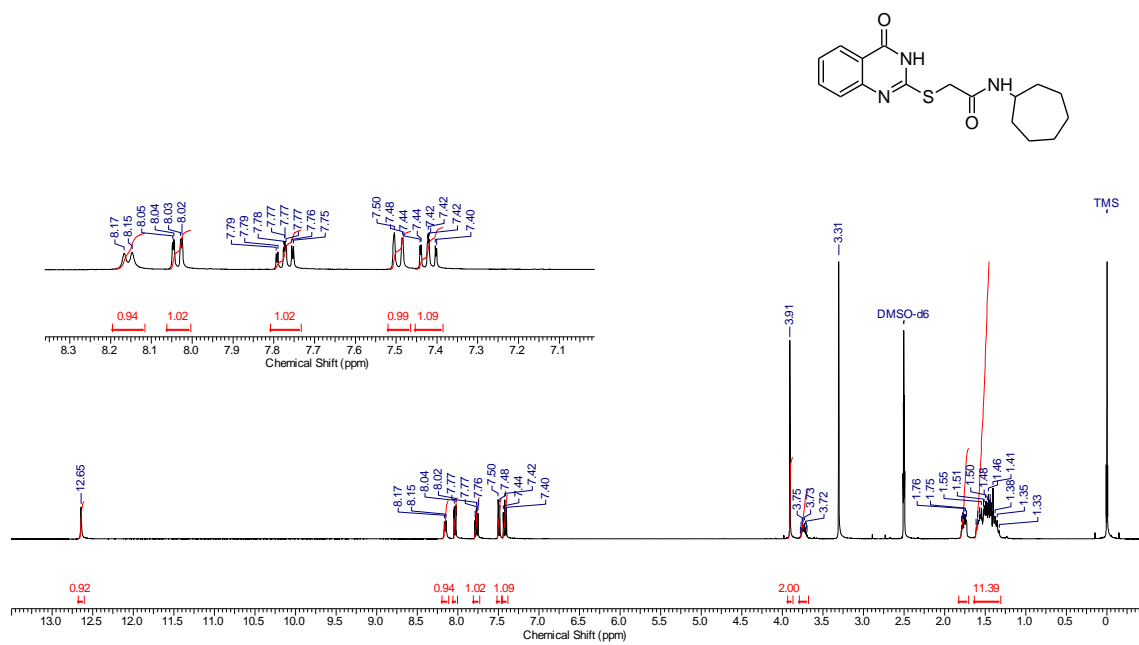


Figure S67. ^1H RMN spectrum of *N*-Cycloheptyl-2-((4-oxo-3,4-dihydroquinazolin-2-yl)thio)acetamide (**9u**) in DMSO-*d*₆.

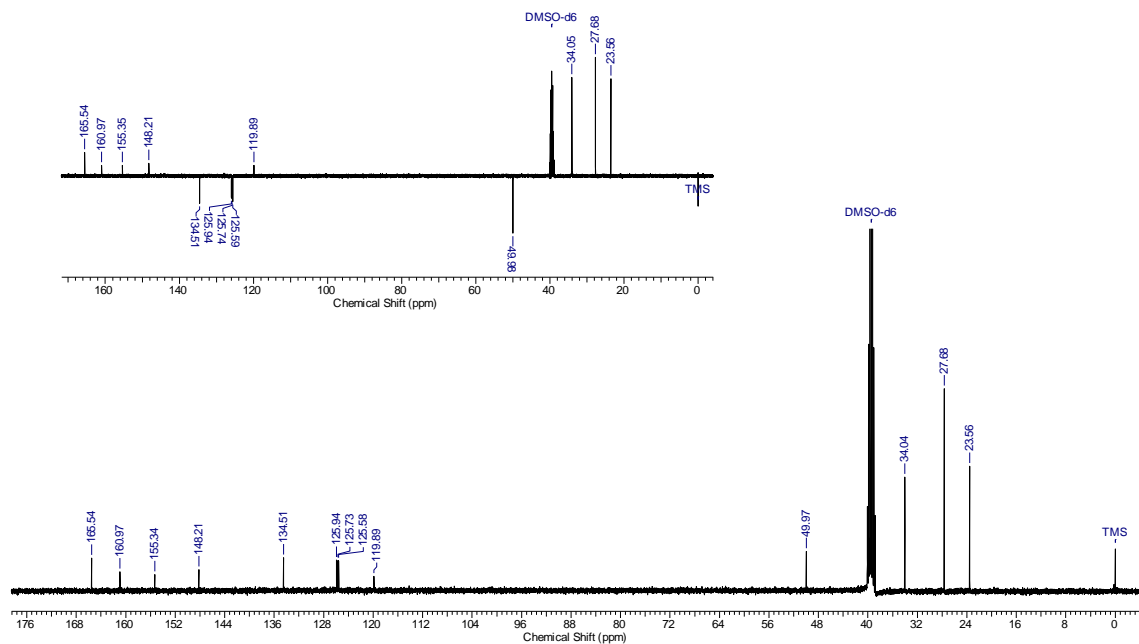


Figure S68. ^{13}C RMN spectrum of *N*-Cycloheptyl-2-((4-oxo-3,4-dihydroquinazolin-2-yl)thio)acetamide (**9u**) in DMSO-*d*₆.

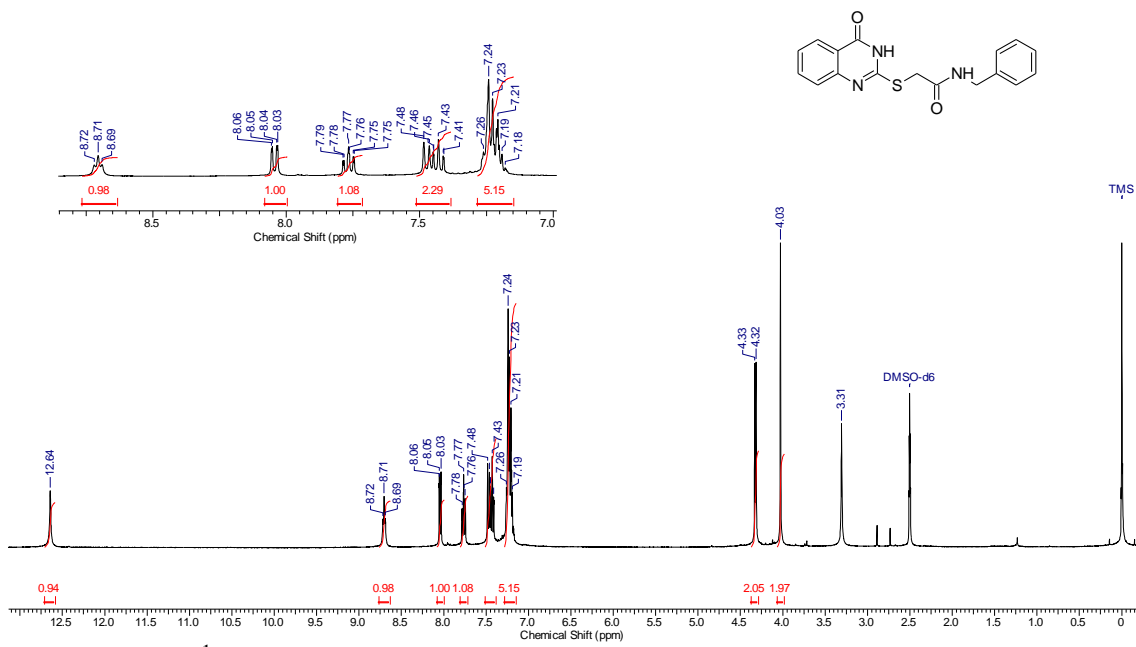


Figure S69. ^1H RMN spectrum of *N*-Benzyl-2-((4-oxo-3,4-dihydroquinazolin-2-yl)thio)acetamide (**9v**) in $\text{DMSO}-d_6$.

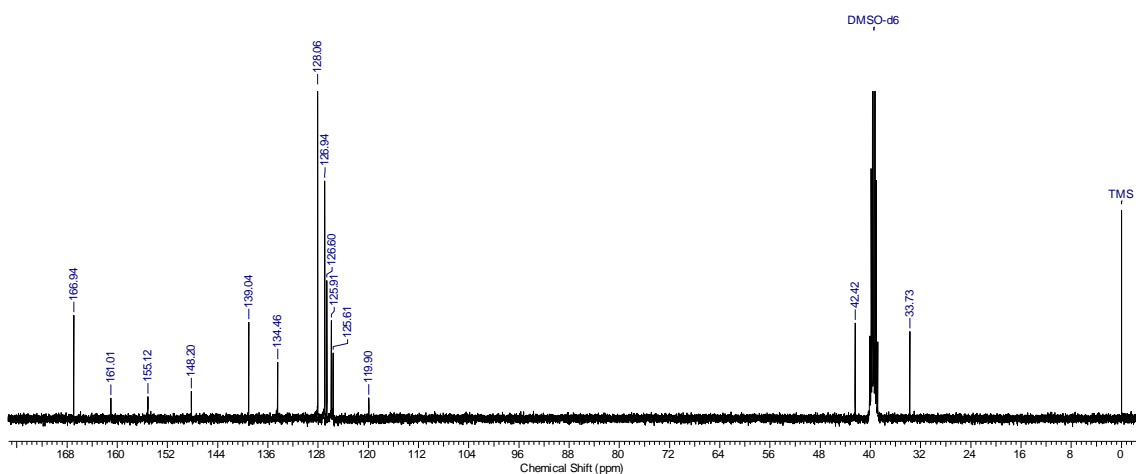


Figure S70. ^{13}C RMN spectrum of *N*-Benzyl-2-((4-oxo-3,4-dihydroquinazolin-2-yl)thio)acetamide (**9v**) in $\text{DMSO}-d_6$.

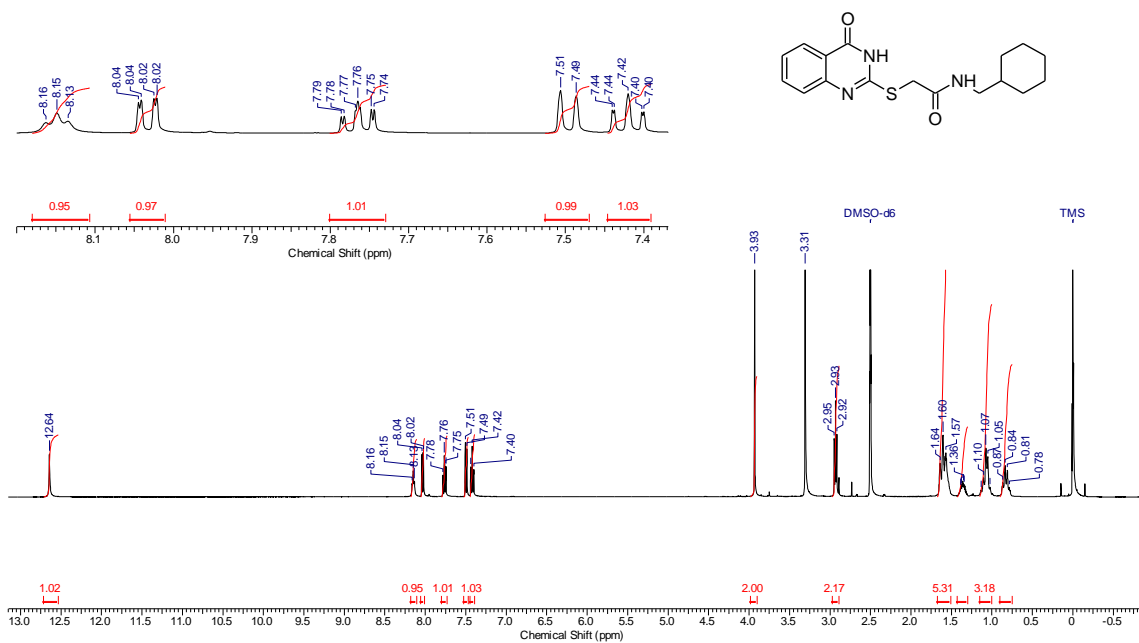


Figure S71. ¹H RMN spectrum of *N*-(Cyclohexylmethyl)-2-((4-oxo-3,4-dihydroquinazolin-2-yl)thio)acetamide (**9w**) in DMSO-*d*₆.

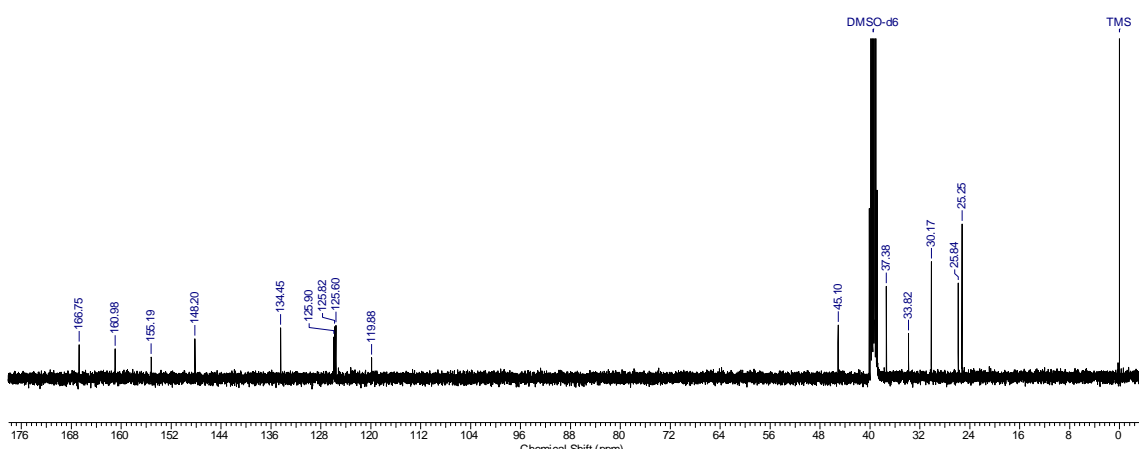


Figure S72. ¹³C RMN spectrum of *N*-(Cyclohexylmethyl)-2-((4-oxo-3,4-dihydroquinazolin-2-yl)thio)acetamide (**9w**) in DMSO-*d*₆.

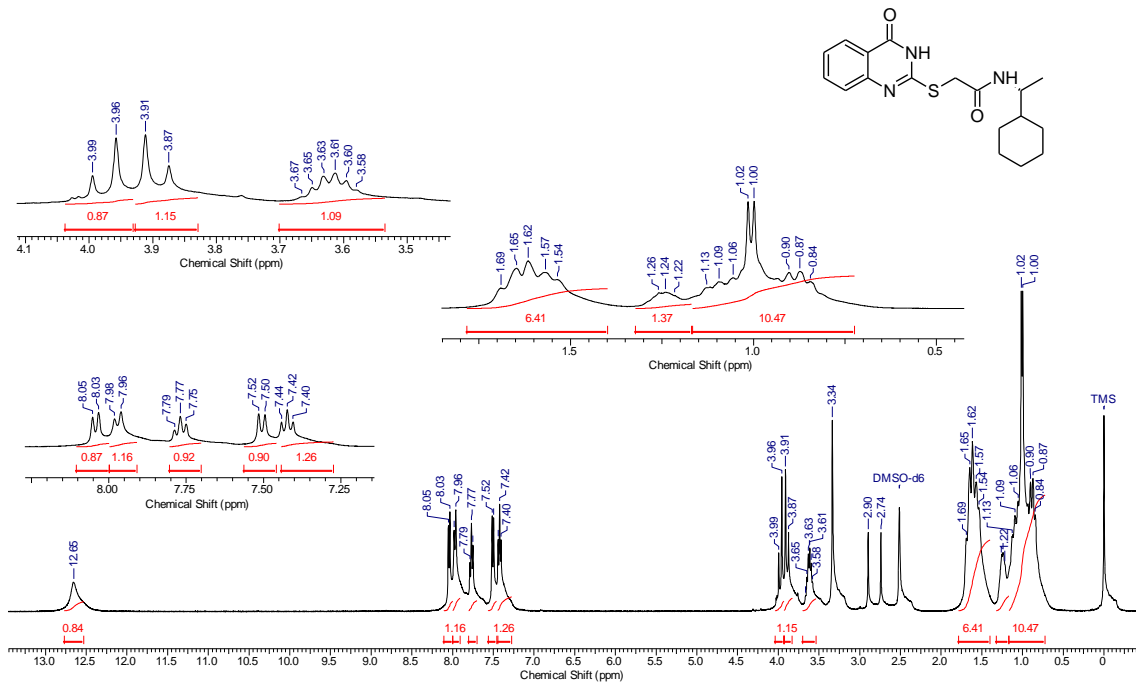


Figure S73. ¹H RMN spectrum of (*S*)-*N*-(1-Cyclohexylethyl)-2-((4-oxo-3,4-dihydroquinazolin-2-yl)thio)acetamide (**9x**) in DMSO-*d*₆.

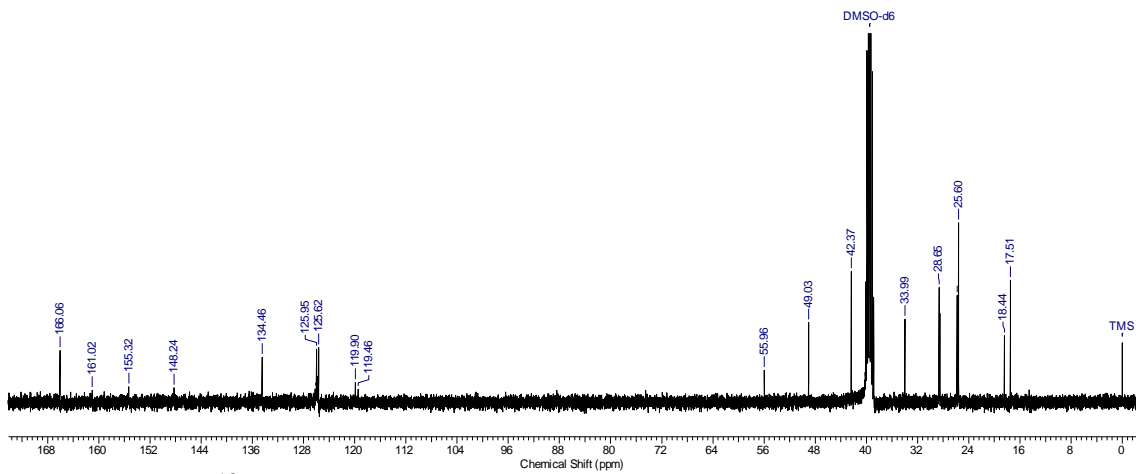


Figure S74. ¹³C RMN spectrum of (*S*)-*N*-(1-Cyclohexylethyl)-2-((4-oxo-3,4-dihydroquinazolin-2-yl)thio)acetamide (**9x**) in DMSO-*d*₆.

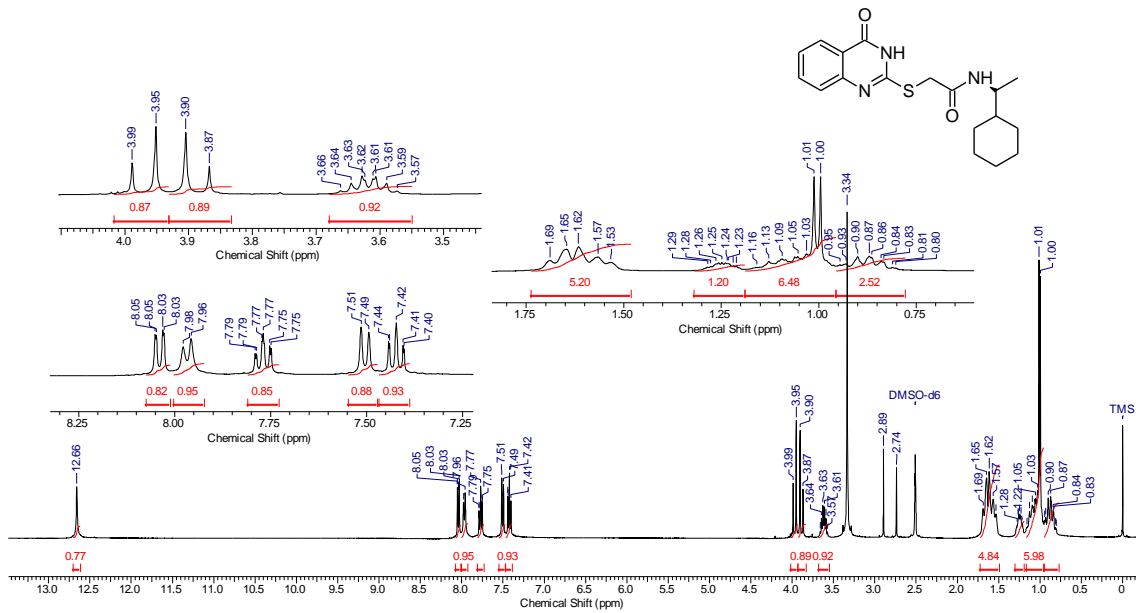


Figure S75. ^1H RMN spectrum of (*R*)-N-(1-Cyclohexylethyl)-2-((4-oxo-3,4-dihydroquinazolin-2-yl)thio)acetamide (**9y**) in DMSO-*d*₆.

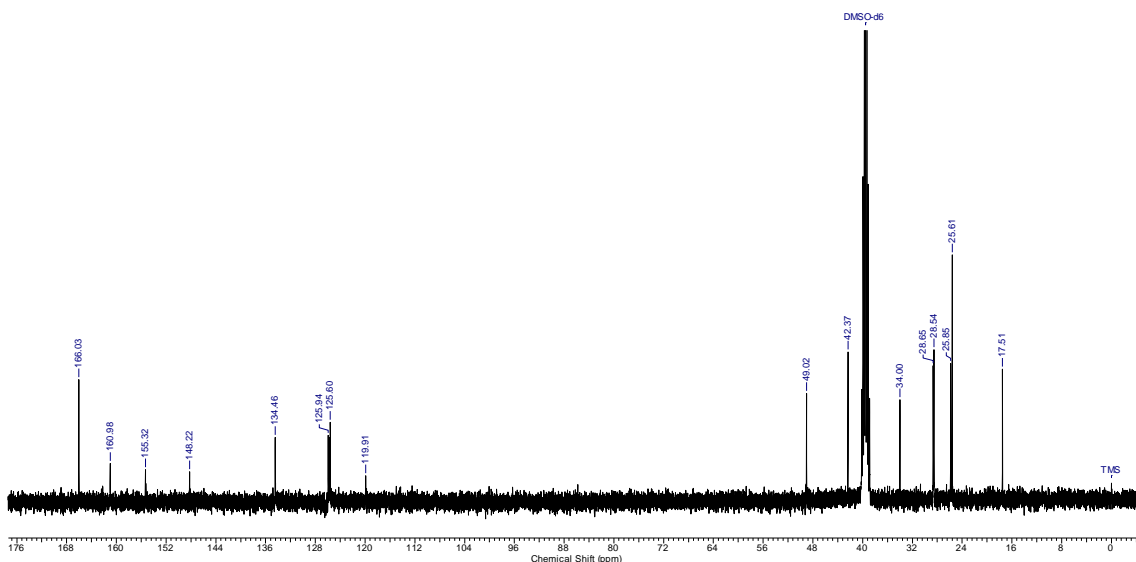


Figure S76. ^{13}C RMN spectrum of (*R*)-N-(1-Cyclohexylethyl)-2-((4-oxo-3,4-dihydroquinazolin-2-yl)thio)acetamide (**9y**) in $\text{DMSO}-d_6$.

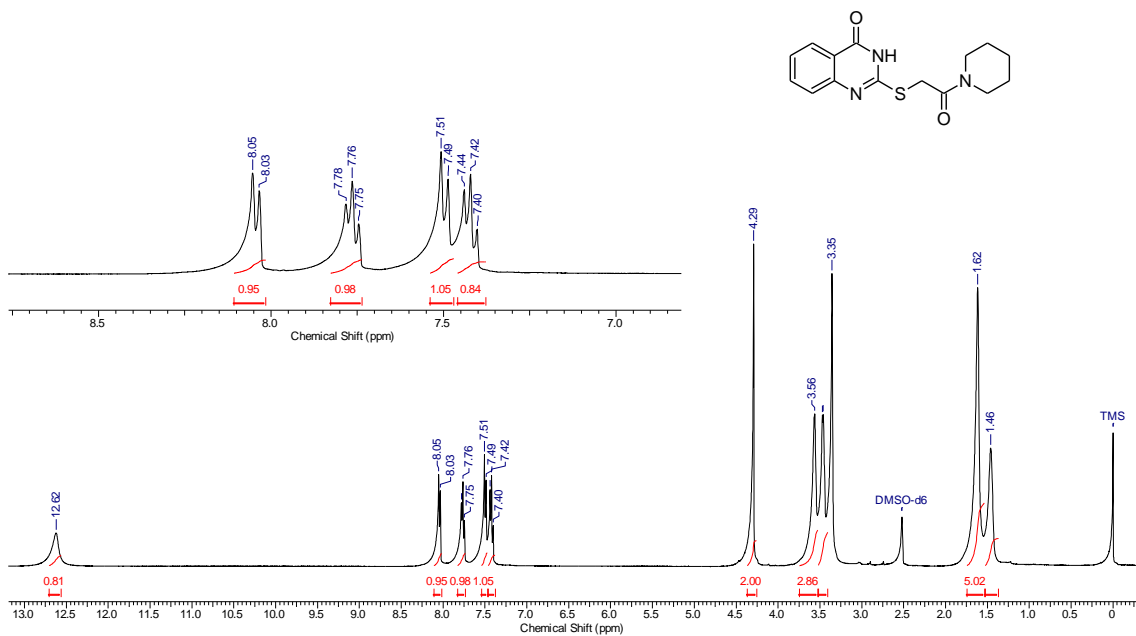


Figure S77. ^{13}C RMN spectrum of 2-((2-Oxo-2-(piperidin-1-yl)ethyl)thio)quinazolin-4(*3H*)-one (**9z**) in $\text{DMSO}-d_6$.

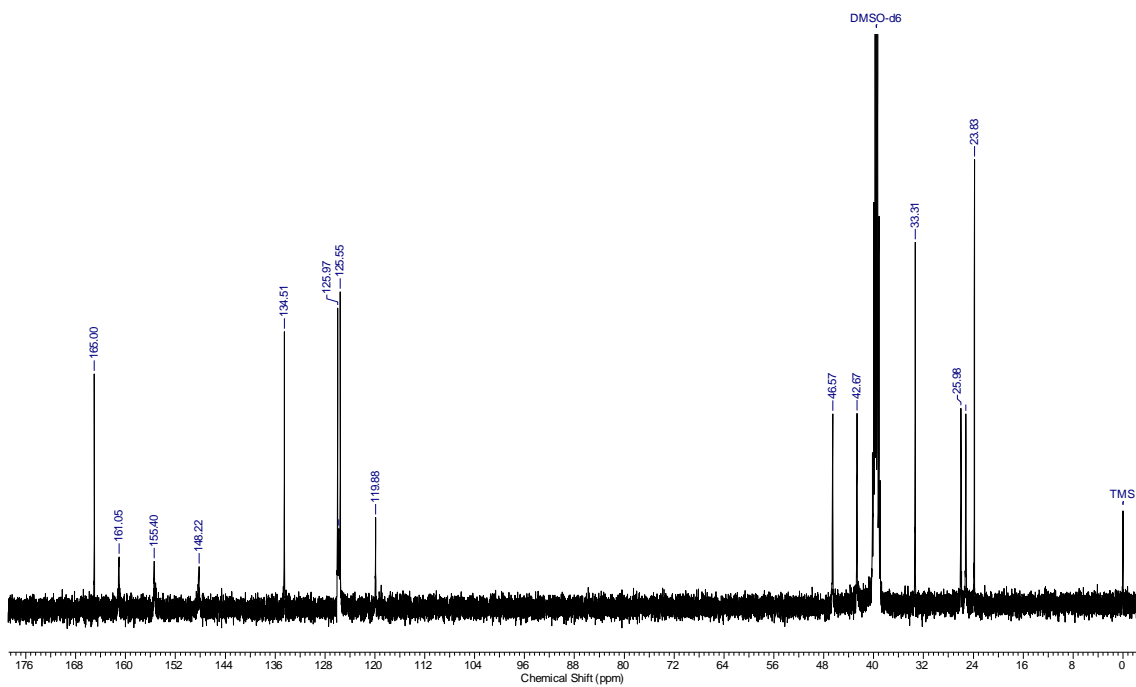


Figure S78. ^{13}C RMN spectrum of 2-((2-Oxo-2-(piperidin-1-yl)ethyl)thio)quinazolin-4(*3H*)-one (**9z**) in $\text{DMSO}-d_6$.

2. Determination of stability of the 3,4-dihydroquinazolin-4-ones **9n**, **9p-s**, **9u**, and **9w** in aqueous media.

Aqueous stability was determined in PBS containing 10% DMSO at 25 °C and 37 °C (**Table S1**). The compounds were incubated for 0, 3, 6, 9, 12, 24 and 48 h and in each time point an aliquot of 200 µL was withdrawn and the measurement of remnant compounds concentration were performed using HPLC. For each compound evaluated a calibration curve with acceptable validation parameters was constructed.

Table S1. Stability of 3,4-dihydroquinazolin-4-ones **9n**, **9p-s**, **9u**, and **9w** at 25 °C and 37 °C.

Entr y	Stability (%E ± SEM)													
	25 °C							37 °C						
	0 h	3 h	6 h	9 h	12 h	24 h	48 h	0 h	3 h	6 h	9 h	12 h	24 h	48 h
9n	100 ± 20	108 ± 13	100 ± 14	118 ± 9	101 ± 5	109 ± 12	126 ± 1	100 ± 4	109 ± 26	111 ± 6	123 ± 3	120 ± 7	127 ± 2	111 ± 9
9p	100 ± 17	128 ± 2	122 ± 17	127 ± 17	137 ± 4	138 ± 16	142 ± 12	100 ± 8	92 ± 7	75 ± 6	71 ± 2	70 ± 4	81 ± 5	80 ± 1
9q	100 ± 21	101 ± 18	102 ± 18	100 ± 19	102 ± 20	100 ± 19	95 ± 17	100 ± 5	96 ± 8	101 ± 5	97 ± 8	100 ± 1	97 ± 1	98 ± 1
9r	100 ± 5	97 ± 13	97 ± 6	99 ± 3	100 ± 2	111 ± 5	125 ± 11	100 ± 11	80 ± 23	59 ± 12	69 ± 6	70 ± 7	43 ± 11	48 ± 18
9s	100 ± 7	76 ± 14	67 ± 18	64 ± 6	47 ± 18	26 ± 24	20 ± 9	100 ± 13	83 ± 5	87 ± 6	77 ± 3	70 ± 4	51 ± 14	50 ± 6
9u	100 ± 4	80 ± 2	90 ± 2	91 ± 6	92 ± 2	122 ± 5	123 ± 4	100 ± 3	81 ± 3	67 ± 4	68 ± 12	81 ± 11	66 ± 2	71 ± 1
9w	100 ± 13	103 ± 12	115 ± 4	116 ± 8	112 ± 1	114 ± 3	125 ± 8	100 ± 12	106 ± 5	109 ± 7	112 ± 16	111 ± 10	104 ± 8	105 ± 6

CAPÍTULO 3

CONSIDERAÇÕES FINAIS

No presente trabalho foram obtidas duas séries de moléculas, sintetizadas a partir da abordagem de hibridação molecular, envolvendo os núcleos heterocíclicos *1H*-benzo[*d*]imidazol e 3,4-diidroquinazolin-4-ona como inibidores do crescimento de *Mycobacterium tuberculosis* (Mtb). Todos os 39 compostos, sendo 13 derivados contendo o núcleo *1H*-benzo[*d*]imidaol e 26 derivados contendo o núcleo 3,4-diidroquinazolin-4-ona, foram caracterizados por técnicas espectroscópicas.

Os compostos da classe *1H*-benzo[*d*]imidazol foram obtidos em rendimentos satisfatórios, variando entre 51 – 98% e com valores maiores ou iguais a 90% para pureza relativa e devidamente caracterizados. Contudo, a classe não mostrou inibição efetiva frente à cepa laboratorial de Mtb H37Rv apresentando concentrações inibitórias mínimas maiores do que 16 μM . Consequentemente, estes resultados não justificaram prosseguir com a realização dos ensaios de inibição do crescimento em isolados clínicos de Mtb e com os demais testes biológicos propostos. Dessa forma, mais estudos devem ser realizados visando à otimização estrutural desta classe para obter estruturas químicas mais promissoras frente ao Mtb.

A série dos compostos híbridos contendo o anel heterocíclico 2-mercaptopquinazolinona foi obtida em rendimentos satisfatórios com valores de pureza maiores ou iguais a 90%. Além disso, foram alcançados novos compostos anti-TB. Na avaliação da inibição do crescimento da cepa H37Rv de Mtb 7 compostos demonstraram valores promissores ($< 1 \mu\text{M}$) e, consequentemente, foram selecionados para a realização dos testes propostos no presente projeto.

Dando continuidade aos estudos de atividade biológica, estes 7 compostos (9n, 9p-s, 9u e 9w) foram então submetidos a testes de inibição de crescimento frente a isolados clínicos de Mtb, demonstrando uma inibição efetiva no crescimento dos isolados, com inibições melhores do que as apresentadas pelo fármaco controle isoniazida (INH). Foram também realizados testes de citotoxicidade, estabilidade, cardiotoxicidade, comportamento e morfologia em peixe-zebra. Todos estes compostos se mostraram não-citotóxicos nas linhagens celulares HepG2, HaCat e Vero, sem cardiotoxicidade aparente e sem efeito no comportamento e morfologia dos peixes-zebra.

Por fim, os resultados sugerem que a exploração de novos grupamentos funcionais e do estudo dos parâmetros físico-químicos envolvidos na relação entre a estrutura química com a atividade biológica pode levar a novos compostos efetivos na inibição do crescimento do Mtb.

REFERÊNCIAS

- ANDRIES, K. et al.. A Diarylquinoline Drug Active on the ATP Synthase of *Mycobacterium tuberculosis*. **Science**, v. 307, n. 5707, Jan. 2005. Disponível em: <<https://www.ncbi.nlm.nih.gov/pubmed/15591164>>. Acesso em: 31 ago. 2017.
- ASIF, M.. Chemical Characteristics, Synthetic Methods and Biological Potential of Quinazoline and Quinazolinone Derivatives. **International Journal of Medicinal Chemistry**, v. 2014, nov. 2014. Disponível em: <<https://www.hindawi.com/journals/ijmc/2014/395637/>>. Acesso em 31 ago. 2017.
- BALLELL, L. et al.. Fueling open-source drug discovery: 177 small-molecule leads against tuberculosis. **ChemMedChem**, v. 8, n. 2, fev. 2013. Disponível em: <<http://www.ncbi.nlm.nih.gov/pubmed/23307663>>. Acesso em: 12 set. 2017.
- BRASIL. Ministério da Saúde. Secretaria de Vigilância em Saúde. **Boletim Epidemiológico: Especial Tuberculose**, v. 43, mar. 2012.
- BRASIL. Sinan Net. Tuberculose - Casos confirmados notificados no Sistema de Informação de Agravos de Notificação - Rio Grande do Sul, 2017. Disponível em: <<http://tabnet.datasus.gov.br/cgi/tabcgi.exe?sinannet/cnv/tubercrs.def>>. Acesso em: 25 ago. 2017.
- CENTERS FOR DISEASE CONTROL AND PREVENTION. Provisional CDC guidelines for the use and safety monitoring of bedaquiline fumarate (Sirturo) for the treatment of multidrug-resistant tuberculosis. **MMWR Recommendations and Reports**, v. 62, n. 9, 2013. Disponível em: <<http://www.ncbi.nlm.nih.gov/pubmed/24157696>>. Acesso em: 20 out. 2017.
- CHAN, E. D.; ISEMAN, Michael D.. Current medical treatment for tuberculosis. **British Medical Journal**, v. 325, n. 7375, nov. 2002. Disponível em: <<https://www.ncbi.nlm.nih.gov/pubmed/123307663>>. Acesso em: 12 set. 2017.
- DAVE, R. S. et al.. Synthesis, characterization and antimicrobial activity of new quinazolin- 4(3H)-one schiff base derivatives. **Journal of Chemical and Pharmaceutical Research**, v. 4, n. 11, 2012.. Disponível em: <<http://www.jocpr.com/articles/synthesis-characterization-and-antimicrobial-activity-of-new-quinazolin43hone-schiff-base-derivatives.pdf>>. Acesso em: 12 set. 2017.
- DEVI, K. A.; SARANGAPANI, M.; SRIRAM.. Synthesis and Antimicrobial activity of some Quinazolinones Derivatives. **International Journal of Drug Development and Research**, v. 4, n. 3, set. 2012. Disponível em: <<http://www.ijddr.in/drug-development/synthesis-and-antimicrobial-activity-of-some-quinazolinonesderivatives.pdf>>. Acesso em: 12 set. 2017.
- DORMAN, S. E.; CHAISSON, R. E.. From magic bullets back to the Magic Mountain: the rise of extensively drug-resistant tuberculosis. **Nature Medicine**, v. 13, n. 3, mar. 2007. Disponível em:

<<http://www.nature.com/doifinder/10.1038/nm0307-295>>. Acesso em: 30 ago. 2017.

DOVER, L. G.; COXON, G. D.. Current status and research strategies in tuberculosis drug development. **Journal of Medicinal Chemistry**, v. 54 n. 18, set. 2011. Disponível em: <<https://www.ncbi.nlm.nih.gov/pubmed/21823589>>. Acesso em: 12 set. 2017.

EL-BADRY, Y. A.; ANTER, N. A.; EL-SHESHTAWY, H. S.. Synthesis and evaluation of new polysubstituted quinazoline derivatives as potential antimicrobial agents. **Der Pharma Chemica**, v. 4, n. 3, 2012. Disponível em: <<http://derpharmacemica.com/archive.html>>. Acesso em: 12 set. 2017.

ELSTON, J. W. T.; THAKER, H. K. B.. Co-infection with human immunodeficiency virus and tuberculosis. **Indian journal of dermatology, venereology and leprology**, v. 74, n. 3, mai. 2008. Disponível em: <<http://www.ncbi.nlm.nih.gov/pubmed/18583782>>. Acesso em: 30 ago. 2017.

EUROPEAN MEDICINES AGENCY. **Assessment report**: Deltyba, dec. 2013. Disponível em: <http://www.ema.europa.eu/docs/en_GB/document_library/EPAR_-_Public_assessment_report/human/002552/WC500166234.pdf>. Acesso em: 30 ago. 2017.

FLYNN, J. L.; CHAN, J.. Immunology of tuberculosis. **Annual Review of Immunology**, v.19, 2011. Disponível em: <<https://www.ncbi.nlm.nih.gov/pubmed/11244032>>. Acesso: em 12 set. 2017.

GAURRAND, S. et al.. Conformational analysis of r207910, a new drug candidate for the treatment of tuberculosis, by a combined NMR and molecular modeling approach. **Chemical biology & drug design**, v. 68, n. 2, ago. 2006. Disponível em: <<http://www.ncbi.nlm.nih.gov/pubmed/16999772>>. Acesso em: 30 ago. 2017.

GHORAB, M. M. et al.. Synthesis and pharmacophore modeling of novel quinazolines bearing a biologically active sulfonamide moiety. **Acta Pharmaceutica**, v. 63, n. 1, mar. 2013. Disponível em: <<http://www.ncbi.nlm.nih.gov/pubmed/23482309>>. Acesso em: 12 set. 2017.

GIACOBBO, B. C. et al.. New insights into the SAR and drug combination synergy of 2-(quinolin-4-yloxy)acetamides against *Mycobacterium tuberculosis*. **European Journal of Medicinal Chemistry**, v. 126, jan. 2017. Disponível em: <<http://www.sciencedirect.com/science/article/pii/S0223523416309862>>. Acesso em: 12 set. 2017.

HOAGLAND, D. et al.. New agents for the treatment of drug-resistant *Mycobacterium tuberculosis*. **Advanced Drug Delivery Reviews**, v.102, jul. 2016. Disponível em: <<https://www.ncbi.nlm.nih.gov/pubmed/27151308>>. Acesso em: 30 ago. 2017.

HUITRIC, E. et al.. Rates and mechanisms of resistance development in *Mycobacterium tuberculosis* to a novel diarylquinoline ATP synthase inhibitor. **Antimicrobial Agents and Chemotherapy**, v. 54, n. 3, mar. 2010. Disponível em: <<https://www.ncbi.nlm.nih.gov/pubmed/20038615>>. Acesso em: 20 out.

2017.

JAFARI, E. et al.. Quinazolinone and quinazoline derivatives: Recent structures with potent antimicrobial and cytotoxic activities. **Research in Pharmaceutical Sciences**, v. 11, n. 1, jan. 2016. Disponível em:

<https://www.ncbi.nlm.nih.gov/pmc/articles/PMC4794932/>. Acesso em: 12 set. 2017.

JASSAL, M.; BISHAI W. R.. Extensively drug-resistant tuberculosis. **The Lancet. Infectious diseases**, v. 9, n. 1, jan. 2009. Disponível em: <http://www.ncbi.nlm.nih.gov/pubmed/18990610>. Acesso em: 31 ago. 2017.

KAUFMANN, S. H.. How can immunology contribute to the control of tuberculosis? **Nature reviews Immunology**, v. 1, n. 1, out. 2001. Disponível em: <<https://www.ncbi.nlm.nih.gov/pubmed/11905811>>. Acesso em: 31 ago. 2017.

KOUL, A. et al.. The challenge of new drug discovery for tuberculosis. **Nature**, v. 469, n. 7331, jan. 2011. Disponível em: <https://www.ncbi.nlm.nih.gov/pubmed/21270886>. Acesso em: 12 set. 2017.

KSHIRSAGAR, U. A.. Recent developments in the chemistry of quinazolinone alkaloids. **Organic & Biomolecular Chemistry**, v. 13, n. 36, set. 2015. Disponível em: <<https://www.ncbi.nlm.nih.gov/pubmed/26278395>>. Acesso em: 20 out. 2017.

MA, Z. et al.. Global tuberculosis drug development pipeline: the need and the reality. **The Lancet**, v. 375, n. 9731, jun. 2010. Disponível em: <https://www.ncbi.nlm.nih.gov/pubmed/20488518>. Acesso em: 12 set. 2017.

MATSUMOTO, M. et al.. OPC-67683, a nitro-dihydro-imidazooxazole derivative with promising action against tuberculosis in vitro and in mice. **PLoS Medicine**, v. 3, n. 11, nov. 2006. Disponível em: <<https://www.ncbi.nlm.nih.gov/pubmed/17132069>>. Acesso em: 20 out. 2017.

NEPALI, K. et al.. Rational approaches, design strategies, structure activity relationship and mechanistic insights for anticancer hybrids. **European Journal of Medicinal Chemistry**, v. 77, abr. 2014. Disponível em: <http://www.ncbi.nlm.nih.gov/pubmed/24685980>. Acesso em: 12 set. 2017.

PAI, M. et al.. Tuberculosis. **Nature Reviews Disease Primers**, v. 2, p. 16076, out. 2016. Disponível em: <<http://www.nature.com/articles/nrdp201676>>. Acesso em: 31 ago. 2017.

PALOMINO, J. C.; MARTIN, A.. TMC207 becomes bedaquiline, a new anti-TB drug. **Future microbiology**, v. 8, n. 9, set. 2013. Disponível em: <http://www.ncbi.nlm.nih.gov/pubmed/24020736>. Acesso em: 31 ago. 2017.

PEDGAONKAR, G. S. et al.. Development of 2-(4-oxoquinazolin-3(4H)-yl)acetamide derivatives as novel enoyl-acyl carrier protein reductase (InhA) inhibitors for the treatment of tuberculosis. **European Journal of Medicinal Chemistry**, v. 86, n. 1, out. 2014. Disponível em: <https://www.ncbi.nlm.nih.gov/pubmed/25218910>. Acesso em: 12 set. 2017.

PETIT, S. et al.. Absolute configuration and structural features of R207910, a

- novel anti-tuberculosis agent. **Journal of Molecular Structure**, 2007. v. 837, n. 1–3, jun. 2007. Disponível em: <<http://www.sciencedirect.com/science/article/pii/S0022286006008416>>. Acesso em: 30 ago. 2017.
- PHUMMARIN, N. et al.. SAR and identification of 2-(quinolin-4-yloxy)acetamides as *Mycobacterium tuberculosis* cytochrome bc₁ inhibitors. **Medicinal Chemical Communication**, v. 7, n. 11, nov. 2016. Disponível em: <<https://www.ncbi.nlm.nih.gov/pmc/articles/PMC5292992/>>. Acesso em: 12 set. 2017.
- PISSINATE, K. et al.. 2-(Quinolin-4-yloxy)acetamides Are Active against Drug-Susceptible and Drug-Resistant *Mycobacterium tuberculosis* Strains. **ACS Medicinal Chemistry Letters**, v. 7, n. 3, jan. 2016. Disponível em: <<https://www.ncbi.nlm.nih.gov/pubmed/26985307>>. Acesso em 20 out. 2017.
- RAMASWAMY, S.; MUSSER, J. M.. Molecular genetic basis of antimicrobial agent resistance in *Mycobacterium tuberculosis*: 1998 update. **Tubercle and lung disease**, v. 79, n. 1, 1998. Disponível em: <<http://www.ncbi.nlm.nih.gov/pubmed/10645439>>. Acesso em 20 out. 2017.
- RAWAL, T.; BUTANI, S.. Combating tuberculosis infection: A forbidding challenge. **Indian Journal of Pharmaceutical Sciences**, v. 78, n. 1, jan. 2016. Disponível em: <<https://www.ncbi.nlm.nih.gov/pubmed/27168676>>. Acesso em 12 set. 2017.
- RYBNIKER, J. et al.. Lansoprazole is an antituberculous prodrug targeting cytochrome bc₁. **Nature communications**, v. 6, n. 7659, jul. 2015. Disponível em: <<https://www.nature.com/articles/ncomms8659>>. Acesso em 30 ago. 2017.
- SZUMOWSK, J. D.; LYNCH, J. B.. Profile of delamanid for the treatment of multidrug-resistant tuberculosis. **Drug Design, Development and Therapy**, v. 9, jan. 2015. Disponível em: <<https://www.ncbi.nlm.nih.gov/pmc/articles/PMC4319680/>>. Acesso em 12 set. 2017.
- TADOLINI, M. et al.. First case of extensively drug-resistant tuberculosis treated with both delamanid and bedaquiline. **European Respiratory Journal**, v. 48, n. 3, set. 2016.
- VELAYATI, A. A. et al.. Emergence of new forms of totally drug-resistant tuberculosis bacilli: Super extensively drug-resistant tuberculosis or totally drug-resistant strains in Iran. **Chest**, v. 136, n. 2, ago. 2009. Disponível em: <<https://www.ncbi.nlm.nih.gov/pubmed/19349380>>. Acesso em 20 out. 2017.
- VIEGAS-JUNIOR, C. et al.. Molecular Hybridization: A Useful Tool in the Design of New Drug Prototypes. **Current Medicinal Chemistry**, v. 14, n. 17, 2007. Disponível em: <<https://www.ncbi.nlm.nih.gov/pubmed/17627520>>. Acesso em 12 set. 2017.
- WALLIS, R. S. et al. Tuberculosis-advances in development of new drugs, treatment regimens, host-directed therapies, and biomarkers. **The Lancet Infectious Diseases**, v. 16, n. 4, abr. 2016. Disponível em: <<https://www.ncbi.nlm.nih.gov/pubmed/27036358>>. Acesso em: 12 set. 2017.

World HealthOrganization. **Global Tuberculosis Control: Surveillance, Planning, Financing.** Geneva, 2003. Disponível em:<http://apps.who.int/iris/bitstream/10665/63835/14/WHO_CDS_TB_2003.316.pdf>. Acesso em: 12 set. 2017.

World HealthOrganization. **Global tuberculosis report 2015.** Disponível em: <<http://www.who.int/tb/publications/2015/en/>>. Acesso em: 30 ago. 2017.

World HealthOrganization. **Global tuberculosis report 2016.** Disponível em: <<http://www.who.int/tb/publications/2016/en/>>. Acesso em: 30 ago. 2017.

World HealthOrganization. **The use of delamanid in the treatment of multidrug-resistant tuberculosis:** Interim policy guidance. 2014. Disponível em: <http://apps.who.int/iris/bitstream/10665/137334/1/WHO_HTM_TB_2014.23_en_g.pdf>. Acesso em: 20 out. 2017.

YEW, W. W.; LEUNG, C. C.. Management of multidrug-resistant tuberculosis : Update 2007. **Respirology**, v. 13, n. 1, jan. 2008. Disponível em: <<https://www.ncbi.nlm.nih.gov/pubmed/18197909>>. Acesso em: 20 out. 2017.

YOUNG, D. B.; STARK, J.; KIRSCHNER, D. E.. Systems biology of persistent infection: tuberculosis as a case study. **Nature Reviews Microbiology**, v. 6, n. 7, jul. 2008. Disponível em: <<https://www.ncbi.nlm.nih.gov/pubmed/18536727>>. Acesso em 12 set. 2017.

ZAHRT, T. C.. Molecular mechanisms regulating persistent *Mycobacterium tuberculosis* infection. **Microbes and Infection**, v. 5, n. 2, fev. 2003. Disponível em: <<https://www.ncbi.nlm.nih.gov/pubmed/12650774>>. Acesso em 20 out. 2017.

ZAYED, M. F. ; HASSAN, M. H.. Synthesis and biological evaluation studies of novel quinazolinone derivatives as antibacterial and anti-inflammatory agents. **Saudi Pharmaceutical Journal**, v. 22, n. 2, abr. 2014. Disponível em: <<https://www.sciencedirect.com/science/article/pii/S1319016413000364>>. Acesso em: 12 set. 2017.

ANEXOS:

1. Carta de aprovação da Comissão de Ética no Uso de Animais da PUCRS.



S I P E S Q
Sistema de Pesquisas da PUCRS

Código SIPESQ: 7249

Porto Alegre, 5 de julho de 2016.

Prezado(a) Pesquisador(a),

A Comissão de Ética no Uso de Animais da PUCRS apreciou e aprovou o Projeto de Pesquisa "AVALIAÇÃO DOS PARÂMETROS ASSOCIADOS À CARDIOTOXICIDADE DE COMPOSTOS CANDIDATOS A FÁRMACOS PARA O TRATAMENTO DA TUBERCULOSE UTILIZANDO O ZEBRAFISH (*Danio rerio*)" coordenado por CARLA DENISE BONAN.

Sua investigação, respeitando com detalhe as descrições contidas no projeto e formulários avaliados pela CEUA, está autorizada a partir da presente data.

Informamos que é necessário o encaminhamento de relatório final quando finalizar esta investigação. Adicionalmente, ressaltamos que conforme previsto na Lei no. 11.794, de 08 de outubro de 2008 (Lei Arouca), que regulamenta os procedimentos para o uso científico de animais, é função da CEUA zelar pelo cumprimento dos procedimentos informados, realizando inspeções periódicas nos locais de pesquisa.

Nº de Animais	Espécie	Duração do Projeto
6720	Zebrafish	05/07/2016 - 05/07/2018

Atenciosamente,

Comissão de Ética no Uso de Animais (CEUA)

2. Carta de submissão deste trabalho para o *European Journal of Medicinal Chemistry*.

Your recent submission to EJMECH

E European Journal of Medicinal Chemistry <eesserver@eesmail.elsevier.com>
Ontem, 10:50
Você ▾

Dear Dr. Fernanda Souza Macchi,

You have been listed as a Co-Author of the following submission:

Journal: European Journal of Medicinal Chemistry

Corresponding Author: Pablo Machado

Co-Authors: Fernanda Souza Macchi, Ms; Kenia Pissinate, PhD; Anne Drumond Villela, PhD; Bruno Lopes Abba Nathalia Sperotto, MS; Adílio da Silva Dadda, MS; Fernanda Teixeira Subtil, MS; Talita Freitas de Freitas; Ana Bizarro, PhD; Luiz Augusto Basso, PhD; Diógenes Santiago Santos, PhD;

Title: 1H-Benzo[d]imidazoles and 3,4-dihydroquinazolin-4-ones: design, synthesis and antitubercular activity

If you did not co-author this submission, please contact the Corresponding Author of this submission at pablo.

An Open Researcher and Contributor ID (ORCID) is a unique digital identifier to which you can link your publis

We would like to invite you to link your ORCID ID to this submission. If the submission is accepted, your ORCID account will also be updated.

To do this, visit our dedicated page in EES. There you can link to an existing ORCID ID or register for one and li

<https://ees.elsevier.com/ejmech/l.asp?i=509367&l=97SVQ8M2>

More information on ORCID can be found on the ORCID website, <http://www.ORCID.org>, or on our help page:

Like other Publishers, Elsevier supports ORCID - an open, non-profit, community based effort - and has adapted their unique ORCID IDs.

Thank you,

European Journal of Medicinal Chemistry